





3 1293 10476 0461

**LIBRARY**  
**Michigan State**  
**University**

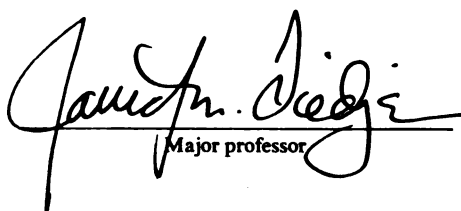
This is to certify that the  
dissertation entitled  
Kinetics of Hydrogen Consumption by  
Methanogenic Consortia and Cultures  
of Hydrogen-Consuming Anaerobes

presented by

Joseph Arlen Robinson

has been accepted towards fulfillment  
of the requirements for

Ph.D. degree in Microbiology

  
Major professor

Date November 9, 1982



RETURNING MATERIALS:  
Place in book drop to  
remove this checkout from  
your record. FINES will  
be charged if book is  
returned after the date  
stamped below.

~~SEP 1 1993~~

SEP 2 5 1993

SEP 10 1993

SEP 27 1993

FEB 7 1994

MAR 1 1994

MAR 1 1994

MAR 1 1994

MAR 1 1994

KINETICS OF HYDROGEN CONSUMPTION BY METHANOGENIC CONSORTIA  
AND CULTURES OF HYDROGEN-CONSUMING ANAEROBES

by

Joseph Arlen Robinson

A DISSERTATION

Submitted to  
Michigan State University  
in partial fulfillment of the requirements  
for the degree of

DOCTOR OF PHILOSOPHY

Department of Microbiology and Public Health

1982



## ABSTRACT

### KINETICS OF HYDROGEN CONSUMPTION BY METHANOGENIC CONSORTIA AND CULTURES OF HYDROGEN-CONSUMING ANAEROBES

by

Joseph Arlen Robinson

Hydrogen plays a central role in the breakdown of organic matter in anaerobic habitats, influencing the nature of the fermentation endproducts and possibly the rates of initial substrate degradation. Until recently, attention had focused primarily on the influence  $H_2$ -consumers exert on the types of endproducts generated from bacteria capable of reducing protons to  $H_2$  (facultative or obligate syntrophs). Currently, interest in  $H_2$  dynamics of anaerobic ecosystems has focused on (i) estimating in situ rates of  $H_2$  consumption and turnover, and (ii) quantitating competition for  $H_2$  among  $H_2$ -consuming anaerobes, such as sulfate-reducing and methanogenic bacteria.

I examined the kinetics of  $H_2$  consumption by samples from natural anaerobic habitats, pure cultures of  $H_2$ -consuming anaerobes, and co-cultures comprised of methanogenic and sulfate-reducing bacteria. In addition, I studied the turnover of ruminal  $H_2$  and the influence organic loading rates have on endogenous  $H_2$  and  $CH_4$  production in vitro. These kinetic studies were performed using a gas-recirculation system that allowed precise measurements of gaseous phase  $H_2$  and  $CH_4$ . Uptake and growth kinetic parameters were estimated for the natural samples and suspensions of  $H_2$ -consumers by fitting  $H_2$  depletion (progress curve)

Joseph Arlen Robinson

data to integrated forms of Michaelis-Menten and Monod equations.

H<sub>2</sub> K<sub>m</sub> values for samples from eutrophic lake sediment, anaerobic digester sludge and rumen fluid were similar, approximately 6 uM. Maximum potential H<sub>2</sub> consumption rates (V<sub>max</sub> estimates) suggested a ratio of activity for rumen fluid, sludge and sediment of about 100:10:1, presumably reflecting the relative densities of H<sub>2</sub>-consuming bacteria--primarily methanogens--occurring in these anaerobic habitats. H<sub>2</sub> K<sub>m</sub> estimates of the four methanogens studied ranged from 2 uM for Methanospirillum PM1 to 12 uM for Methanosarcina barkeri MS, while the other two methanogens--Methanospirillum hungatei JF-1 and Methanobacterium PM2--had mean half-saturation constants for H<sub>2</sub> uptake of 5 uM. Average H<sub>2</sub> K<sub>m</sub> estimates for the sulfate-reducers, Desulfovibrio strains G11 and PS1, were 1 and 0.7 uM, respectively. H<sub>2</sub> V<sub>max</sub> values for the six H<sub>2</sub> consumers assayed were not significantly different when normalized to total protein.

The average half-saturation constant for growth (K<sub>s</sub>), yield coefficient (Y<sub>H<sub>2</sub></sub>) and maximum specific growth rate (u<sub>max</sub>) of G11 were 3 uM, 0.8 g protein/mol H<sub>2</sub> and 0.06/h, respectively. Initial studies with JF-1 suggested that its K<sub>s</sub> for growth on limiting H<sub>2</sub> was higher than the mean value for G11, falling in the range of 2-10 uM. There was an apparent correlation among uptake and growth half-saturation constants estimated for G11 and JF-1. This correlation was corroborated by the finding that the K<sub>m</sub> of Methanospirillum PM1 was lower than that of JF-1 and that it grew significantly faster than JF-1.

The above uptake and growth kinetic parameters predict that sulfate-reducers will outcompete methanogens in habitats where sulfate

Joseph Arlen Robinson

is not limiting.. The partitioning of  $H_2$ , under resting conditions, was used to predict the fate of  $H_2$  when the densities of these competing bacterial groups are relatively fixed. On the other hand, Monod kinetic parameters must be used to predict the outcome of competition for  $H_2$  and the partitioning of this gaseous substrate when growth occurs. A consortium of  $H_2$ -consuming organisms having different affinities for  $H_2$  will exhibit an apparent  $K_m$  that depends on the fractions that the individual groups (e.g., sulfate-reducers, methanogens) comprise of the total  $H_2$ -consuming activity. This dependence was successfully predicted for various mixtures of Desulfovibrio G11 and Methanospirillum JF-1.

Retention times for  $H_2$  turnover in vitro calculated from estimates of ruminal Michaelis-Menten parameters and  $CH_4$  production data were equivalent once the  $H_2$  pool attained steady-state. Retention times varied from 0.1-0.3 sec for strained rumen fluid and diluted whole contents. Retention times for ruminal  $H_2$  in vivo were approximated to be 0.02 sec (mid-point of range) by correcting retention time estimates determined for diluted whole contents by the ratio of total particulates to strained rumen fluid used in these experiments. Endogenous  $H_2$  concentrations and  $CH_4$  production rates rapidly increased when strained rumen fluid samples were amended with finely ground hay. Additions of 5-10 g of milled hay resulted in increased  $H_2$  levels that peaked after several hours; 50 g or greater additions of ground hay typically resulted in extremely high  $H_2$  concentrations that never peaked. In the latter experiments, a decrease in pH accompanied the accumulation of high  $H_2$  concentrations. Further, calculated rates of  $H_2$  production were several times greater than  $V_{max}$  estimates of  $H_2$  consumption obtained

Joseph Arlen Robinson

for strained rumen fluid.

In all of the above kinetic studies,  $H_2$  was measured in the gas phase and liquid phase concentrations were calculated by multiplying the former by the appropriate Bunsen absorption coefficient. But this is only valid when the gaseous and aqueous phases are in equilibrium (i.e., when a phase-transfer limitation does not exist). In accord with this, I developed a mathematical model that predicted conditions leading to phase-transfer limited gaseous substrate consumption by resting and growing cells. For gaseous substrate ( $H_2$ ) consumption by resting bacteria the following criteria indicate that a phase-transfer limitation exists: (i) the apparent  $K_m$  shows a strong dependence on the initial substrate concentration and the magnitude of the sink (i.e.,  $V_{max}$ ) in the aqueous phase; and (ii) the apparent Michaelis-Menten parameters exhibit dependence on stirring speed and the ratio of aqueous to gaseous phase volume. Similar principles apply to Michaelis-Menten gaseous product formation from either gaseous or non-gaseous substrates, and gaseous substrate consumption by growing cells.

**To Patricia-Marie and my loving parents,  
Russell and Nancy Robinson**

In 1863 an unofficial visitor to the Whitehouse drew from Lincoln the remark that he had a great reverence for learning. "This is not because I am not an educated man. I feel the need of reading. It is a loss to a man not to have grown up among books". The visitor replied with: "Men of force can get along pretty well without books. They do their own thinking instead of adopting what other men think". "Yes", said Lincoln, "but books serve to show a man that those original thoughts of his aren't very new, after all".

"Say not, 'I have found the truth', but rather, 'I have found a truth'".

Kahlil Gibran

## ACKNOWLEDGEMENTS

I am much indebted to Dr. James Tiedje. Not only did he provide a superb intellectual environment in which I could grow, but his continual support encouraged me to strive for scientific excellence. I am also indebted to the superb graduate students and post-docs that it was my pleasure to work with over the past five years. Any successes I have enjoyed thus far, I owe in large part to the high caliber of science maintained by Dr. Tiedje and the people who have worked for him in his laboratory.

I thank the members of my guidance committee--Drs. Mike Klug, Clarence Suelter and C. A. Reddy. Special thanks go to Dr. Klug for supporting a summer's stay at the Kellogg Biological Station.

I thank Walter J. Smolenski and Marilyn Boucher for their excellent technical assistance over the past three years. Their help in media preparation and routine culturing of the bacteria used in this study is much appreciated.

I owe a great deal to my loving wife, Patricia-Marie. She has made many sacrifices since I became obsessed with microbial ecology, but her support never waned even through the long evenings I spent away from home.

How can I ever say enough to thank my parents for their unrelenting support? They played a major role in making my years in graduate school the best ones of my life to date. The diversions Patti and I shared with them relieved many of the frustrations of being a graduate student. My only regret is I never learned how to make Dupont 3F; sorry Dad--I doubt if Jim knows either.

# TABLE OF CONTENTS

	Page
LIST OF TABLES .....	vi1
LIST OF FIGURES .....	viii1
INTRODUCTION .....	1
LITERATURE CITED .....	5
ARTICLE I (CHAPTER I). KINETICS OF HYDROGEN CONSUMPTION BY RUMEN FLUID, ANAEROBIC DIGESTOR SLUDGE AND SEDIMENT	7
ABSTRACT .....	8
INTRODUCTION .....	9
MATERIALS AND METHODS .....	11
PHASE-TRANSFER MODEL .....	17
RESULTS .....	21
DISCUSSION .....	42
LITERATURE CITED .....	49
ARTICLE II (CHAPTER II). TURNOVER OF HYDROGEN IN RUMEN FLUID .....	52
ABSTRACT .....	53
INTRODUCTION .....	54
MATERIALS AND METHODS .....	55
RESULTS .....	58
DISCUSSION .....	71
LITERATURE CITED .....	76
ARTICLE III (CHAPTER III). RESOURCE COMPETITION AMONG SULFATE- REDUCERS AND METHANOGENS FOR HYDROGEN .....	78
ABSTRACT .....	79
INTRODUCTION .....	80
MATERIALS AND METHODS .....	82
RESULTS .....	89
DISCUSSION .....	112
LITERATURE CITED .....	122
APPENDIX A. PHASE-TRANSFER KINETICS .....	126
LITERATURE CITED .....	153
APPENDIX B. PROGRESS CURVE ANALYSIS .....	154
LITERATURE CITED .....	195
APPENDIX C. COMPUTER PROGRAMS FOR DATA ANALYSIS .....	197



LITERATURE CITED .....	225
------------------------	-----

## LIST OF TABLES

Table	ARTICLE I	Page
1	Summary of Michaelis-Menten kinetic parameters for rumen fluid, Holt digester sludge and Wintergreen sediment .....	26
	ARTICLE II	
1	Retention times (sec) of ruminal H <sub>2</sub> calculated from endogenous H <sub>2</sub> production versus H <sub>2</sub> consumption rates .....	72
	ARTICLE III	
1	Summary of H <sub>2</sub> kinetic parameters for methanogenic and sulfate-reducing bacteria .....	100
2	H <sub>2</sub> K <sub>m</sub> estimates for <u>Desulfovibrio</u> strains G11 and PS1 at different initial H <sub>2</sub> concentrations .....	101
3	Michaelis-Menten parameters for product appearance by methanogenic and sulfate-reducing bacteria .....	104
4	Monod growth kinetic parameters for <u>Desulfovibrio</u> G11 .....	111
	APPENDIX A	
1	Comparison of nonlinear versus linear analysis of Michaelis-Menten progress curve data containing simple or relative errors .....	170

## LIST OF FIGURES

Figure	ARTICLE I	Page
1	Gas-recirculation system used for H <sub>2</sub> consumption and CH <sub>4</sub> production experiments .....	13
2	Theoretical curves dmr phase-transfer and non-transfer limited gaseous substrate consumption ....	20
3	Gaseous phase data for phase-transfer limited (first-order) H <sub>2</sub> consumption by undiluted rumen fluid (URF) and Portland sludge (PS), and non-transfer limited (mixed order) H <sub>2</sub> consumption by 20-fold diluted rumen fluid (DRF) .....	23
4	Calculated aqueous phase data for Michaelis-Menten H <sub>2</sub> consumption by diluted rumen fluid (DRF), Holt sludge (HS) and Wintergreen sediment (WS) .....	25
5	Dependence of apparent H <sub>2</sub> K <sub>m</sub> on magnitude of the biological sink under phase-transfer and non-transfer limited conditions .....	29
6	Effect of an increase in endogenous substrate production (A) and an increase in V <sub>max</sub> with time (B) on Michaelis-Menten progress curves .....	31
7	Errors in apparent V <sub>max</sub> (A) and K <sub>m</sub> (B) resulting from concomitant endogenous H <sub>2</sub> production during the course of progress curve experiments .....	34
8	CH <sub>4</sub> production data and calculated rates of H <sub>2</sub> production for undiluted rumen fluid .....	36
9	Relationship between endogenously produced H <sub>2</sub> and H <sub>2</sub> concentrations monitored during a progress curve using replicate suspensions of diluted rumen fluid (DRF) .....	38
10	Relationship between endogenously produced H <sub>2</sub> and H <sub>2</sub> concentrations monitored during a progress curve using replicate samples of undiluted Holt sludge (HS) .....	40
ARTICLE II		
1	Endogenous CH <sub>4</sub> production by two samples of strained rumen fluid (SRF) and diluted whole rumen contents (WC) .....	60
2	Endogenous dissolved H <sub>2</sub> concentrations and	

	calculated rates of H <sub>2</sub> production for strained (squares) and diluted whole contents (circles) ....	62
3	H <sub>2</sub> retention times for strained rumen fluid and diluted whole contents estimated from total CH <sub>4</sub> production rate data (Figure 2) .....	64
4	Dissolved H <sub>2</sub> concentrations for strained rumen fluid amended with 50 (triangles), 10 (circles) or 1 (squares) g of finely milled hay .....	67
5	CH <sub>4</sub> production by strained rumen fluid amended with 50 (triangles), 10 (circles) or 1 (squares) g of finely milled hay .....	69

### ARTICLE III

1	H <sub>2</sub> progress curve data for <u>Methanospirillum hungatei</u> JF-1 at two different initial H <sub>2</sub> concentrations .....	91
2	H <sub>2</sub> progress curves for <u>Methanosarcina barkeri</u> MS versus theoretical curves calculated from best-estimates of Michaelis-Menten parameters .....	93
3	H <sub>2</sub> progress curve data for <u>Methanospirillum</u> PM1 (squares) and <u>Methanobacterium</u> PM2 (triangles) versus theoretical curves calculated from best-estimates of V <sub>max</sub> , K <sub>m</sub> and S <sub>0</sub> .....	95
4	H <sub>2</sub> progress curve data for <u>Desulfovibrio</u> G11 at two different initial concentrations of H <sub>2</sub> plotted against theoretical curves .....	97
5	H <sub>2</sub> progress curve data for <u>Desulfovibrio</u> PS1 plotted against theoretical Michaelis-Menten curves at two different initial H <sub>2</sub> concentrations .....	99
6	CH <sub>4</sub> and dissolved sulfide appearance data versus theoretical curves calculated using best-estimates of V <sub>max</sub> and K <sub>m</sub> .....	103
7	Apparent H <sub>2</sub> K <sub>m</sub> at different ratios of sulfate-reducing activity (organism 1) to total H <sub>2</sub> -consuming capacity .....	107
8	Comparison of theoretical curve with measured H <sub>2</sub> concentrations (squares) for growth of <u>Desulfovibrio</u> G11 growing on H <sub>2</sub> as the sole electron donor ....	110
9	Fifty-percent partitioning curves for mixtures of sulfate-reducing and methanogenic bacteria .....	118

## APPENDIX A

1	Influence of $K_{1a}$ on gaseous substrate consumption not limited by phase-transfer .....	130
2	Influence of $K_{1a}$ on gaseous substrate consumption limited by mass-transport .....	132
3	Gaseous substrate consumption by growing cells severely limited by mass-transport .....	135
4	Gaseous substrate consumption by growing cells moderately limited by phase-transfer .....	137
5	Gaseous substrate consumption by growing cells not limited by mass-transport .....	139
6	Influence of $K_{1a}$ on ratio of aqueous to gaseous phase concentrations of a gaseous product produced from a non-gaseous substrate .....	143
7	Gaseous product formation from a non-gaseous substrate for different values of $K_{1a}$ .....	146
8	Influence of gaseous substrate solubility on $K_{m,app}$ and $V_{max,app}$ estimated from aqueous phase data ..	148
9	Influence of gaseous substrate solubility on $K_{m,app}$ and $V_{max,app}$ estimated from for total mass (mol) of gaseous substrate being consumed with time .....	150

## APPENDIX B

1	Plots of Michaelis-Menten progress curve data transformed according to [B.3] (A), [B.4] (B) and [B.5] (C) with simple error bars of $\pm 0.01$ units .....	158
2	Plots of Michaelis-Menten progress curve data transformed according to [B.3] (A), [B.4] (B) and [B.5] (C) with relative error bars of $\pm 0.005$ units ....	162
3	Sensitivity coefficients for $K_m$ and $V_{max}$ .....	168
4	Sensitivity coefficients for $S_0$ derived from [B.1] versus [B.2] .....	172
5	Sigmoidal substrate consumption (S) and biomass formation (X) for cells growing in batch .....	177
6	Linearized discretized Monod data .....	180
7	Sensitivity coefficients for $u_{max}$ , $K_s$ and Y ...	182

8	Residuals for H <sub>2</sub> progress curve data fitted to [B.2] using nonlinear least-squares analysis .....	186
9	Simulated Monod progress curve data containing simple errors (standard deviation=0.01 units) fitted to the integrated form of the Michaelis-Menten equation [B.2] .....	189
10	Residuals for H <sub>2</sub> removal from an empty flask containing H <sub>2</sub> due to sampling .....	191
11	Residuals for H <sub>2</sub> standard tank sampled with time	193

## INTRODUCTION AND EXPERIMENTAL OBJECTIVES

In the past 10-15 years, interest in  $H_2$  and the role it plays as an intermediate in the anaerobic dissimilation of organic matter has risen dramatically. This methanogenic precursor is believed to have a significant influence on pathways of anaerobic metabolism via interspecies  $H_2$  transfer (7,18,19). The earliest quantitative work on  $H_2$  kinetics and turnover in anaerobic habitats--specifically, the rumen--was published by Hungate and co-workers (5,6). Recently, several papers have appeared that document  $H_2$ 's role and the kinetics of  $H_2$  consumption in other anaerobic ecosystems. The majority of these studies focused on  $H_2$  dynamics in lacustrine and marine sediments (1,2,4,11,13,14,16,17). Further, estimates of uptake constants for a methanogen and sulfate-reducer have appeared within the past several months (9) which agree with estimates obtained for methanogenic habitats. Between these two phases of activity,  $H_2$ 's importance in the anaerobic processing of organic matter was primarily assessed through studies on co-cultures of proton-reducing and  $H_2$ -consuming organisms (3,8,10,12,15,18). These studies dealt with products produced from organic matter dissimilation when  $H_2$ -consuming organisms (sulfate-reducers or methanogens) functioned in concert with a proton-reducing organism. Now there is renewed interest in estimating kinetic constants for  $H_2$  consumption in anaerobic ecosystems and additionally, in determining kinetic constants for pure cultures of methanogenic bacteria and other  $H_2$ -consuming anaerobes--specifically, sulfate-reducing bacteria. This interest stems from the need to estimate in situ rates of  $H_2$  consumption and the partitioning of  $H_2$

between competing populations of methanogenic and sulfate-reducing bacteria in habitats where sulfate is not limiting.

The primary goals of my doctoral research was to estimate kinetic constants for  $H_2$  consumption by (i) samples of anaerobic ecosystems, (ii) pure cultures of methanogenic and sulfate-reducing bacteria in both resting and growing states, and (iii) defined co-cultures of methanogens and sulfate-reducers. Knowledge of kinetic constants for  $H_2$  consumption by anaerobic habitats may be used and interpreted in several ways. Firstly, the affinities of various habitats--such as, eutrophic lake sediment, anaerobic digester sludge and rumen fluid--for  $H_2$  can be compared using estimates of half-saturation constants ( $K_m$ ,  $K_s$ ). These half-saturation constants presumably reflect the overall affinity of the  $H_2$ -consuming organisms for  $H_2$  present in these habitats. Maximum potential rates of activity ( $H_2$   $V_{max}$ 's) reflect the densities of methanogens (also sulfate reducers and  $H_2$ -consuming acetogens, if present) occurring in the same habitats and represent better estimates of the active  $H_2$ -consuming biomass than direct or indirect bacterial counts. Thirdly, estimates of  $H_2$  kinetic parameters, along with knowledge of the endogenous  $H_2$  concentration, can be used to predict in situ  $H_2$  retention times when this intermediate is at steady-state.

In Chapter I, I present estimates of Michaelis-Menten kinetic parameters for  $H_2$  consumption by rumen fluid, anaerobic digester sludge and eutrophic sediment. The kinetic constants for rumen fluid and data on endogenous  $CH_4$  production are used in Chapter II to approximate endogenous  $H_2$  turnover and demonstrate the equivalence of  $H_2$  retention times calculated from  $H_2$  production and consumption data when the  $H_2$  pool has attained steady-state. Chapter II also contains data showing



the influence of organic loading rates on endogenous ruminal  $H_2$  and  $CH_4$  production.

In addition to presenting estimates of  $H_2$  uptake parameters for natural anaerobic ecosystems in Chapter I, I also describe criteria that may be used to assess whether gaseous substrate (e.g.,  $H_2$ ,  $O_2$ ) consumption is limited by mass-transport across an aqueous-gaseous phase interface and examine the influence endogenous  $H_2$  production has on estimates of Michaelis-Menten kinetic parameters. Mass-transport limitations must be circumvented before meaningful estimates of biological kinetic parameters can be obtained (see Appendix A).

Chapter III contains estimates of Michaelis-Menten (uptake) and Monod (growth) kinetic parameters for pure cultures of methanogenic and sulfate-reducing bacteria. Estimates of Michaelis-Menten kinetic parameters can be used to predict the partitioning of limiting  $H_2$  between these two functional groups of bacteria and apparent uptake constants for mixtures of these microorganisms. Estimates of Monod growth parameters also predict the fate of an initial limiting amount of  $H_2$  when its consumed by a mixture of growing methanogens and sulfate-reducers. Further, Monod growth parameters, unlike uptake parameters, predict which  $H_2$ -consumer will eventually outgrow the other assuming  $H_2$  is the only limiting substrate.

Appendices A through C contain information relevant to all three chapters. Appendix A provides more details than Chapter I on the influence of mass-transport on rates of gaseous substrate consumption by growing or resting bacterial cells. Further, Appendix A contains systems of differential equations that describe gaseous product formation from either gaseous or nongaseous substrates. In Appendix B

are details on the nonlinear regression analyses applied to the progress curve (i.e., substrate depletion) data shown in Chapters I and III. Finally, Appendix C contains several computer programs written for analysis of the kinetic data presented in this dissertation.

## LITERATURE CITED

1. Abram, J. W., and D. B. Nedwell. 1978. Hydrogen as a substrate for methanogenesis and sulfate reduction in anaerobic saltmarsh sediment. *Arch. Microbiol.* 117:93-97.
2. Abram, J. W., and D. B. Nedwell. 1978. Inhibition of methanogenesis by sulfate-reducing bacteria competing for transferred hydrogen. *Arch. Microbiol.* 117:89-92.
3. Bryant, M. P., L. L. Campbell, C. A. Reddy, and M. R. Crabill. 1977. Growth of Desulfovibrio in lactate or ethanol media low in sulfate in association with H<sub>2</sub>-utilizing methanogenic bacteria. *Appl. Environ. Microbiol.* 33:1162-1169.
4. Cappenberg, T. E. 1974. Interrelationships between sulfate-reducing and methane-producing bacteria in bottom deposits of a fresh-water lake. I. Field observations. *Antonie van Leeuwenhoek J. Microbiol. Serol.* 40:235-295.
5. Hungate, R. E. 1967. Hydrogen as an intermediate in the rumen fermentation. *Arch. Microbiol.* 59: 158-164.
6. Hungate, R. E., W. Smith, T. Bauchop, J. Yu, and J. C. Rabinowitz. 1970. Formate as an intermediate in the bovine rumen fermentation. *J. Bacteriol.* 102:389-397.
7. Hungate, R. E. 1975. The rumen microbial ecosystem. *Ann. Rev. Ecol. Syst.* 6: 39-66.
8. Iannotti, E. L., D. Kafkewitz, M. J. Wolin, and M. P. Bryant. 1973. Glucose fermentation products of Ruminococcus albus grown in continuous culture with Vibrio succinogenes: Changes caused by interspecies transfer of H<sub>2</sub>. *J. Bacteriol.* 114: 1231-1240.
9. Kristjansson, J. R., P. Schonheit, and R. K. Thauer. 1982. Different K<sub>s</sub> values for hydrogen of methanogenic bacteria and sulfate-reducing bacteria: An explanation for the apparent inhibition of methanogenesis by sulfate. *Arch. Microbiol.* 131:278-282.
10. Latham, M. J., and M. J. Wolin. 1977. Fermentation of cellulose by Ruminococcus flavefaciens in the presence and absence of Methanobacterium ruminantium. *Appl. Environ. Microbiol.* 34: 297-301.
11. Lovely, D. R., D. Dwyer, and M. J. Klug. 1982. Kinetic analysis of competition between sulfate reducers and methanogens for hydrogen in sediments. *Appl. Environ. Microbiol.* 43: 1373-1379.
12. McInerney, J. M., and M. P. Bryant. 1981. Anaerobic degradation of

lactate by syntrophic association of Methanosarcina barkeri and Desulfovibrio species and effect of H<sub>2</sub> on acetate degradation. Appl. Environ. Microbiol. 41:346-354.

13. Mountfort, D. O., R. A. Asher, E. L. Mays, and J. M. Tiedje. 1980. Carbon and electron flow in mud and sandflat intertidal sediments of Delaware inlet, Nelson, New Zealand. Appl. Environ. Microbiol. 39:686-694.
14. Robinson, J. A., and J. M. Tiedje. Kinetics of hydrogen consumption by rumen fluid, anaerobic digester sludge and sediment. Appl. Environ. Microbiol. in press (AEM no. 364).
15. Scheifinger, C. C., B. Linehan, and M. J. Wolin. 1975. H<sub>2</sub> production by Selenomonas ruminantium in the presence and absence of methanogenic bacteria. Appl. Environ. Microbiol. 29: 480-483.
16. Strayer, R. F., and J. M. Tiedje. 1978. Kinetic parameters of the conversion of methane precursors to methane in hypereutrophic lake sediment. Appl. Environ. Microbiol. 36:330-340.
17. Winfrey, M. R., and J. G. Zeikus. 1977. Effect of sulfate on carbon and electron flow during microbial methanogenesis in freshwater sediments. Appl. Environ. Microbiol. 33:275-281.
18. Wolin, M. J. 1974. Metabolic interactions among intestinal microorganisms. Amer. J. Clin. Nutr. 27: 1320-1328.
19. Zehnder, A. J. B. 1978. Ecology of methane formation. In R. Mitchell (ed.), Water pollution microbiology. Vol. 2. John Wiley and Sons, Inc., New York. p. 349-376.

**ARTICLE I (CHAPTER I)**

**KINETICS OF HYDROGEN CONSUMPTION BY RUMEN FLUID,  
ANAEROBIC DIGESTOR SLUDGE AND SEDIMENT**

**by**

**Joseph A. Robinson and James M. Tiedje**

## ABSTRACT

Michaelis-Menten kinetic parameters for  $H_2$  consumption by these three methanogenic habitats were determined from progress curve and initial velocity experiments. Additionally, the influences of mass-transfer resistance, endogenous  $H_2$  production and growth on apparent Michaelis-Menten kinetic parameters were investigated.  $H_2$  consumption by undiluted rumen fluid and sludge from a digester with a typical retention time was limited by transfer of  $H_2$  across the gas-liquid interface;  $H_2$  consumption could not be saturated and apparent  $K_m$ 's were dependent on initial  $H_2$  concentrations and the magnitude of  $V_{max}$ . Once rumen fluid was diluted 20-fold,  $H_2$   $K_m$ 's became relatively constant and were independent of the initial  $H_2$  concentration and the magnitude of  $V_{max}$ .  $H_2$  consumption by digester sludge with a long retention time and hypereutrophic lake sediment was not phase-transfer limited, and exhibited Michaelis-Menten kinetics.  $H_2$   $K_m$ 's for these habitats were relatively constant with means of 5.8, 6.0 and 7.1  $\mu M$  for rumen fluid, digester sludge and sediment, respectively.  $V_{max}$  estimates suggested a ratio of activity of approximately 100 (rumen fluid):10 (sludge):1 (sediment); their ranges were rumen fluid (14-28  $mM h^{-1}$ ), Holt sludge (0.7-4.3  $mM h^{-1}$ ) and Wintergreen sediment (0.13-0.49  $mM h^{-1}$ ). Potential errors in the Michaelis-Menten kinetic parameters, resulting from endogenously produced  $H_2$  were less than 15% for rumen fluid and less than 10% for lake sediment or digester sludge. Increases in  $V_{max}$ , during the course of progress curve experiments, were not great enough to produce systematic deviations from Michaelis-Menten kinetics. Conditions that create phase-transfer limitations for gaseous substrate consumption were elucidated using a mathematical model that combined mass-transport and Michaelis-Menten kinetics.

## INTRODUCTION

Hydrogen is a key intermediate in the degradation of organic matter, affecting both the rate of this process and the nature of the endproducts (4,12,34,35). Due to  $H_2$ 's central role in methanogenic habitats, the kinetics of  $H_2$  consumption has received considerable attention in the past few years, with most investigators concentrating on  $H_2$  kinetics in eutrophic lake (29,33) and marine (1,2,20) sediments, and anaerobic digester sludge (15,26).  $H_2$  kinetics in the rumen has been studied to a lesser extent (7,10,13).

Many investigators, particularly those studying  $H_2$  kinetics in digester sludge (15,26), overlooked the influence mass-transfer resistance may have had on their experiments. That mass-transfer of gaseous substrates (e.g.,  $O_2$ ) can limit microbial activity and growth has been understood for some time (3,22,23). But microbiologists investigating  $H_2$  kinetics in methanogenic habitats have often implicitly assumed their incubation systems circumvented potentially rate-limiting movement of  $H_2$  across the gas-liquid interface. Gross over-estimates of half-saturation constants (viz.,  $K_m$ ,  $K_s$ ) result if data, obtained under mass-transfer (phase-transfer) limited conditions, are used to compute estimates of these parameters. Ngian, Lin and Martin (21) have demonstrated that mass-transfer resistance can significantly increase apparent transport  $K_m$ 's for organisms that form aggregates in biological reactors. They argue, as does Shieh (27), that mass-transfer resistances must be eliminated if biological parameters, independent of reaction vessel geometries, are to be estimated. Thus, we initially examined the influence inter-phase movement of  $H_2$  has on apparent kinetic parameters (viz.,  $K_m$ ,  $V_{max}$ ) when consumption of  $H_2$  is monitored in the gaseous

phase, and determined the magnitude of errors associated with Michaelis-Menten kinetic parameters calculated from data obtained under phase-transfer limited conditions. We developed a model (PHASIM) to evaluate effects of mass-transfer resistance on Michaelis-Menten kinetic parameters. The model is generally useful since it describes the influence mass-transfer resistance has on substrate consumption occurring in one phase of a multi-phase system, where the substrate partitions among the various phases (gas, liquid or solid).

The other goals of the present study were to: (1) compare the kinetics of  $H_2$  consumption in rumen fluid, hypereutrophic lake sediment and anaerobic sludge; and (2) to assess the influence that endogenous  $H_2$  production and growth have on apparent Michaelis-Menten kinetic parameters for  $H_2$ .



## MATERIALS AND METHODS

Habitats sampled. Samples of rumen fluid were obtained from a fistulated cow that was fed daily 5.44 kg of hay ad libitum. Samples of rumen fluid were withdrawn from the cow according to a previously described procedure (23); a cheese-cloth screen reduced the proportion of particulate solids from that found in vivo. Samples were usually obtained prior to feeding to minimize variability in endogenous H<sub>2</sub> production rates. Rumen fluid was used within 30 min after it was collected.

Anaerobic digester sludge was obtained from municipal waste treatment plants in Holt and Portland, MI. Lake sediment samples were taken from the pelagic zone of hypereutrophic Wintergreen lake (Hickory Corners, MI) using an Eckman dredge. Mason jars were completely filled with the samples and sealed with metal canning lids. Samples were stored at 5-10°C for 1 week or less before being used.

Experimental apparatus for measurement of H<sub>2</sub> and CH<sub>4</sub>. All experiments were performed using the gas-recirculation system depicted in Figure 1, which is patterned after the one described by Kaspar and Tiedje (16). Five-hundred-milliliter volumes of either undiluted rumen fluid, diluted rumen fluid, Wintergreen sediment, or digester sludge were anaerobically transferred to a 2-l flask, using a modification of the Hungate technique (11). The flask was stoppered, placed in a water bath (held at 39°C for rumen fluid, 30°C for sludge, or 9°C for sediment) and attached to the gas-recirculation system. Prior to the beginning of each experiment, the headspace of the flask was flushed out the vent with CO<sub>2</sub>

Figure 1. Gas-recirculation system used for  $H_2$  consumption and  $CH_4$  production experiments. The heavier line indicates the path of gas circulation between sample flask and  $H_2$  GC sampling loop. Components are detailed in Materials and Methods.

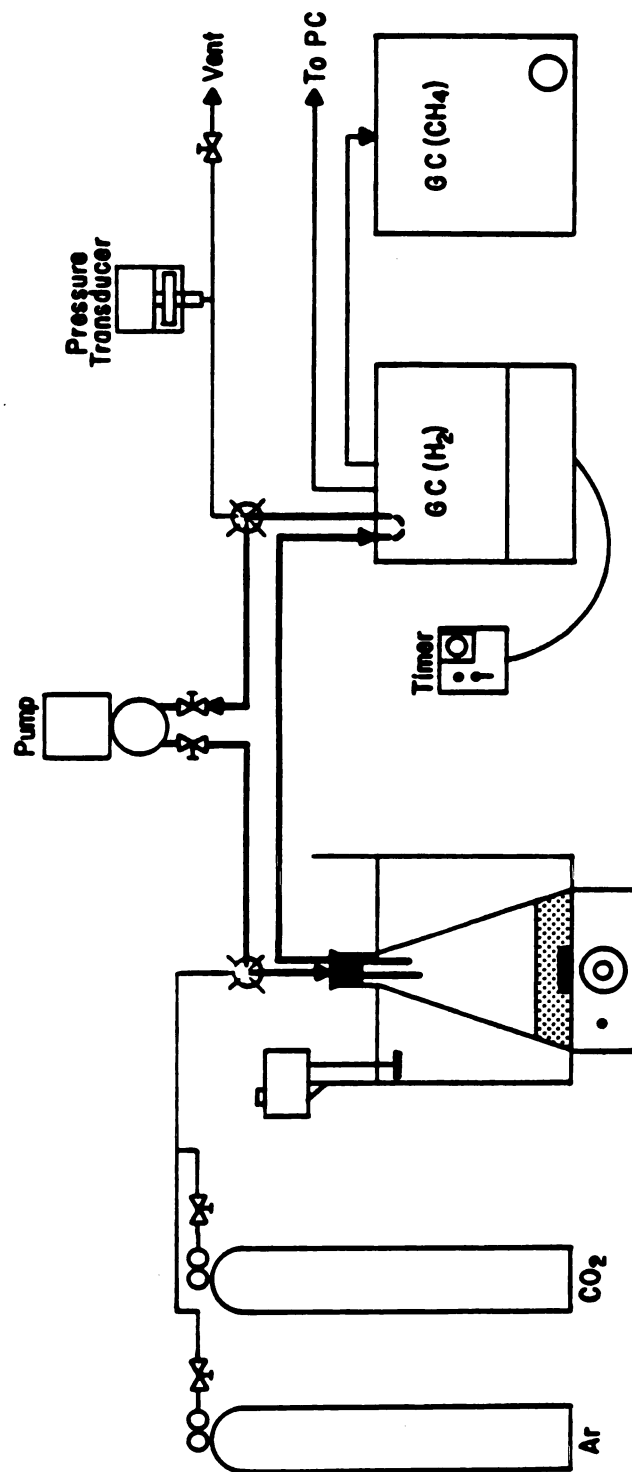


Figure 1

(for rumen fluid), 30% CO<sub>2</sub>/70% Ar (for sludge), or 5% CO<sub>2</sub>/95% Ar (for sediment) for about 15-30 min. Trace levels of O<sub>2</sub> were removed from the sparge gas by passing it through hot copper filings. After the flushing period, the gas-recirculation system was closed and the headspace of the flask was recirculated, via a bellows-type pump (Universal Electric Co., Owosso, MI), through a 3-ml gas sampling loop in a Carle AGC-111 gas chromatograph (Carle Instruments Inc., Anaheim, CA). A magnetic stirrer set at near-maximal speed mixed the aqueous phase in the 2-l flask. Argon, at a flow rate of 20 ml min<sup>-1</sup>, was used as the carrier gas for the Carle GC, and gas separation was made using two tandem columns held at 30°C; the first column was Porapak T (1.2-m length, 3.2-mm i.d.), while the second was Molecular Sieve 5A (2.7-m length, 3.2-mm i.d.). Injections were automatically performed with a timer (Carle Instruments Inc., Anaheim, CA) attached to the valve switching mechanism in the H<sub>2</sub> GC. The H<sub>2</sub> retention time was ca. 3 min. After the H<sub>2</sub> passed through the microthermistor detector, the gas flow was reversed by the timer and the rest of the gas sample (including the CH<sub>4</sub> in the original 3-ml injection) was backflushed to a Varian 600-D GC (Varian Instrument Group, Walnut Creek, CA) equipped with a flame ionization detector. The backflush stream of Ar, at a flow rate of 40 ml min<sup>-1</sup>, served as the carrier gas for the second (CH<sub>4</sub>-detecting) GC, and gas separation in this instrument was effected with a 1.5-m (3.2-mm i.d.) column of Porapak Q at room temperature. H<sub>2</sub> and CH<sub>4</sub> peak areas were determined with integrators. The pressure transducer (Unimeasure, Grants Pass, OR) was used to check for leaks in the gas-recirculation system.

Bunsen coefficients, for the three temperatures of incubation, were calculated using an equation that describes the solubility of a gas as a

function of temperature (32).

Initial velocity and progress curve experiments. For initial velocity experiments rumen fluid (diluted or undiluted) was incubated with five different initial  $H_2$  concentrations. Consumption of  $H_2$  was monitored at 10 min intervals for 2 h, and initial velocity estimates were obtained by evaluating the first-derivatives of the best-fit lines for  $H_2$  disappearance at  $t=0$ . Estimates of  $K_m$  and  $V_{max}$  for  $H_2$  consumption were determined from initial velocity-substrate concentration ( $v-s$ ) pairs using (i) an unweighted Lineweaver-Burk analysis, (ii) the direct linear plot of Cornish-Bowden (9) and, (iii) a non-linear regression analysis that involved fitting the  $v-s$  pairs directly to a rectangular hyperbola (6). For progress curve experiments, a saturating concentration of  $H_2$  [calculated from  $K_m$  estimates determined by Hungate et. al. (13), and Strayer and Tiedje (29)] was incubated with diluted rumen fluid, Holt sludge or Wintergreen sediment. The  $H_2$  concentration was monitored until it had decreased to 10% or less of the value measured at the first time point.  $V_{max}$  and  $K_m$  estimates were calculated from the progress curve data using a computer program that performed a non-linear regression analysis of Michaelis-Menten progress curve data (Mike Betlach, Ph. D. Thesis, Michigan State University, East Lansing, 1979), according to the procedure outlined by Duggleby and Morrison (8).  $H_2$   $V_{max}$ 's for rumen fluid were multiplied by the dilution factor required to overcome the phase-transfer limitation.

Measurement of endogenous  $H_2$  production rates. Experiments to determine endogenous concentrations and rates of  $H_2$  production by rumen fluid, digester sludge, or lake sediment were essentially the same as the progress curve and initial velocity experiments, except that  $H_2$  was not

added. Rates of endogenous  $\text{CH}_4$  production were calculated by fitting the  $\text{CH}_4$  concentration data to linear or one-term power curves and evaluating the first-derivatives of these equations. Rates of endogenous  $\text{H}_2$  production were calculated for rumen fluid, sewage sludge, and lake sediment by first multiplying the  $\text{CH}_4$  production rates by four and then, assuming that 100% (10), 30% (14,28) and 37% (17), respectively, of the  $\text{CH}_4$  generated in these habitats comes from chemolithotrophic methanogenesis. Rates of  $\text{H}_2$  production were calculated during times when the endogenous  $\text{H}_2$  pool, which was concomitantly measured with  $\text{CH}_4$ , had attained an approximately steady-state condition.

## PHASE-TRANSFER MODEL

If the rate at which a gaseous substrate crosses the gas-liquid interface is slower than the rate of biological consumption, then substrate consumption is phase-transfer limited and approximately first-order, whether the initial substrate concentration is greater than the  $K_m$  or not. But if the rate of interface transfer is rapid enough to supply the biological demand, then substrate consumption will not be transfer limited, and the kinetic pattern observed will be controlled by the biological process. In this case, and assuming the biological process exhibits saturation kinetics, a Michaelis-Menten progress curve will be observed for gaseous substrate consumption.

We developed a model (PHASIM) to elucidate conditions leading to phase-transfer limitations for consumption of a gaseous substrate. The model consists of two differential equations. The first equation describes consumption of a gaseous substrate in the gas phase:

$$dG/dt = -k_{1a}(BG - A)$$

where,  $G$ =concentration of the gaseous substrate in the gas phase,  $A$ =concentration of the gaseous substrate dissolved in the aqueous phase,  $k_{1a}$ =volumetric transfer coefficient,  $B$ =Bunsen absorption coefficient, and  $t$ =time. The above equation derives from Fick's first law of diffusion (23,31), and in its most general form, describes mass transport across any inter-phase boundary (e.g., gas-liquid interface). The rate of biological consumption was assumed to conform to Michaelis-Menten kinetics. The following equation describes the behavior of the substrate dissolved in the aqueous phase:

$$dA/dt = k_{1a}(BG - A) - [V_{max}A / (K_m + A)]$$

where,  $V_{\max}$ =the maximum rate of consumption of A and  $K_m$ =the half-saturation constant for substrate consumption. The model also allowed for endogenous production of the substrate and a doubling of  $V_{\max}$  with time, the latter simulating growth during the period of substrate consumption. Solution curves (viz., G vs. t, A vs. t) for the above differential equations were estimated using a fourth-order Runge-Kutta technique (5). Our model is similar to one previously described for  $O_2$  uptake by growing cells in a shake flask (30).

Figure 2 depicts the results of two PHASIM simulations. When the  $k_{1a}$  was less than  $V_{\max}$ , then phase-transfer limited consumption occurred. On the other hand, a Michaelis-Menten progress curve resulted when the  $k_{1a}$  was greater than  $V_{\max}$ . Parameter values for these simulations were chosen arbitrarily. In general, substrate depletion will be first-order under phase-transfer limitations regardless of the initial substrate concentration, whereas gaseous substrate depletion will exhibit Michaelis-Menten kinetics in the absence of a transfer limitation. When the  $K_{1a}$  and  $V_{\max}$  are similar in magnitude then the kinetic pattern will be both first-order and Michaelis-Menten.



Figure 2. Theoretical curves for phase-transfer and non-transfer limited gaseous substrate consumption. The two curves were generated using the PHASIM model. Note that depletion of a saturating concentration of a gaseous substrate is first-order under transfer limited conditions.

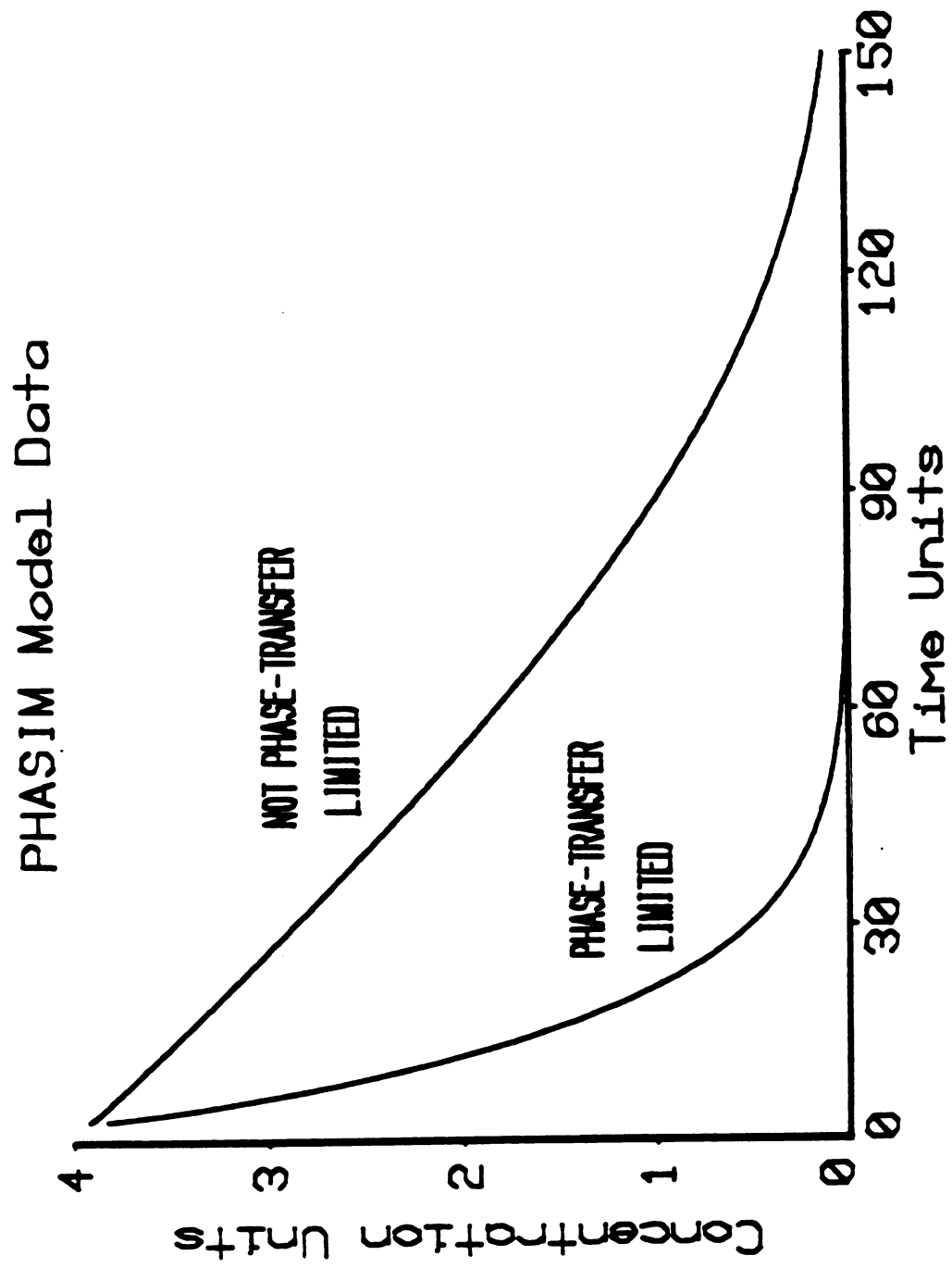


Figure 2

## RESULTS

Consumption of H<sub>2</sub> by rumen fluid, sediment and sludge. Consumption of initially saturating levels of H<sub>2</sub> by undiluted rumen fluid and Portland digester sludge was first-order and thus phase-transfer limited (Figure 3). Coefficients of determination ( $r^2$ 's) of 1.00 were obtained when these data were fitted to one-term exponential equations. H<sub>2</sub> progress curve data for Portland sludge and undiluted rumen fluid could not be fitted to the integrated Michaelis-Menten equation, due to their first-order nature.

We chose dilution as a means of circumventing the transfer limitation. Rumen fluid was diluted to varying degrees with artificial saliva (19), and incubated with a saturating concentration of H<sub>2</sub>. H<sub>2</sub> consumption by 20-fold diluted rumen fluid conformed to Michaelis-Menten kinetics (Figure 3), and thus was not phase-transfer limited. These experiments were repeated several times and it was found that the critical dilution factor required to overcome phase-transfer limited consumption of H<sub>2</sub> was between 10- and 20-fold. The  $V_{\max}$  (corrected for dilution) and  $K_m$  for H<sub>2</sub> consumption by rumen fluid were calculated from the data depicted in Figure 4 to be 28 mM h<sup>-1</sup> and 9.1 uM, respectively.

Hydrogen consumption by undiluted Wintergreen sediment and Holt digester sludge exhibited Michaelis-Menten kinetics (Figure 4). Consumption of added H<sub>2</sub> by sediment was occasionally phase-transfer limited (data not shown), but this was due to the relatively high viscosity of sediment rather than to the presence of a large biological sink. Estimates of  $V_{\max}$  and  $K_m$  for diluted rumen fluid, Holt sludge and

Figure 3. Gaseous phase data for phase-transfer limited (first-order)  $H_2$  consumption by undiluted rumen fluid (URF) and Portland sludge (PS), and non-transfer limited (mixed order)  $H_2$  consumption by 20-fold diluted rumen fluid (DRF). The solid lines are best-fit one-term exponential (undiluted rumen fluid and Portland sludge) and theoretical Michaelis-Menten curves (diluted rumen fluid) calculated from the data.

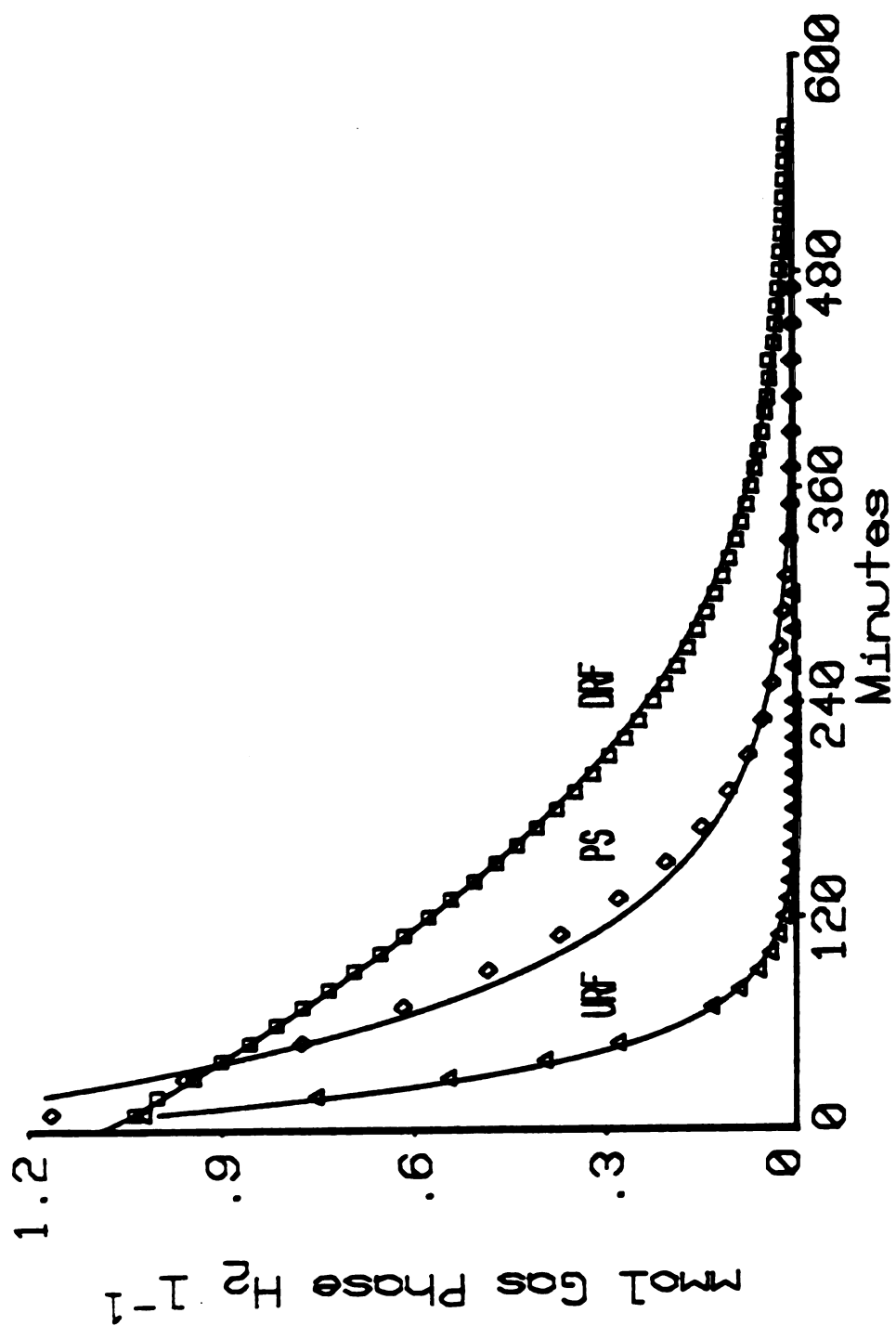


Figure 3

Figure 4. Calculated aqueous phase data for Michaelis-Menten  $H_2$  consumption by diluted rumen fluid (DRF), Holt sludge (HS) and Wintergreen sediment (WS). The solid lines are theoretical curves calculated using the  $V_{max}$  and  $K_m$  estimates obtained from nonlinear analysis of the progress curve data and illustrate the high precision with which the kinetic constants were estimated.

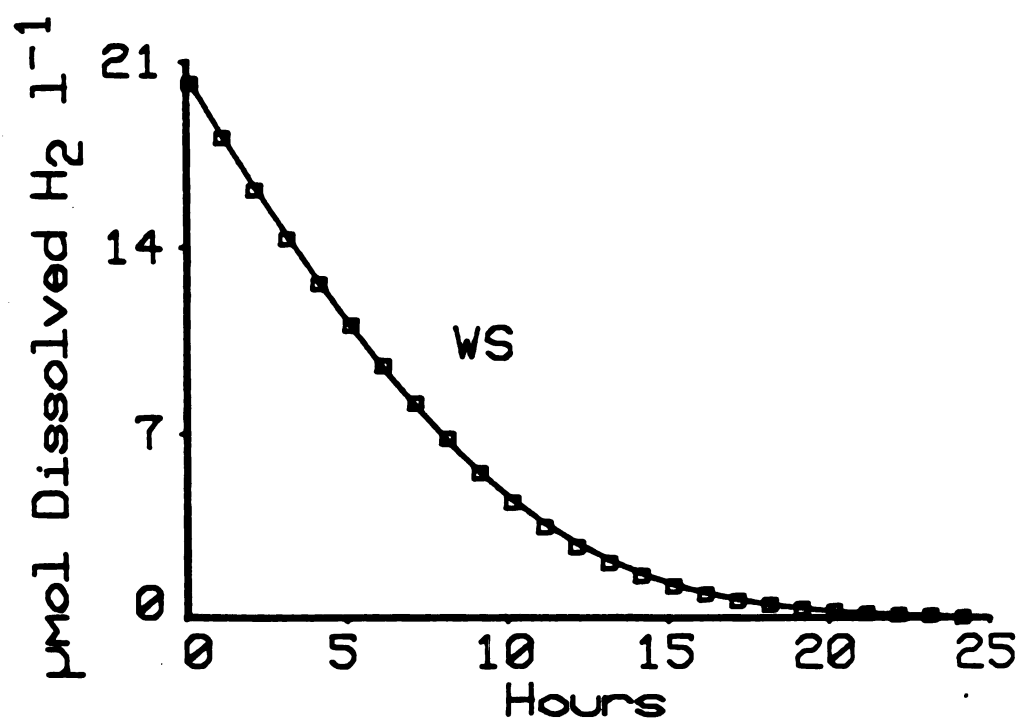
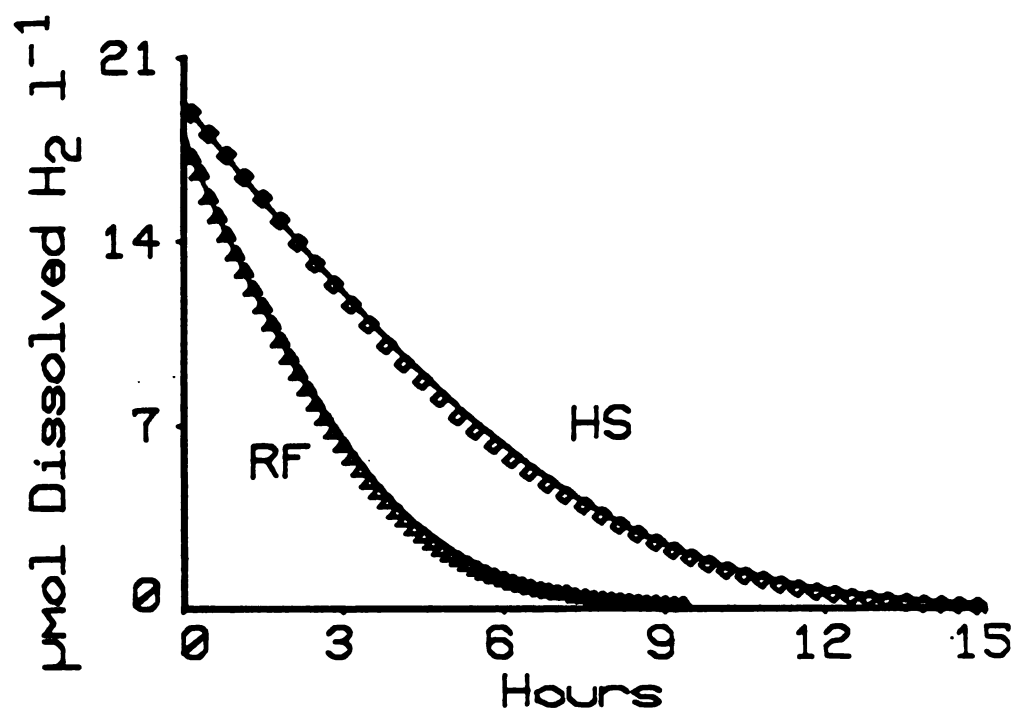


Figure 4

Table 1. Summary of Michaelis-Menten kinetic parameters for rumen fluid, Holt digester sludge and Wintergreen sediment<sup>a</sup>

Anaerobic habitat	$V_{\max}$ (mM h <sup>-1</sup> ) <sup>b</sup>	$K_m$ (uM) <sup>c</sup>
Rumen fluid	28.3 +/- 0.37	9.08 +/- 0.26
	13.3 +/- 0.15	7.19 +/- 0.30
	19.8 +/- 0.71	6.00 +/- 0.64
	14.6 +/- 0.39	4.31 +/- 0.41
	13.5 +/- 0.21	4.23 +/- 0.23
	17.0 +/- 0.70	4.21 +/- 0.50
Holt digester sludge	0.70 +/- 0.01	6.80 +/- 0.30
	4.30 +/- 0.22	6.72 +/- 0.85
	2.98 +/- 0.08	6.22 +/- 0.43
	2.55 +/- 0.04	6.12 +/- 0.26
	2.29 +/- 0.10	5.85 +/- 0.59
	3.26 +/- 0.16	4.42 +/- 0.66
Wintergreen sediment	0.49 +/- 0.01	8.58 +/- 0.49
	0.13 +/- 0.01	5.63 +/- 0.38

<sup>a</sup> Parameter estimate +/- SE\*t-value (95% confidence interval); each pair of parameter estimates were determined from a minimum of 12 data pairs. Note SE's are approximate since the integrated form of the Michaelis-Menten model is nonlinear and were calculated assuming no correlation among the measurement errors.

<sup>b</sup> Values are corrected for any dilutions required to overcome phase-transfer limitations and are for total consumption per unit volume of sample assayed.

<sup>c</sup> Estimates are for H<sub>2</sub> dissolved in the aqueous phase, calculated from gaseous phase data using Bunsen Absorption coefficients for pure water.



Wintergreen sediment were determined via nonlinear regression analysis. The goodness-of-fit of the non-transfer limited  $H_2$  depletion data to the integrated Michaelis-Menten equation is illustrated in Figure 4.  $K_m$  estimates for the anaerobic habitats investigated ranged from 4–9  $\mu M$  dissolved  $H_2$  (Table 1).  $V_{max}$ 's for  $H_2$  consumption by rumen fluid, eutrophic sediment and anaerobic digester sludge varied from 0.1 to 28 mmol total  $H_2$  consumed  $l^{-1} h^{-1}$ , with rumen fluid having the highest potential  $H_2$ -consuming capacity and Wintergreen sediment the lowest (Table 1).

Effect of phase-transfer limitation on  $H_2$   $K_m$ . The error associated with  $H_2$   $K_m$  estimates for a phase-transfer limited system was evaluated from initial velocity data obtained for undiluted and diluted rumen fluid. Each batch of rumen fluid was incubated with five different initial  $H_2$  concentrations. Substrate disappearance was monitored for 2 h, and initial velocity estimates were calculated from slopes of the best-fit curves at  $t=0$ . The apparent  $H_2$   $K_m$  estimates were markedly dependent on the rumen fluid concentration when  $H_2$  consumption was transfer limited (Figure 5). In addition,  $H_2$   $K_m$  estimates were dependent on the initial  $H_2$  concentration; the higher the initial substrate concentration, the greater the apparent  $H_2$   $K_m$ . Once the phase-transfer limitation was overcome,  $H_2$   $K_m$ 's remained relatively constant with increasing dilution (Figure 5) and their values were independent of the initial  $H_2$  concentration as expected.

Influence of endogenous  $H_2$  production on  $V_{max}$  and  $K_m$ . The effect of endogenous  $H_2$  production on  $V_{max}$  and  $K_m$  estimates was investigated using the PHASIM model. Several simulations were run using the same  $V_{max}$  and  $K_m$  values, but with increasing linear rates of  $H_2$  production (Figure

Figure 5. Dependence of apparent  $H_2$   $K_m$  on magnitude of the biological sink under phase-transfer and non-transfer limited conditions. Points are  $K_m$  estimates calculated from both linear and non-linear analyses of 5 initial velocity- $H_2$  concentration data pairs. Along with apparent  $K_m$ 's determined from initial-velocity experiments are plotted  $K_m$  estimates obtained from progress curves performed at dilutions of 20 or greater, to demonstrate equivalence of these two kinetic approaches once  $H_2$  consumption is not phase-transfer limited.

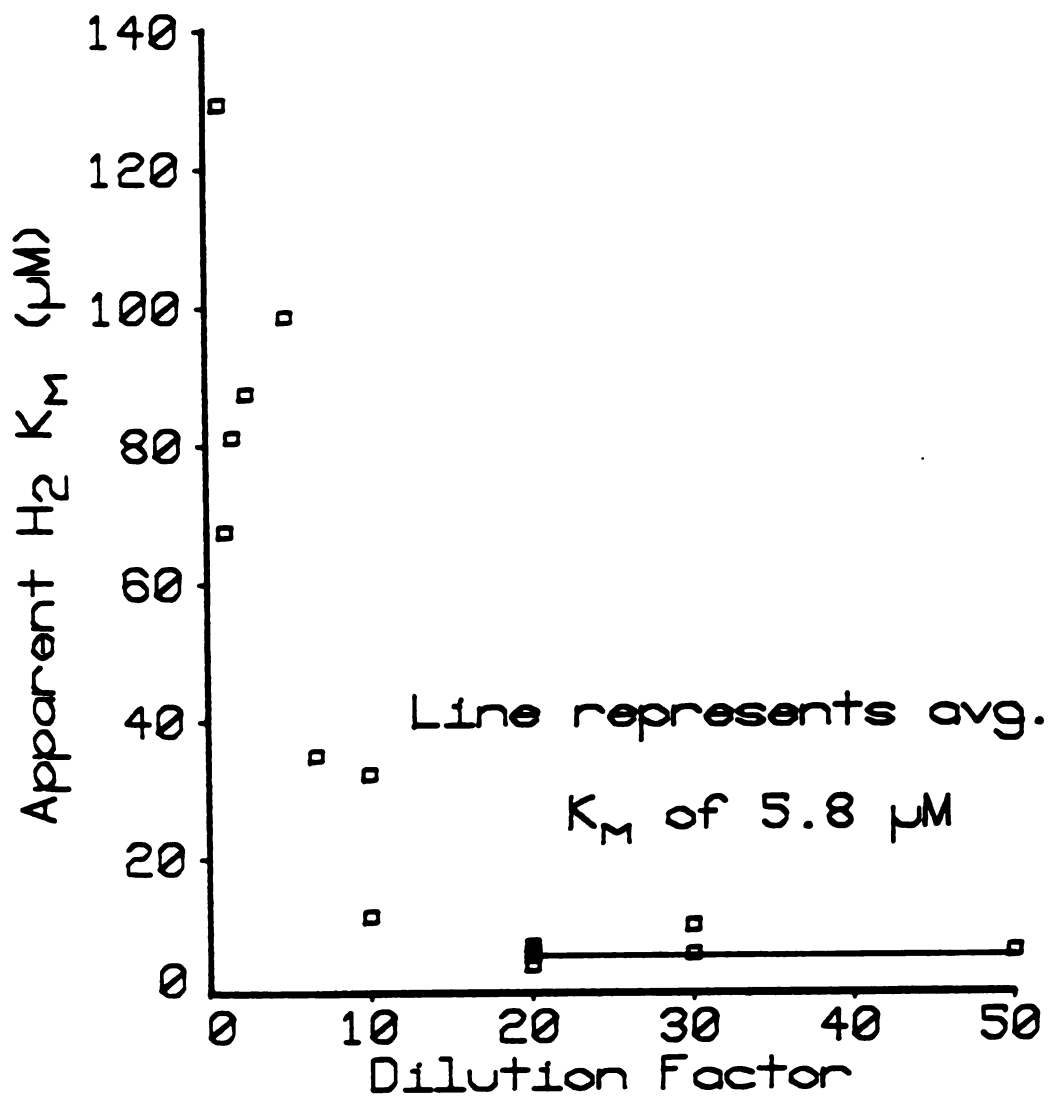


Figure 5

Figure 6. Effect of an increase in endogenous substrate production (A) and an increase in  $V_{\max}$  with time (B) on Michaelis-Menten progress curves. All theoretical curves were generated by PHASIM for gaseous substrate consumption under non-transfer limited conditions. The lowest curve in (A) is the case for no endogenous  $H_2$  production with the succeeding curves above this one representing linear endogenous  $H_2$  production rates equal to 5, 10, 15 and 20% of the  $V_{\max}$  for substrate consumption. The uppermost curve in (B) is identical to the lowest curve in (A) and represents the situation where  $V_{\max}$  remains constant over the course of the progress curve. The lower succeeding curves depict the patterns of substrate consumption where  $V_{\max}$  doubles within 100, 75, 50 and 25% of the total time required for the control progress curve to be 99% complete.

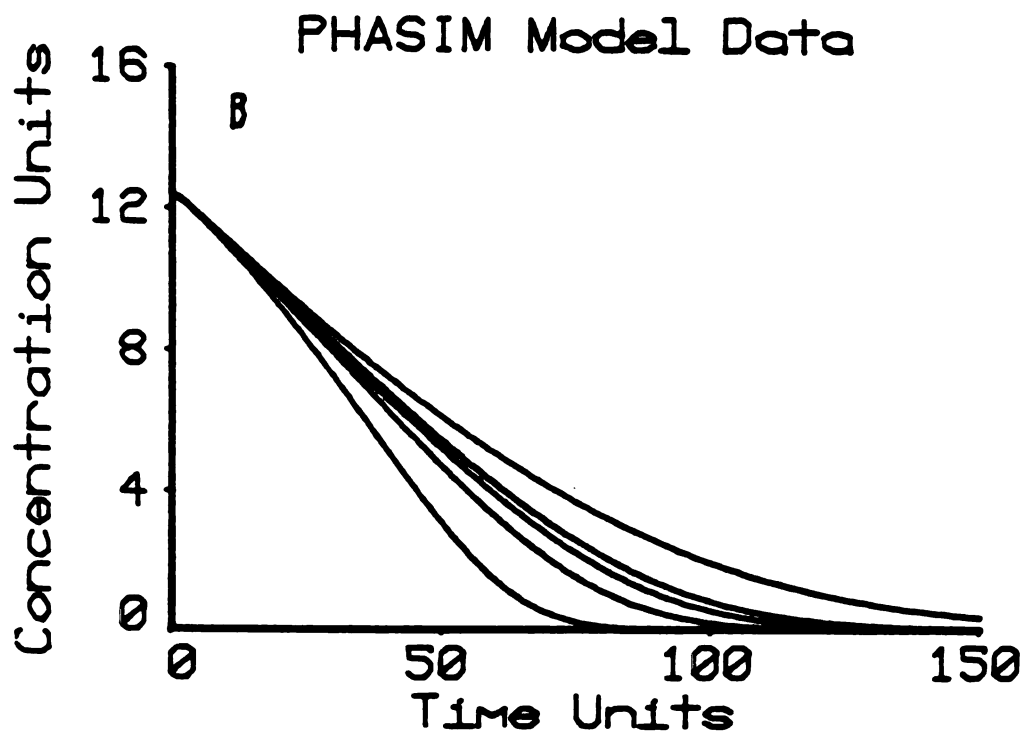
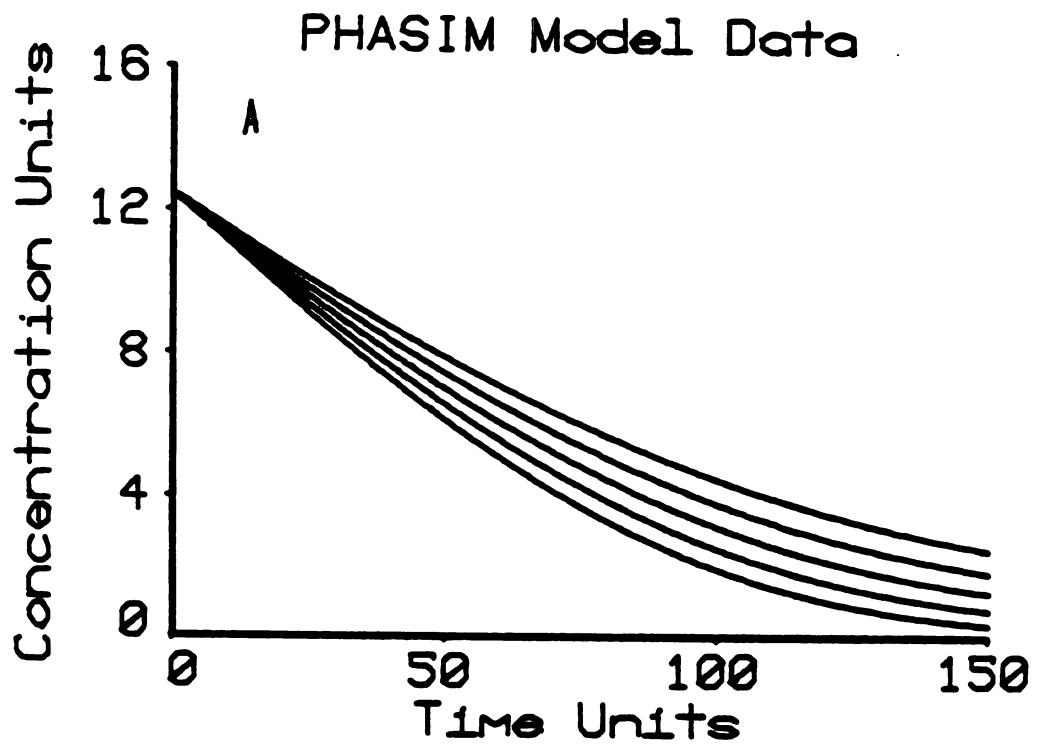


Figure 6

6A). After the simulated data were generated they were analyzed, using the same non-linear regression program employed in analyzing experimental data, to obtain estimates of the kinetic parameters. Rates of endogenous production that were a greater percentage of the maximum rate of substrate consumption produced less error in estimates of  $V_{\max}$  than in  $K_m$  (Figure 7). The apparent  $K_m$ 's increased with increasing rates of endogenous substrate production, whereas apparent  $V_{\max}$ 's decreased with increasing rates of substrate production. In the absence of endogenous substrate production, the kinetic parameters calculated from simulated data equalled the parameter values plugged into the PHASIM model for that particular simulation.

In order to assess the error in calculated  $V_{\max}$  and  $K_m$  estimates for filtered rumen fluid, arising from endogenously produced  $H_2$ , rates of  $H_2$  production were determined for this methanogenic habitat. These rates were subsequently used to calculate potential errors in the kinetic parameters using Figure 7. Undiluted rumen fluid (500 ml) was incubated in the gas-recirculation system, and  $H_2$  and  $CH_4$  concentrations were monitored (Figure 8). Best-fit curves were calculated for the  $CH_4$  data and the first-derivatives of these curves were evaluated at times when endogenous  $H_2$  concentrations were measured. Endogenous rates of ruminal  $H_2$  production were calculated by multiplying calculated  $CH_4$  production rates by 4, and then assuming that 100% of total  $CH_4$  production derives from chemolithotrophic methanogenesis (10). Rates of  $H_2$  production for undiluted rumen fluid, over the period of time the  $H_2$  pool size was relatively constant (Figure 9), ranged from 0.7-0.9  $\mu M h^{-1}$  (Figure 8). These rates equal 4% and 5%, respectively, of the average ruminal  $V_{\max}$  for  $H_2$  consumption. Thus, potential errors

Figure 7. Errors in apparent  $V_{\max}$  (A) and  $K_m$  (B) resulting from concomitant endogenous  $H_2$  production during the course of progress curve experiments. Each theoretical curve was generated from 60 separate simulations, all of which were run under non-transfer limited conditions.

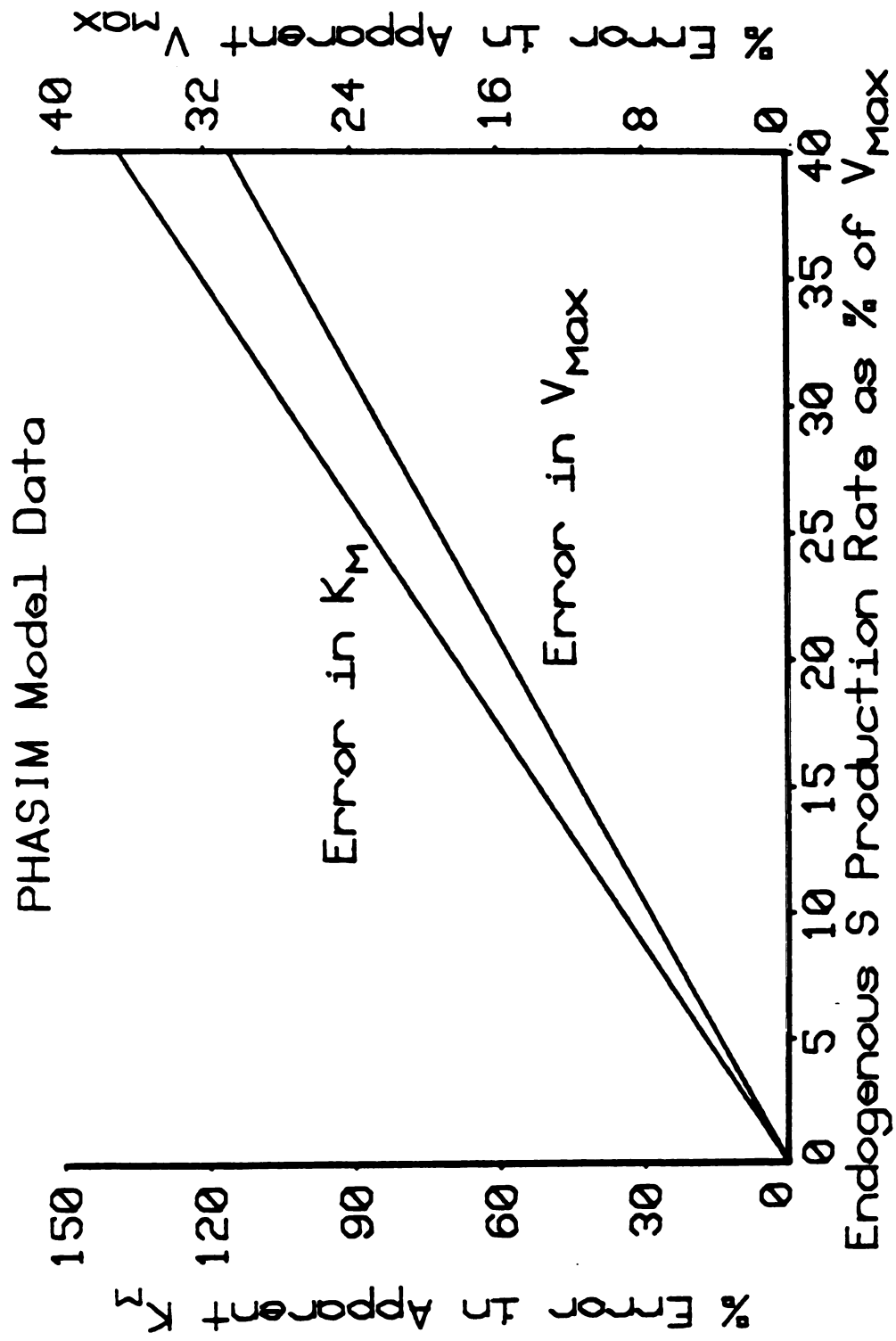


Figure 7



Figure 8.  $\text{CH}_4$  production data and calculated rates of  $\text{H}_2$  production for undiluted rumen fluid. Rates of  $\text{H}_2$  production were calculated by fitting a power curve to the  $\text{CH}_4$  production data, differentiating, and then multiplying the calculated instantaneous  $\text{CH}_4$  production rates by 4. Early high rates of  $\text{H}_2$  production partially result from prior stripping out of the product and substrate gases during the sparging period (see Materials and Methods), while later rates reflect attainment of near steady-state conditions after  $\text{H}_2$  has again equilibrated between the two phases.

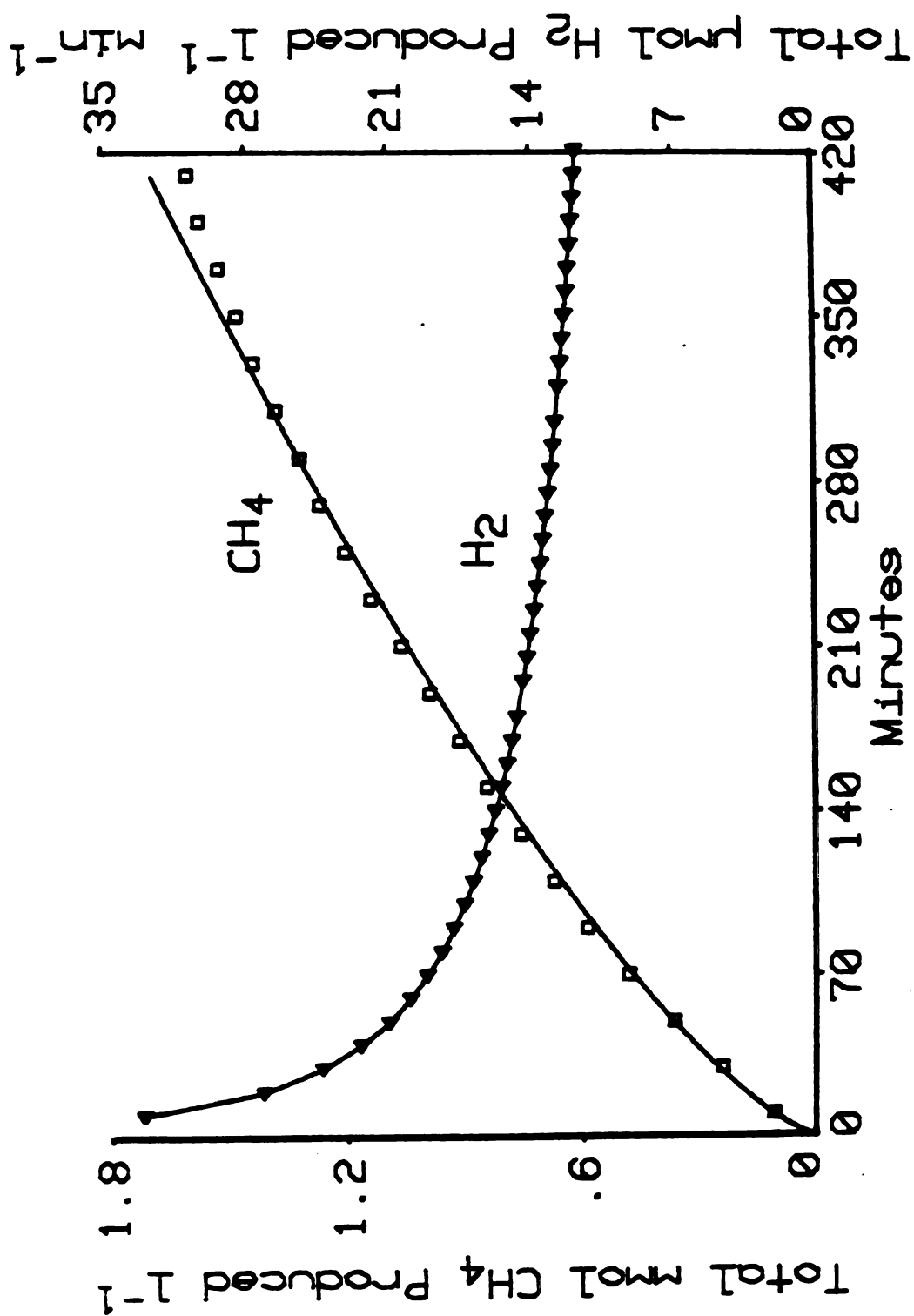


Figure 8

Figure 9. Relationship between endogenously produced  $H_2$  and  $H_2$  concentrations monitored during a progress curve using replicate suspensions of diluted rumen fluid (DRF). Triangles in lower graph are the points at the end of the progress curve that fall within the ordinate-range in which endogenously produced  $H_2$  is plotted.

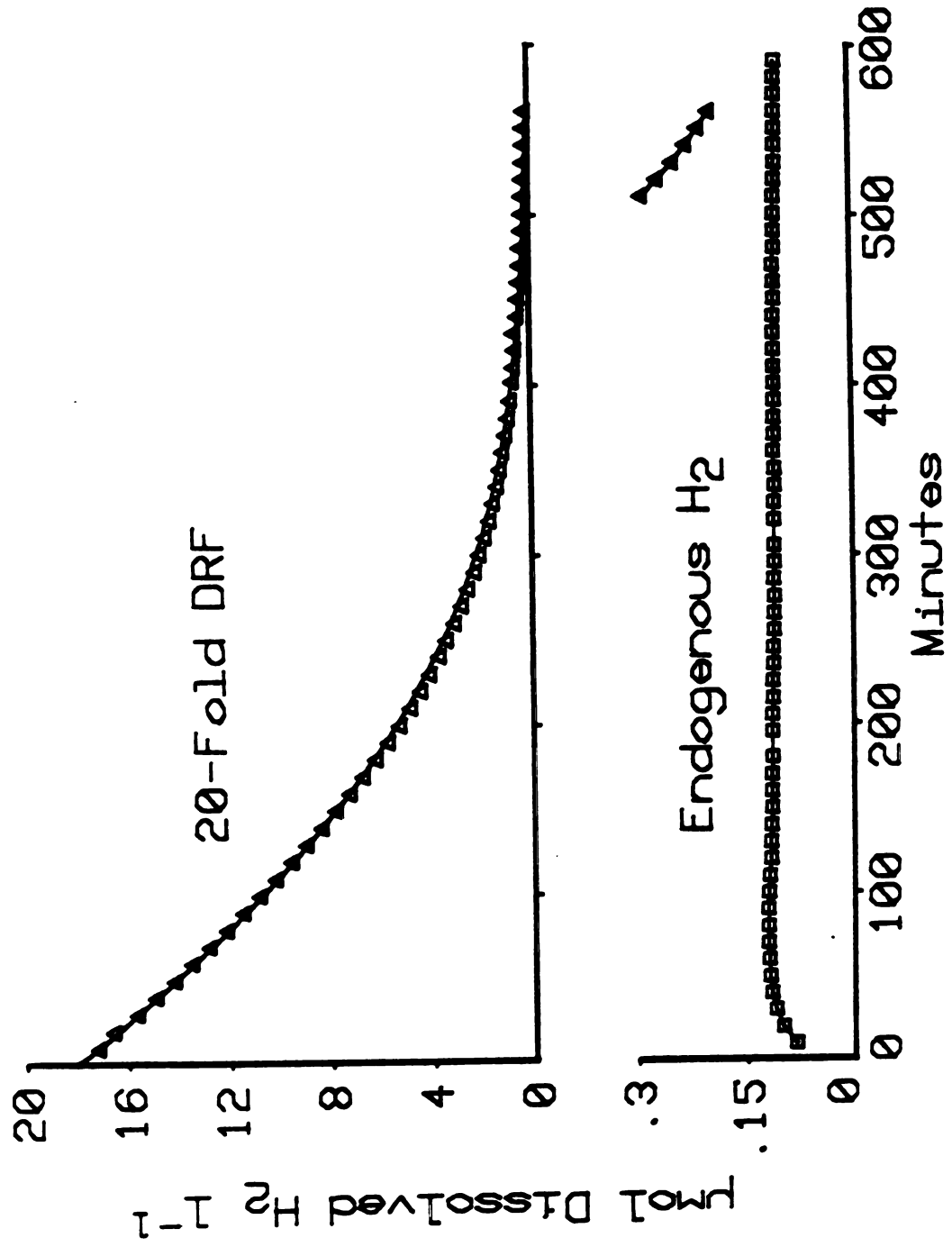


Figure 9

Figure 10. Relationship between endogenously produced  $H_2$  and  $H_2$  concentrations monitored during a progress curve using replicate samples of undiluted Holt sludge (HS). Triangles in lower graph are the points at the end of the progress curve that fall within the ordinate-range in which endogenously produced  $H_2$  is plotted.

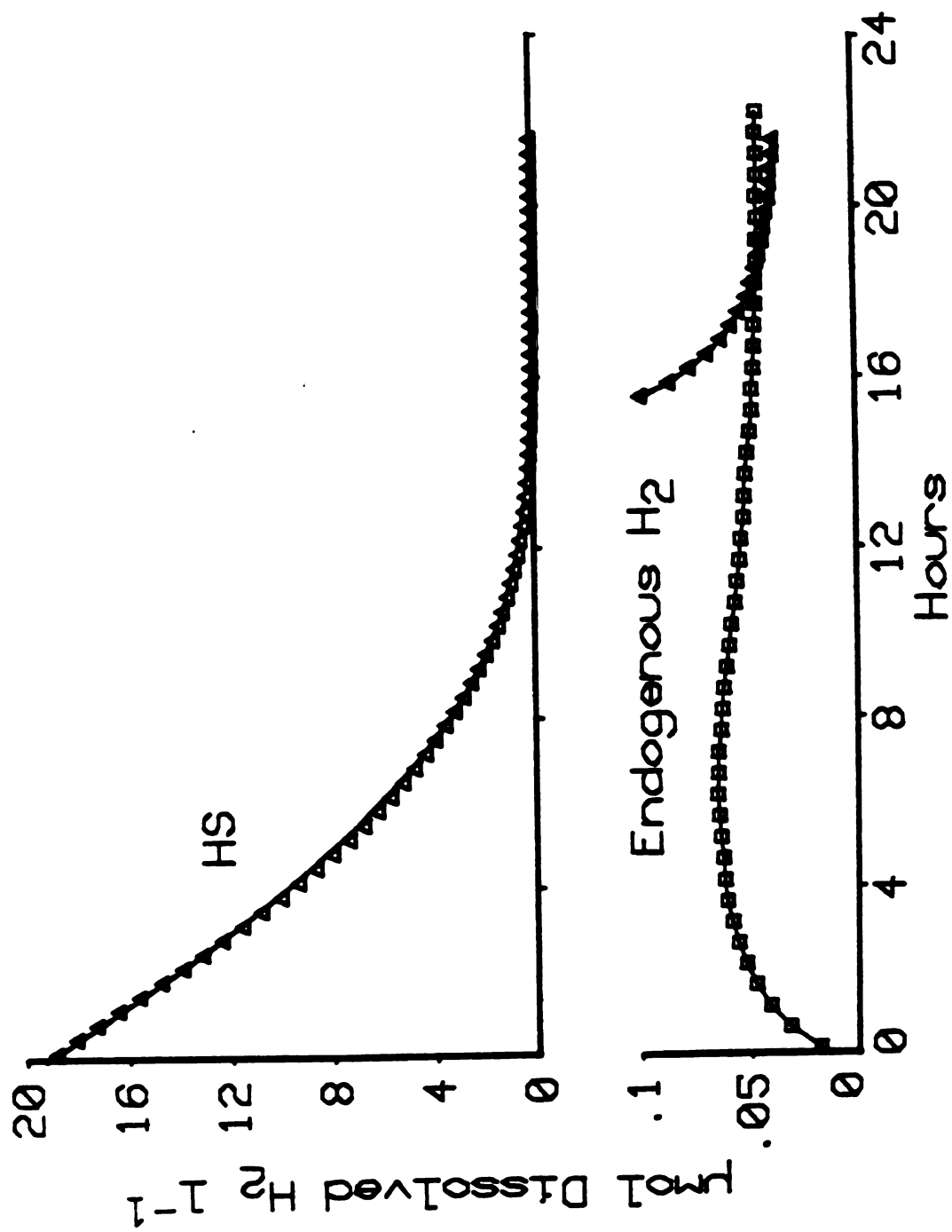


Figure 10

in the  $H_2$   $K_m$  for rumen fluid, after taking into account the possible error associated with the  $V_{max}$  estimate, ranged from 10-15%. In similar experiments with Holt sludge and Wintergreen sediment, we calculated maximum potential errors in  $H_2$   $K_m$ 's to be less than 10%.

Steady-state dissolved  $H_2$  concentrations were typically 0.1  $\mu M$  for diluted rumen fluid (Figure 9), 0.05  $\mu M$  for Holt sludge (Figure 10), and generally less than 0.01  $\mu M$  for Wintergreen sediment (when detectable). These are 40-fold or more below the  $H_2$   $K_m$  estimates. Figures 9 and 10 also show that added  $H_2$  is consumed until the concentration reaches the endogenous  $H_2$  level found in replicate batches.

Effect of growth on  $H_2$   $V_{max}$  and  $K_m$  estimates. The effect of growth on the shape of non-transfer limited  $H_2$  consumption was examined using the PHASIM model. Again, the kinetic parameters, with the exception of  $V_{max}$ , were constant for all simulations. For each simulation, the initial  $V_{max}$  was the same, but the doubling time for  $V_{max}$  was decreased for successive simulations. If  $V_{max}$  increased by a minimum of 25%, during the course of a simulated progress curve, then enough sigmoidicity was introduced into the data to prevent non-linear regression analysis using the Michaelis-Menten kinetic model (Figure 6B). We never observed a degree of sigmoidicity in our  $H_2$  consumption experiments, using rumen fluid, sediment or sludge, that prevented analyzing the progress curve data using our nonlinear regression program.

## DISCUSSION

When consumption of a gaseous substrate is phase-transfer limited, then the kinetic pattern is dictated by the rate of absorption of the gas. According to the fluid-film theory (23,31), the absorption rate of a gas by a liquid is linearly dependent on the difference between the equilibrium concentration of the gas and its concentration in the bulk of the liquid phase. If the solubility of the gaseous substrate is low, such as is the case for  $H_2$ , then disappearance of the gas from the gaseous phase is approximately first-order, regardless of the kinetic nature of substrate consumption by cells in the liquid phase.  $H_2$  consumption by undiluted rumen fluid, using our incubation system, was phase-transfer limited.  $H_2$  consumption could not be saturated and apparent  $K_m$ 's, determined from initial velocity experiments, exhibited a strong dependence on both the initial substrate concentration and the magnitude of the biological sink. Once the transfer limitation was overcome,  $H_2$  consumption could be saturated and  $K_m$ 's became relatively constant (5.8  $\mu M$ ).

When gaseous substrate consumption is not phase-transfer limited, then gaseous phase concentrations may be multiplied by a partition coefficient to obtain aqueous phase substrate concentrations, because the rate-limiting step is biological consumption and not mass-transport. We have found agreement between steady-state aqueous phase  $H_2$  concentrations calculated from gaseous phase data (Figures 9 and 10) and dissolved  $H_2$  measured using a previously published technique (24). Similar results have also been obtained for  $H_2$  progress curve



experiments. Measurement of gaseous phase components (albeit indirect) is usually preferred since it generally can be done with greater ease and precision.

H<sub>2</sub> consumption by eutrophic Wintergreen sediment and Holt sludge generally followed Michaelis-Menten kinetics. Non-transfer limited behavior by Holt sludge was likely a result of its unusually long retention time (38 days). Experiments with other sludges (e.g., Portland), having more typical retention times (17-21 days), all exhibited phase-transfer limited consumption of H<sub>2</sub>. The H<sub>2</sub> K<sub>m</sub>'s for Wintergreen sediments and Holt sludge fell within the range observed for rumen fluid (Table 1). The H<sub>2</sub> V<sub>max</sub>'s for total consumption by sediments and Holt sludge were approximately 100- and 10-fold lower, respectively, than V<sub>max</sub>'s for rumen fluid (Table 1). The difference among the H<sub>2</sub> V<sub>max</sub>'s is partially explained by the different temperatures of incubation. But the broad range among the V<sub>max</sub> estimates primarily reflects the densities of H<sub>2</sub> consuming organisms, principally methanogens, present in these habitats. The V<sub>max</sub>'s for rumen fluid are probably underestimates since solid particulates were partially removed by sampling through cheese-cloth. The variability among the H<sub>2</sub> K<sub>m</sub> estimates probably reflects variability in endogenous H<sub>2</sub> production rates, since the precision of K<sub>m</sub> estimates was high (Table 1). This is supported by the reproducibility of K<sub>m</sub> estimates determined for Methanospirillum hungatei JF-1 and Desulfovibrio G11 (CV's of approximately 10%, versus CV's of about 30% overall for the three habitats studied, unpublished results).

Our H<sub>2</sub> K<sub>m</sub>'s for rumen fluid and eutrophic sediments are slightly higher than previously published estimates. Strayer and Tiedje's (29)

average  $K_m$  for  $H_2$  consumption by Wintergreen sediment was 2.5  $\mu M$ . Hungate et. al. (13) reported an average ruminal  $H_2$   $K_m$  of 1  $\mu M$ . In a series of competition experiments with  $FeCl_2$ - and  $FeSO_4$ -amended Wintergreen sediments, Lovely et. al. (18) determined  $H_2$   $K_m$ 's for the methanogenic population that agree with our estimates. Mass-transfer resistance probably influenced the above sediment  $H_2$  kinetic experiments to a minor extent since  $H_2$  consuming activity is comparatively low in this methanogenic habitat, and these experiments employed reaction vessels having large surface-to-sediment volume ratios. Inter-phase transport could not have influenced  $H_2$  kinetic experiments performed by Hungate and co-workers (13) since dissolved  $H_2$  was directly measured.

Half-saturation constants in the literature for digester sludge differ markedly compared to  $H_2$   $K_m$  estimates we obtained for anaerobic sludge. Half-saturation constants as high as 96 kPa have been reported for  $H_2$  consumption by anaerobic sludge (26). This is equivalent to 720  $\mu M$  at 25°C and 101 kPa total pressure, assuming the gas and liquid phases were in equilibrium. In a more recent study, Kaspar and Wuhrmann (15) calculated that  $H_2$  consumption by digester sludge was half-saturated at 80  $\mu M$  (11 kPa). The high  $K_m$  estimates for sludge probably were determined under phase-transfer limited conditions. Previous investigators have generally performed initial velocity-type experiments, analyzing their rate data using double-reciprocal plots, to obtain estimates of microbial kinetic parameters. For transfer limited systems, initial velocity experiments can be performed and excellent linear fits obtained when the data are transformed for double-reciprocal analysis, even though the rate data are strictly first-order. This is because the reciprocal of a first-order rate equation is a straight

line. In initial velocity experiments using transfer limited rumen fluid we have repeatedly obtained  $r^2$ 's of 0.99 or better for double-reciprocal analyses of the data, but the parameter values determined for such systems are unrealistically high (Figure 5).

Estimates of  $H_2$  Michaelis-Menten parameters are in error if endogenous  $H_2$  production concomitantly occurs with consumption of added  $H_2$ . Under these conditions, overestimates of  $K_m$  and underestimates of  $V_{max}$  are obtained from analysis of the progress curve data, with  $K_m$  being the more sensitive of the two kinetic parameters. In the present study,  $H_2$   $K_m$ 's were maximally overestimated for rumen fluid by 15% and by 10% for Holt sludge and Wintergreen sediment. These error estimates were calculated using the endogenous  $H_2$  production rates and average  $V_{max}$  estimates for these three habitats and Figure 7. Its interesting to note that differences among the endogenous  $H_2$  levels for rumen fluid, sludge and sediment paralleled the ratios of the  $H_2$   $V_{max}$ 's for these habitats.

Errors in  $H_2$   $K_m$  and  $V_{max}$  estimates are also produced if there is a change in activity (i.e.,  $V_{max}$ ) during a progress curve experiment. In contrast to the effect of endogenous  $H_2$  production, an increase in  $V_{max}$  (i.e., growth) with time results in underestimates and overestimates of  $K_m$  and  $V_{max}$ , respectively, when progress curve data are analyzed. Indeed, if  $V_{max}$  increases by a minimum of 25% during the course of substrate consumption, then the resulting degree of sigmoidicity is sufficient to prevent analysis of the data using the Michaelis-Menten model.  $H_2$  consumption by rumen fluid, Holt sludge and Wintergreen sediment exhibited no apparent sigmoidicity and if  $V_{max}$  increased during the course of any of our progress curve experiments, it was not enough

to generate statistically significant deviations from the Michaelis-Menten kinetic model.

The influence of mass-transport on microbial activity is a general one, affecting both substrate consumption and product formation in multi-phase systems. Thus, half-saturation constants for substrate consumption by either growing (25) or resting cells may have questionable significance unless it was established that conditions were not phase-transfer limited. Phase-transfer considerations are also important to production of gaseous products (e.g.,  $\text{CH}_4$ ,  $\text{N}_2\text{O}$ ,  $\text{N}_2$ ) from either gaseous or non-gaseous substrates. Production of a gaseous product from a gaseous substrate mirrors the kinetic behavior of substrate consumption, whether a phase-transfer limitation is in force or not. On the other hand, appearance of a gaseous product in a headspace is rate-limited if inter-phase transport is slower than the rate this product is formed in the liquid phase from a non-gaseous substrate. PHASIM can be used to model this situation by including a third differential equation to describe non-gaseous substrate consumption and by reversing the order of the variables in the mass-transport terms of the other two differential equations.

Several criteria can be used to assess whether a phase-transfer limitation is in force or not. Firstly, under transfer limited conditions consumption of an initially saturating concentration of the substrate is approximately first-order. Consumption of the substrate must be monitored until it is at least 85% complete to assure that strictly first-order behavior can be distinguished from Michaelis-Menten-type kinetics. Secondly, apparent  $K_m$ 's (obtained from initial-velocity studies) are markedly dependent on the magnitude of the

biological sink (i.e.,  $V_{\max}$ ) and the initial substrate concentration under transfer limited conditions, and experiments should be designed to test for these possibilities. If initial velocity studies are to be relied upon, then the v-gaseous s data pairs should be directly fitted to a rectangular hyperbola (i.e., the Michaelis-Menten equation) or a direct linear plot constructed. Plotting of initial velocity results for gaseous substrate consumption to a linearized form of the Michaelis-Menten equation (e.g., Lineweaver-Burk plot) does not alone allow a distinction to be made between transfer limited substrate consumption and saturation kinetics. On occasion, substrate consumption is nearly transfer limited and progress curve analysis of substrate consumption data yields  $K_m$  estimates greater than the initial substrate concentration. This results from the data fitting first-order decay better than to the Michaelis-Menten model, and is apparent when the data are plotted against the theoretical Michaelis-Menten curve along with the best-fit exponential equation. Lastly, apparent  $K_m$ 's determined from initial-velocity data should decrease with increasing dilutions of the original liquid sample, converging to a constant value once the transfer limitation is overcome.

For kinetic investigations of microbial processes that involve gaseous substrates and products it is easier to monitor changes in the concentrations of these compounds in the gaseous than in the liquid phase. But this is appropriate only when it has been verified by the criteria presented above that a phase-transfer limitation does not exist.

## ACKNOWLEDGEMENTS

We thank Derek Lovely for helpful comments on sediment H<sub>2</sub> kinetics, Mike Klug for making available the facilities of his laboratory at the Kellogg Biological Station in Hickory Corners, MI, and the Department of Animal Science for use of their fistulated cows. This work was supported by National Science Foundation Grants DEB 78-05321 and DEB 81-09994.

## LITERATURE CITED

1. Abram, J. W., and D. B. Nedwell. 1978. Hydrogen as a substrate for methanogenesis and sulfate reduction in anaerobic saltmarsh sediment. *Arch. Microbiol.* 117: 93-97.
2. Abram, J. W., and D. B. Nedwell. 1978. Inhibition of methanogenesis by sulphate reducing bacteria competing for transferred hydrogen. *Arch. Microbiol.* 117: 89-92.
3. Brown, D. E. 1970. Aeration in the submerged culture of micro-organisms, p. 125-174. In J. R. Norris and D. W. Ribbons (eds.), Vol. 2. Academic Press Inc., New York.
4. Bryant, M. P. 1979. Microbial methane production-theoretical aspects. *J. Anim. Sci.* 48: 193-201.
5. Burden, R. L., J. D. Faires, and A. C. Reynolds. 1978. Numerical analysis. Prindle, Weber, and Schmidt, Boston, Mass.
6. Cornish-Bowden, A. 1976. Principles of enzyme kinetics. Butterworths, Inc., Boston, Mass.
7. Czerkowski, J. W., C. H. Harfoot, and G. Breckenridge. 1972. The relationship between methane production and concentrations of hydrogen in the aqueous and gaseous phases during rumen fermentation in vitro. *J. Appl. Bacteriol.* 35: 537-551.
8. Duggleby, R. G., and J. F. Morrison. 1977. The analysis of progress curves for enzyme-catalyzed reactions by non-linear regression. *Biochem. Biophys. Acta.* 481: 297-312.
9. Eisenthal, R., and A. Cornish-Bowden. 1974. The direct linear plot. A new graphical procedure for estimating enzyme kinetic parameters *Biochem. J.* 139: 715-720.
10. Hungate, R. E. 1967. Hydrogen as an intermediate in the rumen fermentation. *Arch. Mikrobiol.* 59: 158-164.
11. Hungate, R. E. 1968. A roll tube method for cultivation of strict anaerobes, p. 117-132. In J. R. Norris and D. W. Ribbons (eds.), Vol., 3B. Academic Press Inc., New York.
12. Hungate, R. E. 1975. The rumen microbial ecosystem. *Ann. Rev. Ecol. Syst.* 6: 39-66.
13. Hungate, R. E., W. Smith, T. Bauchop, I. Yu, and J. C. Rabinowitz. 1970. Formate as an intermediate in the bovine rumen fermentation *J. Bacteriol.* 102: 389-397.
14. Jeris, J. S., and P. L. McCarty. 1965. The biochemistry of methane

- using  $^{14}\text{C}$  tracers. J. Water Poll. Control Fed. 37: 178-192.
15. Kaspar, H. F., and K. Wuhrmann. 1978. Kinetic parameters and relative turnovers of some important catabolic reactions in digesting sludge. Appl. Environ. Microbiol. 36: 1-7.
  16. Kaspar, H. F. and J. M. Tiedje. 1980. Response of electron capture detector to  $\text{H}_2$ ,  $\text{O}_2$ ,  $\text{N}_2$ ,  $\text{N}_2\text{O}$ ,  $\text{NO}$  and  $\text{N}_2$ . J. Chromatog. 193:142-147.
  17. Lovely, D. R., and M. J. Klug. 1982. Intermediary metabolism in a eutrophic lake. Appl. Environ. Microbiol. 43: 552-560.
  18. Lovely, D. R., D. F. Dwyer, and M. J. Klug. 1982. Kinetic analysis of competition between sulfate reducers and methanogens for hydrogen in sediments. Appl. Environ. Microbiol. 43: 1373-1379.
  19. McDougall, E. I. 1948. Studies on ruminant saliva. 1. The composition and output of sheep's saliva. Biochem. J. 43:99-109.
  20. Mountfort, D. O., R. A. Asher, E. L. Mays, and J. M. Tiedje. 1980. Carbon and electron flow in mud and saltflat intertidal sediments at Delaware inlet, Nelson, New Zealand. Appl. Environ. Microbiol. 39: 686-694.
  21. Ngian, R. F., S. H. Lin, and W. R. B. Martin. 1977. Effect of mass-transfer resistance on the Lineweaver-Burk plots for flocculating microorganisms. Biotech. Bioeng. 19:1773-1784.
  22. Phillips, D. H., and M. J. Johnson. 1961. Aeration in fermentations. J. Biochem. Microbiol. Technol. 3: 277-309.
  23. Pirt, S. J. 1975. Principles of microbe and cell cultivation. John Wiley and Sons, Inc., New York, New York.
  24. Robinson, J. A., R. F. Strayer, and J. M. Tiedje. 1981. Method for measuring dissolved hydrogen in anaerobic ecosystems: Application to the rumen. Appl. Environ. Microbiol. 41: 545-548.
  25. Schonheit, P., J. Moll, and R. K. Thauer. 1980. Growth parameters ( $K_s$ ,  $U_{\max}$ ,  $Y_s$ ) of Methanobacterium thermoautotrophicum. Arch. Microbiol. 127: 59-65.
  26. Shea, T. G., W. A. Pretorius, R. D. Cole, and E. A. Pearson. 1968. Kinetics of hydrogen assimilation in the methane fermentation. Water Res. 2: 833-848.
  27. Shieh, W. K. 1979. Theoretical analysis of the effect of mass-transfer resistances on the Lineweaver-Burk plot. Biotech. Bioeng. 21: 503-504.
  28. Smith, P. H., and R. A. Mah. 1966. Kinetics of acetate metabolism



- during sludge digestion. Appl. Microbiol. 14: 368-371.
29. Strayer, R. F. and J. M. Tiedje. 1978. Kinetic parameters of the conversion of methane precursors to methane in a hypereutrophic lake sediment. Appl. Environ. Microbiol. 36: 330-340.
  30. Suijdam, J. C., N. W. H. Kossen, and A. C. Joha. 1978. Model for oxygen transfer in a shake flask. Biotech. Bioeng. 20: 1695-1709.
  31. Thibodeaux, L. J. 1979. Chemodynamics. Environmental movement of chemicals in air, water and soil. John Wiley and Sons, Inc., New York, New York.
  32. Wilhelm, E., R. Battino, and R. J. Wilcock. 1977. Low-pressure solubility of gases in liquid water. Chem. Rev. 77: 219-262.
  33. Winfrey, M. R., D. R. Nelson, S. C. Klevickis, and J. G. Zeikus. 1977. Association of hydrogen metabolism with methanogenesis in Lake Mendota sediment. Appl. Environ. Microbiol. 33: 312-318.
  34. Wolin, M. J. 1974. Metabolic interactions among intestinal microorganisms. Amer. J. Clin. Nutr. 27: 1320-1328.
  35. Zehnder, A. J. B. 1978. Ecology of methane formation, p. 349-376. In R. Mitchell (ed.), Vol 2. Water pollution microbiology. John Wiley and Sons Inc., New York, New York.

**ARTICLE II (CHAPTER II)**

**TURNOVER OF HYDROGEN IN RUMEN FLUID**

by

**Joseph A. Robinson and James M. Tiedje**

#### ABSTRACT

Retention times for ruminal  $H_2$  in vitro were estimated using  $CH_4$  production data and estimates of  $H_2$  kinetic parameters. Retention times calculated by the two methods agreed and ranged from 0.2-2 sec.  $H_2$  retention times for whole rumen contents were about 10-fold lower than for strained rumen fluid. Additions of finely ground hay (10 g) significantly increased the endogenous concentrations of  $H_2$  and the  $CH_4$  production rates. Amendment of rumen fluid with 50 g of hay resulted in a pH drop with a concomitant halt in methanogenesis. In this case the  $H_2$  production rate was at least 10-fold higher than for unamended strained rumen fluid and the endogenous  $H_2$  concentration never peaked.

## INTRODUCTION

The rumen is an anaerobic ecosystem in which virtually all of the  $\text{CH}_4$  produced derives from  $\text{H}_2$  (6,7), in contrast to eutrophic lake sediments and anaerobic sludge where acetate is the principal methanogenic precursor (1,11,14). In all three of these anaerobic ecosystems it is thought that  $\text{H}_2$  exerts control on the rate and fate of organic matter dissimilation through interspecies  $\text{H}_2$  transfer (18). But in the rumen, the influence this process exerts on production of fermentative endproducts is potentially greatest since chemolithotrophic methanogenesis dominates ruminal methanogenic activity. Not since the pioneering work of Hungate and co-workers (6,8) has the kinetics of  $\text{H}_2$  consumption been quantitatively examined in the anaerobic ecosystem. We have reexamined ruminal  $\text{H}_2$  dynamics using improved techniques for estimating  $\text{H}_2$  kinetic parameters and endogenous  $\text{H}_2$  concentrations.

In previous papers, we reported on in situ concentrations of ruminal  $\text{H}_2$  (12) and kinetic parameters for  $\text{H}_2$  consumption by rumen fluid (13). These findings are extended in the present manuscript by presenting data on the turnover of  $\text{H}_2$  in rumen fluid, calculated from  $\text{CH}_4$  production data and estimated  $\text{H}_2$  kinetic parameters. Further, we examined the influence organic loading rates have on endogenous ruminal  $\text{H}_2$  production, and compared endogenous  $\text{H}_2$  production rates for strained rumen fluid versus whole contents. A portion of this work was presented at the XVI Conference of Rumen Function held November 11-13 in Chicago, 1981.

## MATERIALS AND METHODS

Collection of rumen samples. Rumen fluid and whole rumen contents were collected from two fistulated Holstein cows, each fed daily 5.44 Kg of hay ad libitum. Rumen samples were generally obtained in the morning after feeding and used within 30 min of collection. Rumen fluid, strained through two layers of cheesecloth, was collected anaerobically in 100- and 250-ml glass syringes using a previously described procedure (12). Whole contents were taken from the floc near the top of the rumen and transferred to a 1-l flask. The flask was filled to the top and sealed with a rubber stopper. Whole rumen contents were diluted 1:4 with strained rumen fluid so that it could be adequately stirred in our incubation system.

Incubation system. The gas-recirculation system used in this study to measure  $H_2$  and  $CH_4$  has been described in detail elsewhere (13). Briefly, 500 ml of rumen fluid or a mixture of rumen fluid (400 ml) plus whole rumen contents (100 ml) were anaerobically transferred to a 2-l flask which was sealed with a butyl rubber stopper. The flask was subsequently immersed in a 39° C water bath, attached to the gas-recirculation system, and the headspace of the flask purged with anaerobe-purity  $CO_2$  (Matheson Gas Products, Joliet, IL) for 15-30 min. The incubation system was then closed to the atmosphere and the headspace of the flask recirculated using a pump through a 3-ml sampling loop in a microthermistor-equipped gas chromatograph.  $CH_4$  in the same 3-ml gas sample was analyzed in a second gas chromatograph using a flame ionization detector. Details on the gas chromatographs and conditions for analysis employed were provided previously (13).

Aqueous phase  $H_2$  and  $CH_4$  concentrations were calculated from gaseous phase concentrations by multiplying the latter by Bunsen absorption coefficients for  $H_2$  and  $CH_4$  (viz., 0.0167 for  $H_2$  and 0.0248 for  $CH_4$ ;  $T = 39^\circ C$ ) calculated from an empirical equation (17). Total quantities of  $H_2$  and  $CH_4$  were calculated using an equation similar to one that has appeared elsewhere (5).

Endogenous rates of  $CH_4$  production. Rates of  $CH_4$  production were calculated by fitting power curves ( $y = ax^b$ ) to  $CH_4$  appearance data, and then evaluating the first-derivatives of the best-fit curves [ $dy/dx = abx^{(b-1)}$ ] at each time the  $CH_4$  concentration was measured. The  $CH_4$  production rates are for total mol of  $CH_4$  present at each sampling point per unit time, normalized to the volume of sample assayed (viz., 500 ml).

Endogenous rates and retention times of  $H_2$ . Since virtually 100% of ruminal  $CH_4$  derives from chemolithotrophic methanogenesis (6,7), endogenous rates of  $H_2$  production were calculated by multiplying  $CH_4$  production rates by four. Retention times of  $H_2$  in vitro were calculated by dividing these rates into measured  $H_2$  concentrations. Retention times for  $H_2$  were also calculated using  $H_2$  kinetic parameters determined by Robinson and Tiedje for rumen fluid (13). The kinetic parameters were used in the Michaelis-Menten equation, which was in turn used to calculate endogenous  $H_2$  consumption rates. Retention times were estimated by dividing the measured  $H_2$  concentrations by calculated in vitro  $H_2$  consumption rates.

Preparation of ground hay. In some experiments, ground hay was added to 2-1 incubation flasks prior to rumen fluid addition. The flask was vigorously flushed with anaerobe-purity  $CO_2$  before rumen fluid was

transferred into it in order to remove O<sub>2</sub> trapped within the hay. The hay was obtained from the same cutting fed to the fistulated cows, and was ground in a Wiley mill equipped with a 2-mm screen.

## RESULTS

Endogenous CH<sub>4</sub> production. Endogenous CH<sub>4</sub> production was measured for both strained rumen fluid and diluted whole rumen contents. In both cases, CH<sub>4</sub> production showed a curvilinear response with time and was several fold higher for whole rumen contents than for strained rumen fluid (Figure 1). CH<sub>4</sub> production by strained rumen fluid and whole rumen contents was determined to not be mass-transport limited using previously established criteria (13).

Endogenous H<sub>2</sub> production rates and retention times. Endogenous H<sub>2</sub> concentrations were measured concomitantly with CH<sub>4</sub> for both strained rumen fluid and diluted whole rumen contents. The endogenous H<sub>2</sub> concentrations were comparable for both and approximately attained steady-state within 2 h. Rates of endogenous H<sub>2</sub> production were calculated by fitting power curves to the CH<sub>4</sub> production data (Figure 1) and evaluating the first-derivatives of the best-fit equations at each sampling point. These instantaneous CH<sub>4</sub> production rates were then multiplied by 4 to obtain instantaneous H<sub>2</sub> production rates. Endogenous H<sub>2</sub> production rates were approximately constant after 2 hours and were about 2-fold greater for diluted whole rumen contents than for strained rumen fluid (Figure 2). For both diluted whole contents and strained rumen fluid, the initial rapid rise in the H<sub>2</sub> concentration was likely a result of re-equilibration of endogenously produced H<sub>2</sub> with the gaseous phase subsequent to purging of the headspaces.

Under steady-state conditions, the retention time of a fermentation intermediate (e.g., H<sub>2</sub>) may be estimated from its production or



Figure 1. Endogenous CH<sub>4</sub> production by two samples of strained rumen fluid (SRF) and diluted whole rumen contents (WC). Curves drawn through the data points are best-fit power curves ( $r^2$ 's=0.998-0.999).

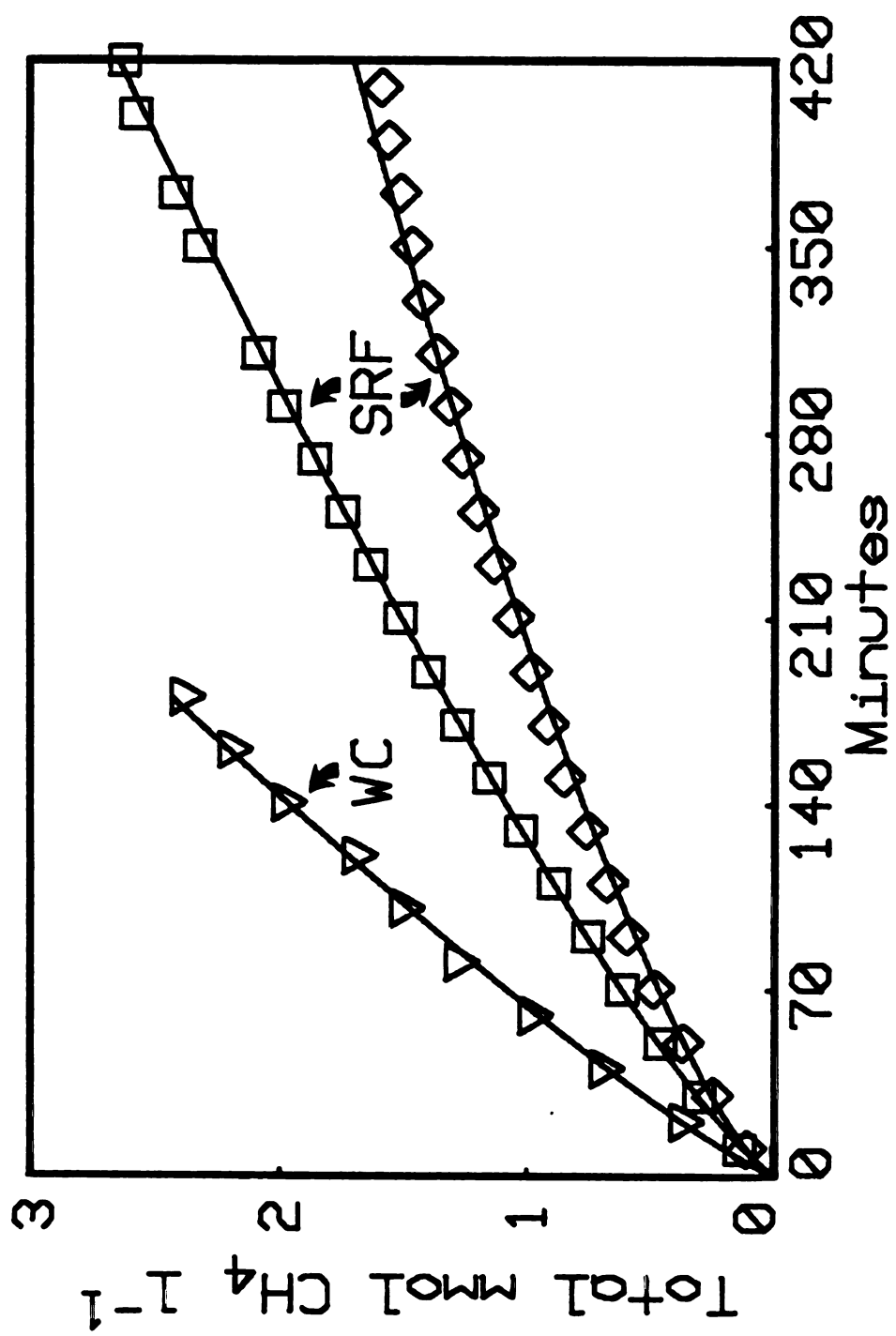


Figure 1

Figure 2. Endogenous dissolved  $H_2$  concentrations and calculated rates of  $H_2$  production for strained (squares) and diluted whole contents (circles). Triangles and diamonds are endogenous  $H_2$  production rates calculated from total  $CH_4$  production data (Figure 1) for diluted whole contents and strained rumen fluid, respectively.

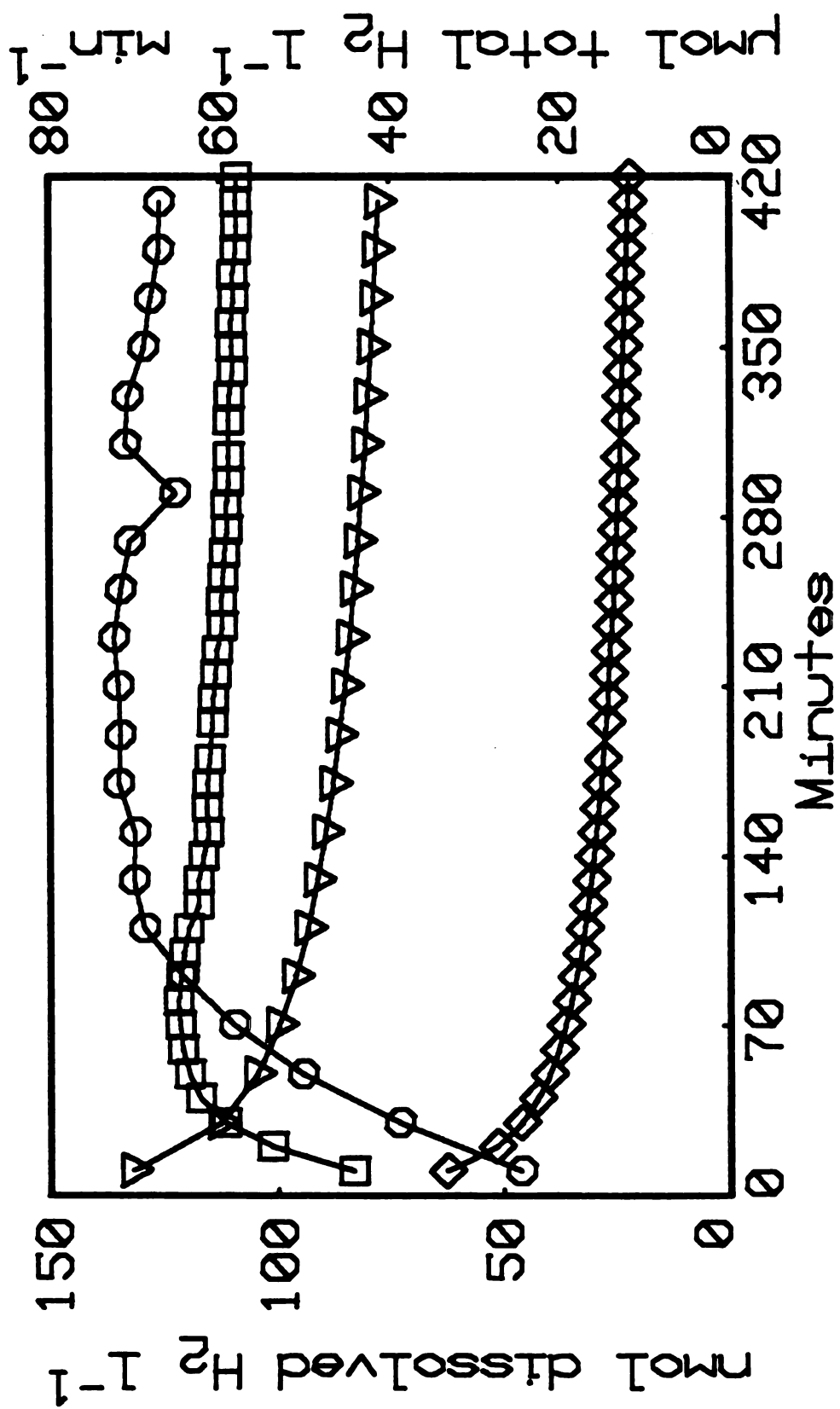


Figure 2

Figure 3. H<sub>2</sub> retention times for strained rumen fluid and diluted whole contents estimated from total CH<sub>4</sub> production rate data (Figure 2). Straight lines parallel to x-axis encompass range of retention times calculated using previously published H<sub>2</sub> kinetic parameters.

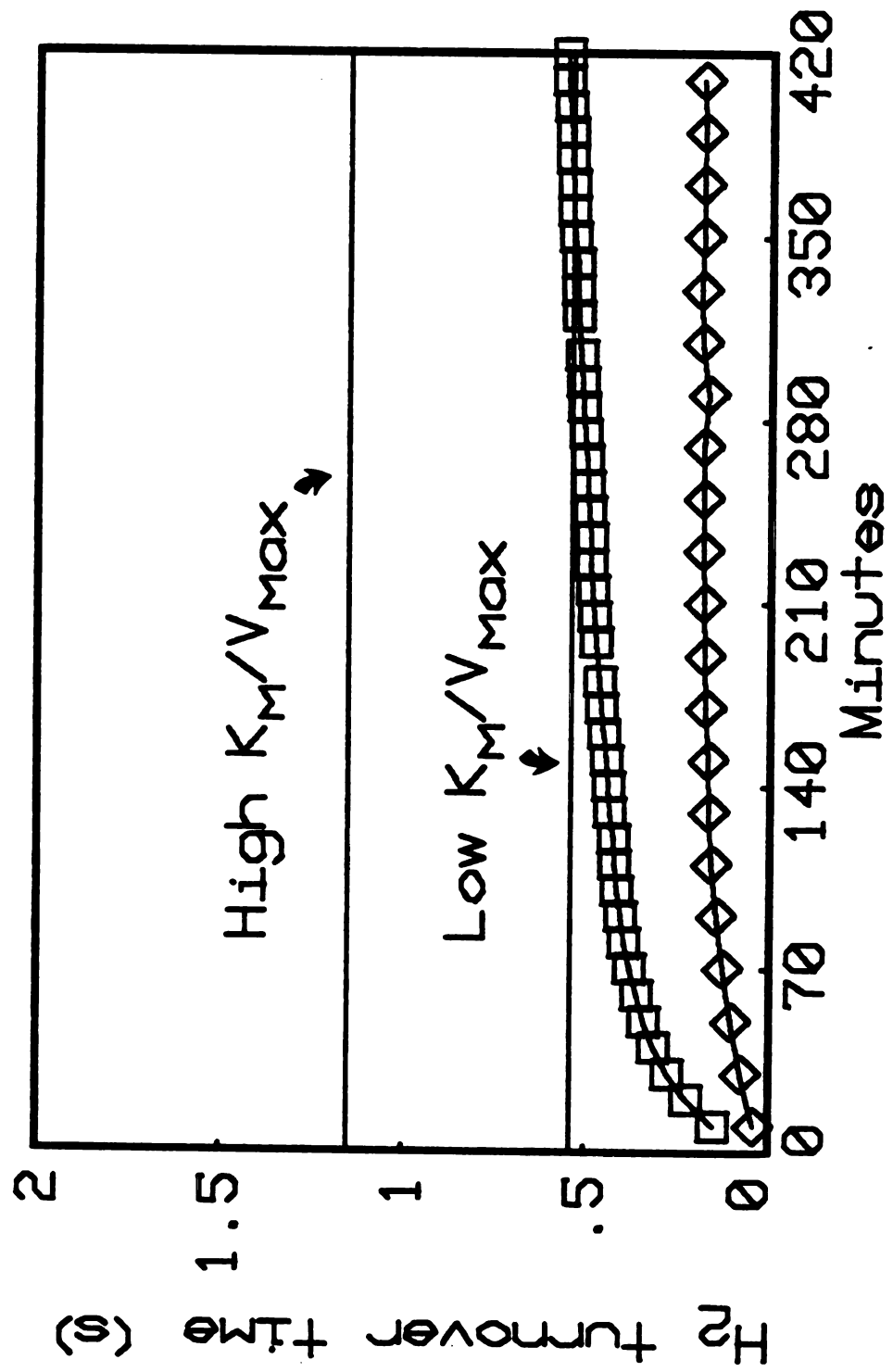


Figure 3

consumption rate. Retention times for endogenously produced  $H_2$  were calculated by dividing measured  $H_2$  concentrations by estimated rates of  $H_2$  production, calculated from the  $CH_4$  data, or by  $H_2$  consumption calculated using previously determined  $V_{max}$  and  $K_m$  estimates (13). Once the  $H_2$  pool approximately attained steady-state,  $H_2$  retention times calculated in the above two ways agreed reasonably well for strained rumen fluid (Figure 3). On the other hand,  $H_2$  retention times for diluted whole rumen contents were slightly shorter than those predicted from estimates of  $H_2$  kinetic parameters for strained rumen fluid.

Influence of organic loading on  $H_2$  production. The response of endogenous  $H_2$  production to organic loading was examined by incubating filtered rumen fluid with 1, 10 or 50 g of ground hay. The endogenous  $H_2$  level in the flask containing 10 g of hay rose approximately 5-fold above endogenous  $H_2$  concentrations measured for unamended rumen fluid (both for diluted whole contents and strained rumen fluid) (Figure 4), and the rate of  $CH_4$  production was correspondingly higher (Figure 5). The endogenous  $H_2$  concentration rose to a maximum (0.57  $\mu M$  dissolved) and subsequently declined. In contrast, when 50 g of hay was incubated with strained rumen fluid the endogenous  $H_2$  concentration increased dramatically and did not peak during the course of the experiment (Figure 4). This particular experiment was prematurely halted because of excess pressure due to outgassing of  $CO_2$  from the liquid phase (the pH had dropped to 5.6).  $CH_4$  production stopped abruptly in the flask containing 50 g of hay (Figure 5). The steady-state  $H_2$  concentration in rumen fluid amended with 1 g of milled hay was comparable (0.12-0.13  $\mu M$  dissolved) with endogenous  $H_2$  concentrations for unamended strained rumen fluid and whole rumen contents (Figure 3). Additional

Figure 4. Dissolved  $H_2$  concentrations for strained rumen fluid amended with 50 (triangles), 10 (circles) or 1 (squares) g of finely milled hay.



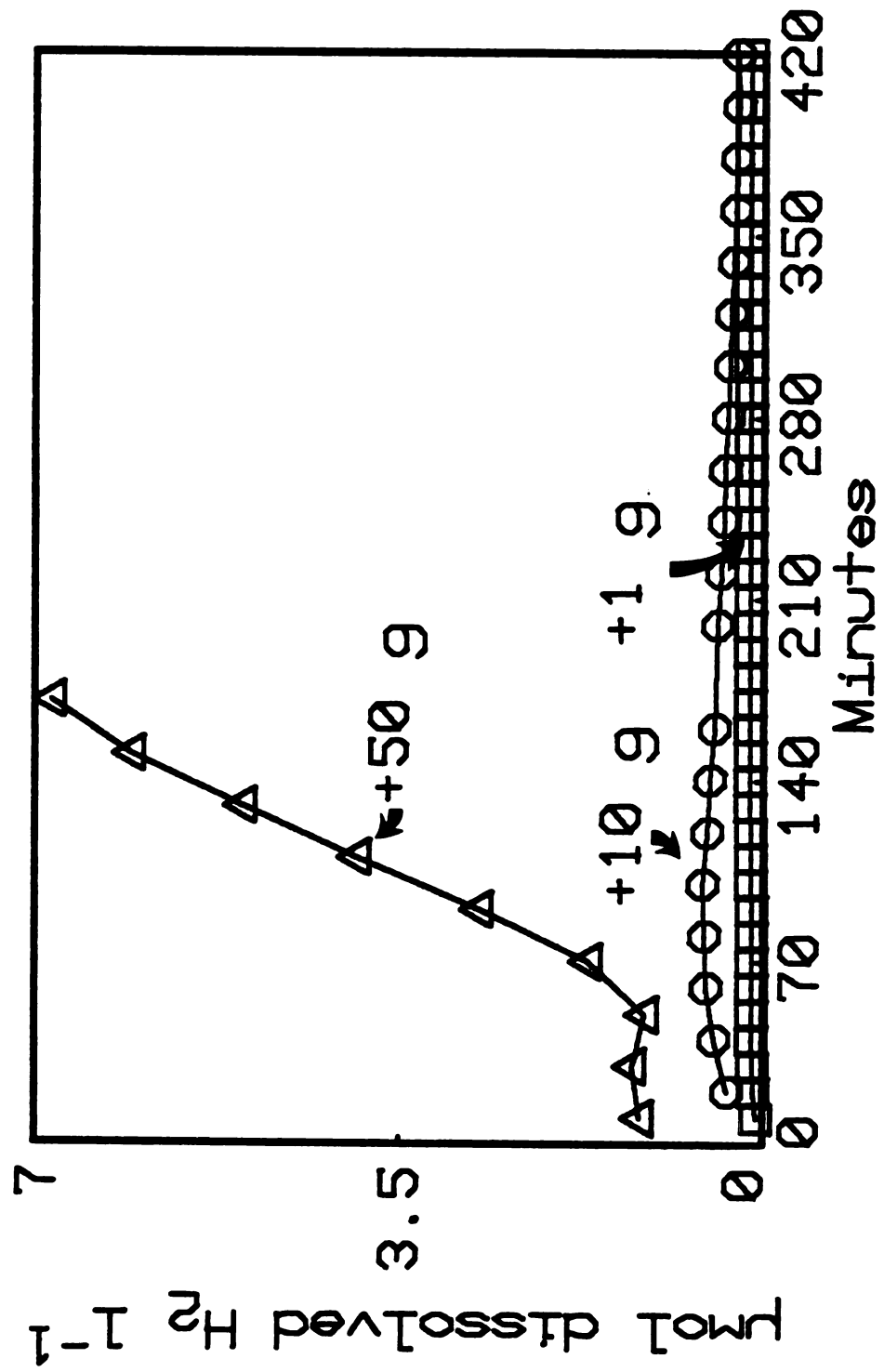


Figure 4

Figure 5.  $\text{CH}_4$  production by strained rumen fluid amended with 50 (triangles), 10 (circles) or 1 (squares) g of finely milled hay.

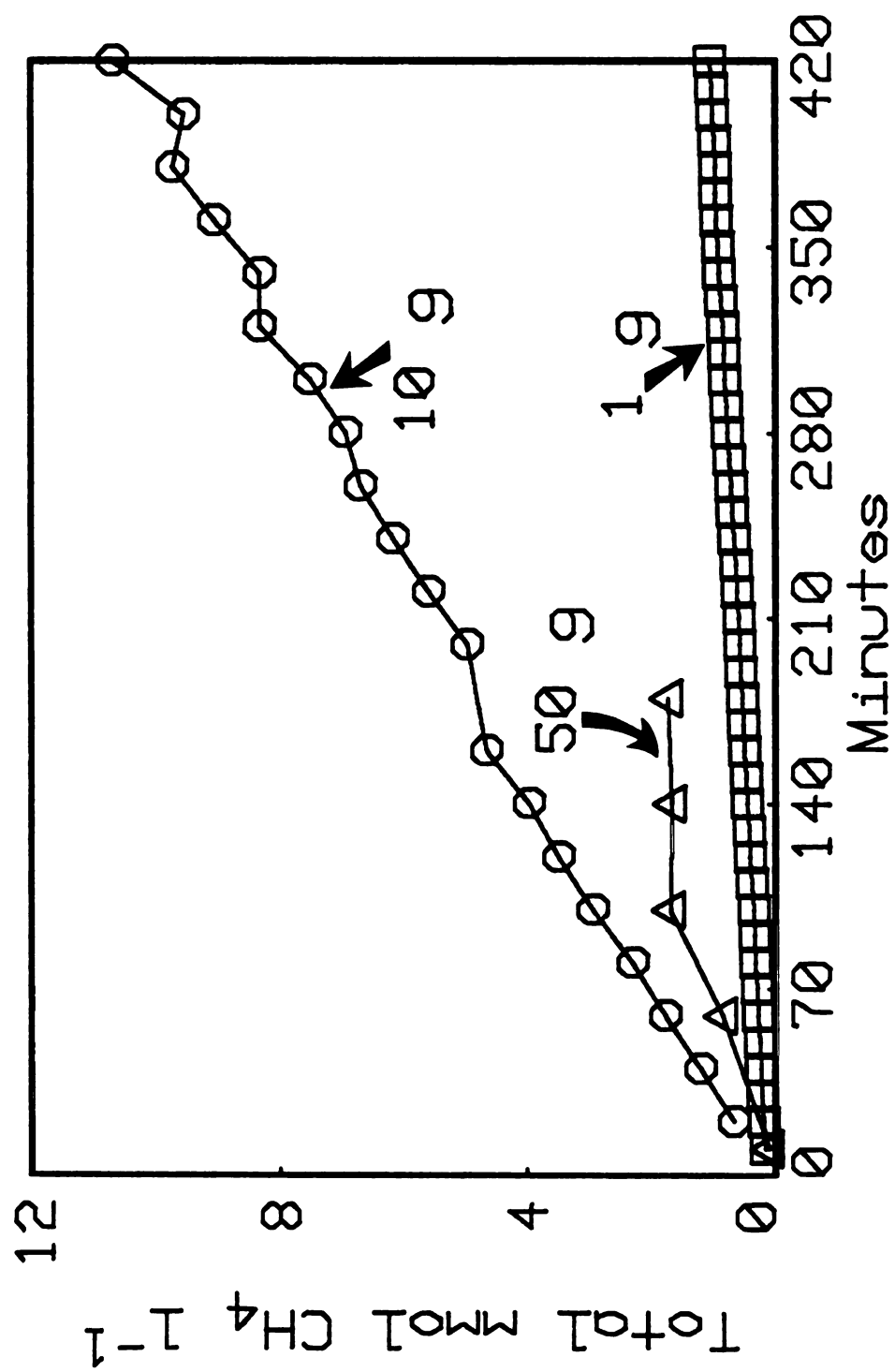


Figure 5

experiments performed using various organic loading rates showed similar trends; additions of 50 or more g of milled hay always resulted in extremely high  $H_2$  concentrations that failed to return to steady-state concentrations.

## DISCUSSION

Under steady-state conditions, the rates of  $H_2$  consumption and production must be equal if the  $H_2$  pool does not vary with time (i.e.,  $dH_2/dt = 0$ ). We observed that the  $H_2$  concentration in unamended strained rumen fluid and diluted whole rumen contents reached approximate steady-state conditions (range: 0.1-0.2  $\mu M$ ) in a relatively short period of time (viz., 2 h). The steady-state was approximate because the  $H_2$  level declined slightly with time. This presumably reflects the gradual depletion of organic substrates in the samples assayed. Qualitatively similar patterns have been observed for endogenous  $H_2$  concentrations measured in fistulated cows maintained solely on a roughage diet; the dissolved  $H_2$  concentration was approximately constant (range: 0.4-2  $\mu M$ ), declining slowly with time after feeding (unpublished results).

The retention times for  $H_2$  we measured in vitro ranged from 0.2-1 sec for strained rumen fluid, and agree well with those calculated from the  $CH_4$  production and dissolved  $H_2$  data of Hungate (6) (Table 1). In a later publication, Czerkawski et. al. studied the kinetics of  $H_2$  consumption and  $CH_4$  production in strained rumen fluid obtained from fistulated sheep. We calculate from their  $CH_4$  production rate and dissolved  $H_2$  data,  $H_2$  retention times ranging from 9-28.4 sec (4). These values are rather high given the low solubility of this gaseous substrate and the characteristically high rates of methane production for undiluted rumen fluid. The  $H_2$  retention times for diluted whole rumen contents were shorter than those for strained rumen fluid presumably reflecting the higher levels of  $H_2$ -consuming biomass present

Table 1. Retention times (sec) of ruminal H<sub>2</sub> calculated from endogenous H<sub>2</sub> production versus H<sub>2</sub> consumption rates.

<u>H<sub>2</sub> production<sup>a</sup></u>	<u>Reference</u>	<u>H<sub>2</sub> consumption<sup>b</sup></u>	<u>Reference</u>
0.82	Hungate (8) <sup>c</sup>	0.08	Hungate (9)
9-28	Czerkowski et. al. (6) <sup>d</sup>	--	--
0.2-1	Present Study	0.8-2	Robinson and Tiedje (12) <sup>e</sup>

<sup>a</sup>Calculated by dividing dissolved H<sub>2</sub> concentration by H<sub>2</sub> production rates (methane production rates x 4).

<sup>b</sup>Calculated by dividing estimated H<sub>2</sub> K<sub>m</sub>'s plus endogenous H<sub>2</sub> concentrations by estimates of H<sub>2</sub> V<sub>max</sub>'s.

<sup>c</sup>Turnover times calculated from entries in Table 1 (8) for experiments where substrates were not added.

<sup>d</sup>Calculated from entries in Table 2 (6) for experiments where rumen fluid was not incubated with added H<sub>2</sub>.

<sup>e</sup>Estimated from H<sub>2</sub> kinetic parameters for strained rumen fluid in Table 1 (12).

in the former.

The above retention time estimates are for  $H_2$  production, calculated from  $CH_4$  production data assuming that 100% of the ruminal  $CH_4$  derives from chemolithrophic methanogenesis.  $H_2$  retention times may be alternately estimated by calculating endogenous rates of  $H_2$  consumption and dividing endogenous  $H_2$  concentrations by these calculated rates. Using the derivative form of the Michaelis-Menten equation, estimates of  $V_{max}$  and  $K_m$  for ruminal  $H_2$  consumption previously obtained (13), and  $H_2$  concentrations measured in vitro, we calculated  $H_2$  retention times similar to those estimated from our in vitro  $CH_4$  production data (Table 1). In a review on the rumen microbial ecosystem (7), Hungate calculated a turnover rate constant for  $H_2$  of  $710 \text{ min}^{-1}$ , which is equivalent to a retention time of 0.08 sec. This value is 10-fold less than the average retention time calculated from Hungate's  $CH_4$  production and  $H_2$  concentration data (6), and about 2-fold below our lowest in vitro estimates. But his retention time estimate is comparable in magnitude to retention times (about 0.3 sec) for diluted whole contents once the latter values have been corrected for dilution.

Several investigators (9,10,16) have shown that ruminal fermentative bacteria are nearly evenly distributed between the particulate and fluid phases of whole rumen contents. Assuming this is true for  $H_2$ -consumers as well, then our estimates of total  $H_2$  production rates and calculated retention times for strained rumen fluid were underestimated and overestimated, respectively, by about 50%. Taking this into account, the retention time of  $H_2$  in whole rumen contents should be 0.2-0.3 sec. Its interesting to note that these values are similar to  $H_2$  retention times estimated for diluted whole contents, but





are almost 10-fold greater than retention times (0.03 sec) for diluted whole contents corrected for a dilution factor of four. Taking the above into account, The retention time of ruminal  $H_2$  in situ is likely between 0.03 and 0.3 sec.

The endogenous  $H_2$  pool responds rapidly to increases in rates of  $H_2$  production. We found in vitro that finely ground hay can increase the rate of  $H_2$  production to such an extent that methanogenic activity is saturated and the  $H_2$  pool size increases. The rate of  $H_2$  production for strained rumen fluid amended with 50 g milled hay ( $65 \text{ mM h}^{-1}$ ) was several fold higher than  $H_2$   $V_{\text{max}}$ 's (mean =  $18 \text{ mM h}^{-1}$ ) estimated for rumen fluid obtained from grain-fed cows before feeding (13).

$H_2$ -consuming activity may become transiently saturated in ruminants fed once daily rations relatively high in carbohydrates; the  $H_2$  pool size increases within several hours post-feeding, but declines to pre-feeding steady-state levels within a few hours, presumably after readily degradable materials have been consumed (12). Czerkawski and Breckenridge found that the dissolved  $H_2$  concentration rapidly rose and then peaked in sheep fed a concentrate diet (5). We believe the above observed spikes in the  $H_2$  concentrations result from increased rates of  $H_2$  production that temporarily saturate  $H_2$ -consuming activity.

Fifty g of milled hay added to 500 ml of rumen fluid ( $0.1 \text{ Kg l}^{-1}$ ) is equivalent to a loading rate  $1/4$  of that the fistulated cows received at feeding ( $0.4 \text{ Kg hay l}^{-1}$ ), assuming a total rumen fluid volume of 50 l. As stated above, the endogenous  $H_2$  pool measured in situ for fistulated cows fed a roughage ration did not spike after feeding, remaining approximately constant during the day. In contrast, the endogenous  $H_2$  concentration dramatically increased in strained rumen

fluid amended with 10 g or more of milled hay. The colonizable surface area of the hay used in our loading experiments was much greater than that for unmilled hay, and this greater surface area would be expected to significantly increase the availability of readily degradable materials resulting in greater endogenous  $H_2$  production rates. We have found endogenous  $CH_4$  production rates and steady-state  $H_2$  concentrations in strained rumen fluid amended with unmilled hay to not be significantly different from values for strained rumen fluid alone (data not shown).

If the level of organic loading is high enough (50 g of finely ground hay in this case), then endogenous  $H_2$  levels may exceed by several hundred-fold the normal endogenous  $H_2$  concentrations. In such a case,  $H_2$  is primarily derived from reactions that are exergonic at  $H_2$  concentrations much greater than those required for interspecies  $H_2$  transfer (15). Although we did not measure them directly, rates of acid production were probably high since the pH typically dropped to values of 5.6-6 when 50 g of hay or more was incubated with strained rumen fluid. During the onset of lactic acid acidosis, a high production rate of lactic acid results in a lowering of the ruminal pH to 5.5, which in turn halts methanogenesis (2).

#### ACKNOWLEDGEMENTS

The authors thank R. E. Hungate and R. B. Hespell for discussions on ruminal  $H_2$  kinetics and ruminant metabolism. This work was supported by National Science Foundation grants DEB 78-05321 and DEB 81-09994.

# LITERATURE CITED

1. Cappenberg, T. E., and R. A. Prins. 1974. Interrelationships between sulfate-reducing and methane-producing bacteria in bottom deposits of a freshwater lake. III. Experiments with <sup>14</sup>C labeled substrates. *Antonie van Leeuwenhoek J. Microbiol. Serol.* 40: 457-469.
2. Counotte, G. H. M., and R. A. Prins. 1978/1979. Regulation of rumen lactate metabolism and the role of lactic acid in nutritional disorders of ruminants. *Vet. Sci. Commun.* 2: 277-303.
3. Czerkawski, J. W., and G. Breckenridge. 1971. Determination of concentration of hydrogen and some other gases dissolved in biological fluids. *Lab. Pract.* 20: 403-405, 413.
4. Czerkawski, J. W., C. G. Harfoot, and G. Breckenridge. 1972. The relationship between methane production and concentrations of hydrogen in the aqueous and gaseous phases during rumen fermentation in vitro. *J. Appl. Bacteriol.* 35: 537-551.
5. Flett, R. J., R. D. Hamilton, and N. E. R. Campbell. 1976. Aquatic acetylene-reduction techniques: solutions to several problems. *Can. J. Microbiol.* 22: 43-51.
6. Hungate, R. E. 1967. Hydrogen as an intermediate in the rumen fermentation. *Arch. Mikrobiol.* 59: 158-164.
7. Hungate, R. E. 1975. The rumen microbial ecosystem. *Ann. Rev. Ecol. Syst.* 6: 39-65.
8. Hungate, R. E., W. Smith, T. Bauchop, I. Yu, and J. C. Rabinowitz. 1970. Formate as an intermediate in the rumen fermentation. *J. Bacteriol.* 102: 384-397.
9. Leedle, J. A. Z., and R. B. Hespell. 1980. Differential carbohydrate media and anaerobic replica plating techniques in delineating carbohydrate-utilizing subgroups in rumen bacterial populations. *Appl. Environ. Microbiol.* 39: 709-719.
10. Leedle, J. A. Z., M. P. Bryant, and R. B. Hespell. 1982. Diurnal variations in bacterial numbers and fluid parameters in ruminal contents of animals fed low- or high-forage diets. *Appl. Environ. Microbiol.* 44: 402-412.
11. Lovely, D. R., and M. J. Klug. 1982. Intermediary metabolism in a eutrophic lake. *Appl. Environ. Microbiol.* 43: 552-560.
12. Robinson, J. A., R. F. Strayer, and J. M. Tiedje. 1981. Method for measuring dissolved hydrogen in anaerobic ecosystems: Application to the rumen. *Appl. Environ. Microbiol.* 41: 545-548.

13. Robinson, J. A., and J. M. Tiedje. Kinetics of hydrogen consumption by rumen fluid, anaerobic digester sludge and sediment. Appl. Environ. Microbiol. in press.
14. Smith, P. H., and R. A. Mah. 1966. Kinetics of acetate metabolism during sludge digestion. Appl. Microbiol. 14: 368-371.
15. Thauer, R. K., K. Jungermann, and K. Decker. 1977. Energy conservation in chemotrophic anaerobic bacteria. Bact. Revs. 41: 100-180.
16. Warner, A. C. I. 1962. Some influencing the rumen microbial population. J. Gen. Microbiol. 28: 129-146.
17. Wilhelm, E., R. Battino, and R. J. Wilcock. 1977. Low-pressure solubility of gases in liquid water. Chem. Rev. 77: 219-262.
18. Wolin, M. J. 1979. The rumen fermentation: A model for microbial interactions in anaerobic ecosystems. Adv. Microb. Ecol. 3: 49-77.

**ARTICLE III (CHAPTER III)**

**RESOURCE COMPETITION AMONG SULFATE-REDUCERS  
AND METHANOGENS FOR HYDROGEN**

by

**Joseph A. Robinson and James M. Tiedje**

## ABSTRACT

Michaelis-Menten (uptake) parameters ( $V_{\max}$  and  $K_m$ ) were estimated for various genera of methanogens and strains of sulfate-reducing bacteria from substrate depletion and product appearance data. In addition, Monod growth kinetic parameters ( $\mu_{\max}$ ,  $K_s$  and  $Y_{H_2}$ ) were determined for Desulfovibrio G11 and approximate values obtained for Methanospirillum hungatei JF-1.  $K_m$  estimates for the methanogenic bacteria ranged from a low of 2  $\mu\text{M}$  (Methanospirillum PM1) to 12  $\mu\text{M}$  for Methanosarcina barkeri MS; Methanospirillum hungatei JF-1 and Methanobacterium PM1 had intermediate  $H_2$   $K_m$  values of about 5  $\mu\text{M}$ . Estimates of  $K_m$  for  $H_2$  of Desulfovibrio PS1 and G11 were lower than values for the methanogens, with means of 0.7 and 1.0  $\mu\text{M}$ , respectively. Significant differences were not observed among the  $H_2$   $V_{\max}$  estimates of methanogenic and sulfate-reducing bacteria when these were normalized to total protein. A two-term Michaelis-Menten equation demonstrated that apparent uptake affinities by resting mixtures of sulfate-reducers plus methanogens depended on the ratio of sulfate-reducing activity to total  $H_2$ -consuming capacity. Half-saturation constants for growth-- $K_s$ --of G11 (2-4  $\mu\text{M}$ ) and JF-1 (2-10  $\mu\text{M}$ ) were comparable in magnitude to their  $K_m$  values for  $H_2$  uptake. Maximum specific growth rates and  $Y_{H_2}$  values appeared to be greater for G11 than for JF-1. These kinetic investigations suggest that sulfate-reducers outcompete methanogens for  $H_2$  whether in a resting or growing state when sulfate is not limiting, and suggest that a correlation exists between uptake and growth kinetic parameters for the bacteria studied.

## INTRODUCTION

The ability of sulfate-reducers to outcompete methanogens in both natural habitats and defined anaerobic consortia has been suggested in a number of previous investigations (1,2,6,7,16,17,18,19,32). Greater affinities for  $H_2$  or acetate (1,2,16,18,31), the effect of  $H_2S$  on methanogenic bacteria (7), and bioenergetic reasons (17,34) have all been invoked to explain the apparent competitive advantage sulfate-reducers have over methanogens. Until recently, quantitative data supporting any of these hypotheses were lacking. In the past year, Kristjansson et. al. (15) and Robinson and Tiedje (J. A. Robinson and J. M. Tiedje, Annu. Meet. Am. Soc. Microbiol., 1982, 195, p. 110) reported on  $H_2$   $K_m$ 's for resting cultures of sulfate-reducing and methanogenic bacteria. Additionally, Lovely et. al. (16) determined  $H_2$  kinetic parameters for lake sediments containing sulfate-reducing and methanogenic activities. All of these studies suggest that sulfate-reducers outcompete methanogens for  $H_2$  under resting conditions, given similar levels of biomass, because of their lower  $K_m$  for  $H_2$ .

This manuscript extends the above findings by including more varied groups of  $H_2$ -consuming anaerobic bacteria. Our results substantiate the claim that sulfate-reducers generally will outcompete methanogens for  $H_2$  when sulfate is not limiting. Using a two-term Michaelis-Menten model we were able to predict apparent uptake affinities for  $H_2$  by several mixtures of sulfate-reducing and methanogenic bacteria. Further, this model predicts that differences in  $H_2$   $K_m$ 's between these two functional groups of bacteria significantly affect which group processes the

greater proportion of a given quantity of  $H_2$  only in the mixed- and first-order regions.

Michaelis-Menten parameters may only be used to evaluate competition between sulfate-reducers and methanogens for  $H_2$  when these bacteria are not growing. In order to evaluate competition among growing bacteria, Monod-type kinetic parameters must be estimated. Therefore, we also determined Monod growth kinetic parameters of sulfate-reducers and methanogens growing in batch on limiting  $H_2$ . Robinson and Tiedje (submitted, AEM no. 723) recently demonstrated the feasibility and advantages of using the integrated Monod equation for estimating growth kinetic parameters, particularly for gaseous substrate consumption. We fitted  $H_2$  depletion data to the integrated Monod equation and the estimated parameters predict that sulfate-reducers can outgrow and hence outcompete methanogens for growth-limiting  $H_2$ . These results correlate with conclusions drawn from estimates of uptake parameters determined for these two groups of bacteria.



## MATERIALS AND METHODS

Organisms. Methanospirillum hungatei JF-1, Methanosarcina barkeriMS and Desulfovibrio G11 were obtained from the culture collection of Marvin P. Bryant. Methanospirillum PM1, Methanobacterium PM2 and Desulfovibrio PS2 were gifts from Dan R. Shelton, who isolated these organisms from an anaerobic aromatic-degrading consortium.

Media and growth conditions. The percentage composition of the growth medium was:  $K_2HPO_4$ , 0.15;  $KH_2PO_4$ , 0.3;  $(NH_4)_2SO_4$ , 0.3; NaCl, 0.6;  $MgSO_4 \times 7H_2O$ , 0.12;  $CaCl_2 \times 2H_2O$ , 0.08; trypticase (BBL), 0.2; resazurin, 0.0001; vitamins, 0.01; trace metals, 0.01; cysteine- $Na_2S$ , 0.038; and  $Na_2CO_3$ , 0.2. The vitamin solution contained in mg/l: biotin, 2; folic acid, 2; pyridoxal-HCl, 10; riboflavin, 5; thiamin, 5; nicotinic acid, 5; pantothenic acid, 5; cyanocobalamin, 5; p-aminobenzoic acid, 5; and lipoic acid, 6. The trace metal solution contained the following compounds in g/l:  $ZnSO_4 \times 7H_2O$ , 0.01;  $MnCl_2 \times 4H_2O$ , 0.003;  $H_3BO_3$ , 0.03;  $CaCl_2 \times 6H_2O$ , 0.02;  $CuCl_2 \times 2H_2O$ , 0.001;  $NiCl_2 \times 6H_2O$ , 0.002;  $Na_2MoO_4 \times 2H_2O$ , 0.003;  $FeCl_2 \times 4H_2O$ , 0.15; and  $Na_2SeO_3$ , 0.01. For growth of the two sulfate-reducers (viz., G11 and PS1) the above medium was supplemented with 3.4 g of  $Na_2SO_4$ /l. On occasion, autoclaved clarified rumen fluid (5%) and yeast extract (Difco; final concentration, 0.2 %) were added to the medium to increase cell yields.

The growth medium was prepared under Ar according to the Hungate anaerobic technique (12) and bacteria were routinely cultured in 160-ml serum vials containing 50 ml of medium. Serum vials were sealed with butyl rubber stoppers held in place with aluminum crimp seals. Before

serum bottles were inoculated the headspaces were evacuated and refilled to 2.5 atm several times with an 80% H<sub>2</sub>-20% CO<sub>2</sub> gas mixture. The gas mixture was passed over hot copper filings to remove trace amounts of O<sub>2</sub>. Serum bottles were incubated on their sides on a rotary shaker at 37°C, and the headspaces of the bottles were repressurized approximately every other day. Methanogenic bacteria were transferred weekly, whereas sulfate-reducers were transferred every 2 or 3 days.

Anaerobic diluent. The anaerobic diluent had the following composition in g/l: KH<sub>2</sub>PO<sub>4</sub>, 0.9; NaCl, 0.9; CaCl<sub>2</sub> x 2H<sub>2</sub>O, 0.027; MgCl<sub>2</sub> x 6H<sub>2</sub>O, 0.02; MnCl<sub>2</sub> x 4H<sub>2</sub>O, 0.01; CoCl<sub>2</sub> x 6H<sub>2</sub>O, 0.001; resazurin, 0.001; Na<sub>2</sub>CO<sub>3</sub>, 4; cysteine-HCl, 0.56; and Na<sub>2</sub>SO<sub>4</sub>, 3.4. It was prepared anaerobically under CO<sub>2</sub> and was pipetted into both 160-ml serum vials (100 ml) and 2-l flasks (300 or 500 ml). In some experiments, the Na<sub>2</sub>SO<sub>4</sub> was omitted.

Resting cell suspensions. Cells were harvested in mid- to late-exponential growth (25-50 ml) using an Amicon ultrafiltration cell (Amicon Corp., Lexington, MA). Millipore filters having a 47-mm diameter (type HA; pore size = 0.45  $\mu$ m) were cut to fit the sterile filtration cell (dia. = 45 mm), and the entire assembly flushed with CO<sub>2</sub> for ca. 30 min prior to the addition of cells. Cultures were anaerobically transferred to the filtration cell using pre-flushed plastic syringes. After the 25-50 ml of culture medium was filtered, the cells trapped on the filter were resuspended in an equal volume of the diluent and filtered again. This was repeated once more and the cells were finally resuspended in 10-25 ml of the anaerobic diluent. This cell suspension was then anaerobically transferred to a 2-l flask containing more anaerobic diluent, typically 300 or 500 ml.

Progress curve experiments. Progress curve experiments were initiated by first attaching the 2-l flask to the gas-recirculation used in previous studies (25). At time zero, ultra-high purity  $H_2$  (Matheson, Joliet, IL) was injected into the headspace of the flask. Its concentration, and the concentration of  $CH_4$  (when measured), were monitored at 20, 30 or 60 min intervals. Each progress curve was terminated when the  $H_2$  concentration in the recirculating gas-stream had reached 1-5% of the  $H_2$  concentration at the first time point. For sulfide appearance experiments, a 2-l flask with a stopper pierced by an 11-gauge maleable connector to which was attached a one-way stainless steel stopcock (Popper and Sons, New Hyde Park, NY) was used. The distal end of the maleable connector was immersed several mm below the aqueous-gaseous phase interface in the flask, and samples were withdrawn from the aqueous phase at 60 min intervals using a sterile 3-ml glass syringe. To avoid absorption of  $H_2S$  by the rubber stopper, thin layers of teflon and then Saran were wrapped over that part of the stopper in contact with the headspace of the flask.

All progress curves were run at 37°C.

$H_2$ ,  $CH_4$  and  $H_2S$  measurements.  $H_2$  and  $CH_4$  were measured in the recirculating gas-stream using gas chromatographs equipped with microthermistor and flame-ionization detectors, respectively. The columns used in these GC's and the chromatographic conditions employed have been previously outlined (25). The liquid phase concentrations and total amounts of both  $H_2$  and  $CH_4$  were calculated using equations that have appeared elsewhere (10).

Sulfide dissolved in the aqueous phase was measured using a modification of the Pachmayr method (22). One-ml samples withdrawn from

the 2-1 flask were injected into 25-ml serum vials each containing 20 ml of a 2% Zn acetate solution. Each vial was sealed with a teflon-backed silicon septum, which was in turn held in place with an aluminum crimp seal. Ten ml of the resulting ZnS suspension was transferred to an 18.5-ml screw cap tube, to which was added 1 ml of acidic 0.2% phenylenediamine reagent and 0.1 ml of an acidic 10% solution of  $\text{FeNH}_4(\text{SO}_4)_2 \times 12\text{H}_2\text{O}$ . The screw cap tube was then sealed with a teflon-lined cap and the absorbance of the solution read after 30 min. Sulfide concentrations were determined by comparing absorbance readings with those for a standard curve prepared using a ZnS solution.

The amount of  $\text{H}_2\text{S}$  in the gaseous phase was estimated by first calculating the fraction of total sulfide in the aqueous phase present as  $\text{H}_2\text{S}$  (aq) (the pH of the anaerobic diluent was 6.7) and then dividing this by the Bunsen absorption coefficient for  $\text{H}_2\text{S}$  at  $37^\circ\text{C}$  (31).

Michaelis-Menten progress curve analysis.  $\text{H}_2$  depletion curves were fitted to the integrated form of the Michaelis-Menten equation (8) using nonlinear regression analysis. In addition to estimating  $K_m$  and  $V_{\max}$  in this way, we also treated the initial  $\text{H}_2$  concentration as another parameter (initial state) to be estimated. Details on fitting substrate depletion data to the integrated form of the Michaelis-Menten equation when the initial substrate concentration is unknown are provided in J. A. Robinson's Ph. D. thesis, Michigan State University, East Lansing, 1982, D.A. no. 00-00000.

$\text{CH}_4$  and sulfide appearance data were also fitted to the integrated form of the Michaelis-Menten equation that describes product appearance in the presence of background levels of the product (i.e., progress curves of unknown origin). Equations required for this analysis have

appeared elsewhere (9,20). Provisional estimates of  $K_m$  and  $V_{max}$  for  $CH_4$  and sulfide were calculated from least-squares analysis using a linearized version of the integrated Michaelis-Menten equation for progress curves of unknown origin (20). An initial estimate of the displacement term  $P_0$  (background concentration of product at  $t = 0$ ) was determined by fitting a straight line to the first 3-6 product concentration-t data pairs and extrapolating back to the product concentration axis. The final concentration of sulfide or  $CH_4$  was taken as an estimate of  $S_0$ ;  $S_0$  was not updated.

All  $K_m$  estimates are for the concentrations of  $H_2$ ,  $CH_4$  or sulfide in the aqueous phase that half-saturate activity, whereas  $V_{max}$  estimates are calculated for the total amount of the substrate or product present in the 2-l flask, normalized to the volume of sample assayed.

Co-culture kinetic experiments. Substrate consumption ( $H_2$ ) by two competing organisms having different affinities and maximum potential activities ( $V_{max}$ 's) cannot be described by a one-term Michaelis-Menten model, but may be predicted using a two-term Michaelis-Menten equation. The latter expression only describes substrate consumption when the total number of catalytic units (i.e., cells) is fixed. This expression has the form

$$-dS/dt = V_1S/(K_1 + S) + V_2S/(K_2 + S)$$

where,  $V_1$  and  $V_2$  are the maximum rates of substrate consumption by organisms one (Desulfovibrio G11) and two (Methalospirillum JF-1), respectively. The constants  $K_1$  and  $K_2$  correspond to the half-saturation constants for the two organisms.

For the co-culture kinetic experiments, G11 and JF-1 were grown in the above described medium and filtered separately. Washed cell

suspensions were either (i) mixed in various ratios and added to 2-flasks containing anaerobic diluent or (ii) one organism was added in increasing increments to a flask already containing the other bacterium. For each mixture of G11 plus JF-1,  $H_2$  and  $CH_4$  progress curve data were obtained and analyzed using the same nonlinear analyses applied to progress curve data obtained using G11 or JF-1 alone.

Theoretical curves describing total  $H_2$  consumed and  $CH_4$  plus sulfide produced for resting suspensions of G11 plus JF-1 were calculated by integrating the above equation along with two one-term Michaelis-Menten equations for formation of the products using numerical integration. Parameter values were those estimated from  $H_2$  depletion data for these two  $H_2$ -consuming anaerobes.

Growth kinetic experiments. Estimates of  $Y_{H_2}$ ,  $u_{max}$  and  $K_s$  for  $H_2$  consumption by Desulfovibrio G11 and Methanospirillum JF-1 growing in batch with limiting  $H_2$  were estimated by fitting sigmoidal  $H_2$  depletion data to the integrated Monod equation. Details on fitting substrate depletion data to the integrated Monod equation using nonlinear least-squares analysis has been previously described (Robinson and Tiedje, AEM submitted, ms no. 723). Estimates of  $K_s$  and  $Y_{H_2}$ , analogous with  $K_m$  and  $V_{max}$ , were calculated from aqueous  $H_2$  concentration data and the total amount of  $H_2$  consumed with time, respectively. The parameter  $u_{max}$  may be estimated from aqueous or gaseous data or the sum of these two, since its value does not depend on the solubility of the gaseous substrate (J. A. Robinson, Ph.D. thesis, Michigan State University, East Lansing, 1982).

For growth kinetic studies, 10-25 ml of a mid-exponential culture of either G11 or JF-1 were filtered as above and added to 300 ml of the

growth medium, in which rumen fluid and trypticase were replaced with 0.2% Na acetate. Monod progress curves were initiated and terminated in the same fashion as those progress curves designed to estimate Michaelis-Menten parameters for  $H_2$ . Biomass formation was followed at hourly intervals by measuring protein content of the growth medium, determined using the Lowry assay with BSA as the standard. Cell suspensions were hydrolyzed in dilute alkali (33) before assays were performed.

## RESULTS

H<sub>2</sub> Michaelis-Menten parameters for methanogenic and sulfate-reducing bacteria. Goodness-of-fit of the H<sub>2</sub> progress curve data, obtained under resting conditions, to the integrated Michaelis-Menten equation is illustrated in Figures 1-5. H<sub>2</sub> K<sub>m</sub> estimates for the sulfate-reducing bacteria were consistently lower (0.7-1  $\mu\text{M}$ ) than those for the methanogens which ranged from 12  $\mu\text{M}$  (Methanosarcina barkeri MS) to approximately 2  $\mu\text{M}$  (Methanospirillum PM1) (Table 1). H<sub>2</sub> V<sub>max</sub> values for the organisms assayed, when normalized to total protein content per flask, exhibited considerable overlap.

For all organisms except Methanosarcina MS, H<sub>2</sub>-consuming activity (V<sub>max</sub>) was stable for three days or greater; MS activity gradually declined over this same period of time. Additionally, substitution of cysteine-HCl with cysteine-Na<sub>2</sub>S as reductant or elimination of Na<sub>2</sub>SO<sub>4</sub> from the anaerobic diluent did not affect apparent K<sub>m</sub> estimates for H<sub>2</sub> consumption by the methanogenic bacteria.

Influence of initial H<sub>2</sub> concentration on apparent K<sub>m</sub>. Under phase-transfer limited conditions, the apparent K<sub>m</sub> for H<sub>2</sub> will depend on the initial substrate concentration (S<sub>0</sub>) (25), which is inconsistent with the Michaelis-Menten model. To be certain the H<sub>2</sub> K<sub>m</sub> estimates in Table 1 were not obtained under mass-transport limited conditions and to check for product inhibition of substrate consumption we performed H<sub>2</sub> progress curves at different initial H<sub>2</sub> concentrations. No apparent dependence of half-saturation constants for H<sub>2</sub> uptake on the initial H<sub>2</sub> concentration was found for Desulfovibrio strains G11 and PS1 (Table 2);



Figure 1.  $H_2$  progress curve data for Methanospirillum hungatei JF-1 at two different initial  $H_2$  concentrations. Continuous curves are theoretical progress curves calculated from best-estimates of  $V_{max}$ ,  $K_m$  and  $S_0$  obtained via nonlinear regression analysis.

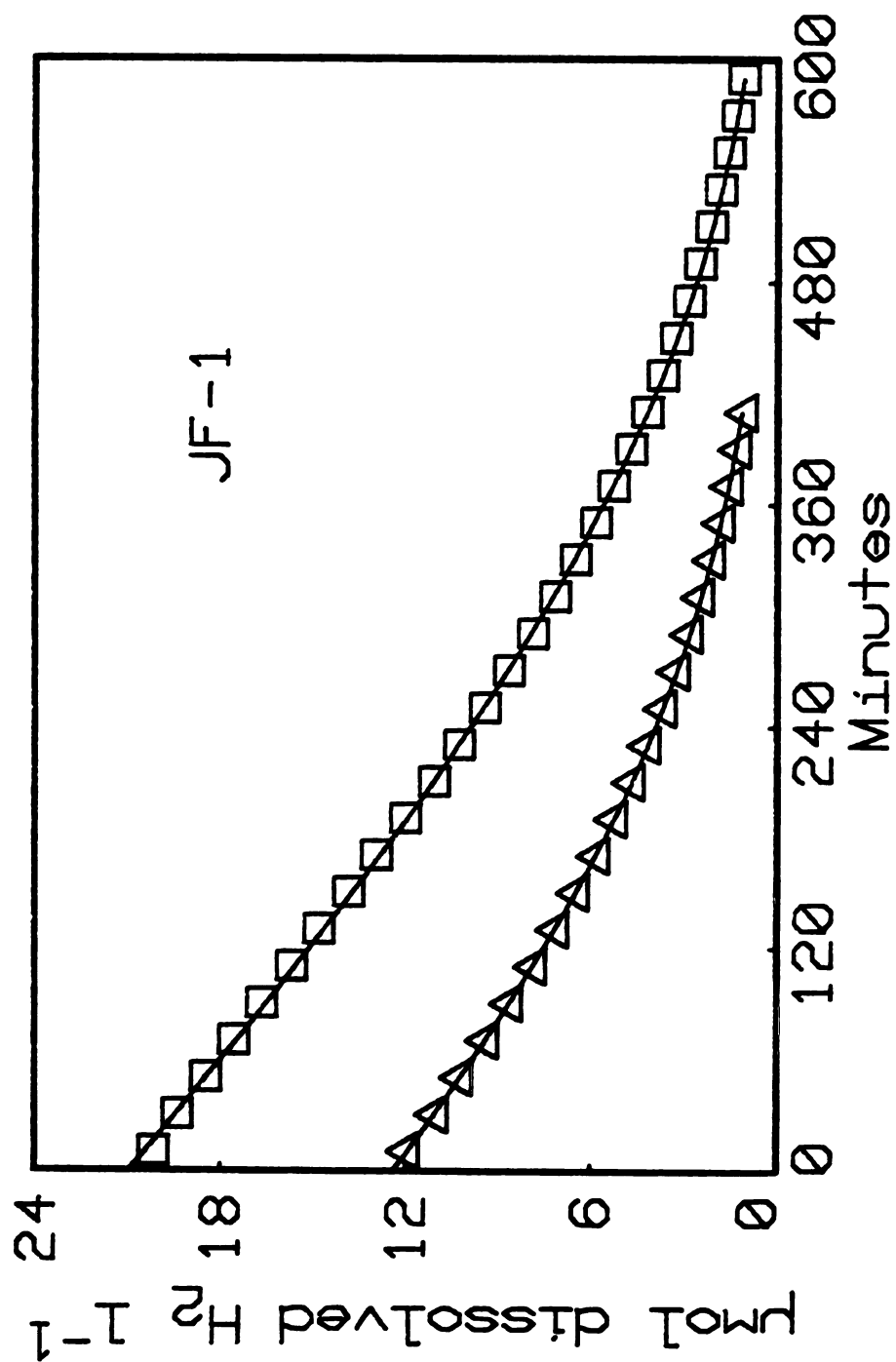


Figure 1

Figure 2. H<sub>2</sub> progress curves for Methanosarcina barkeri MS versus theoretical curves calculated from best-estimates of Michaelis-Menten parameters.

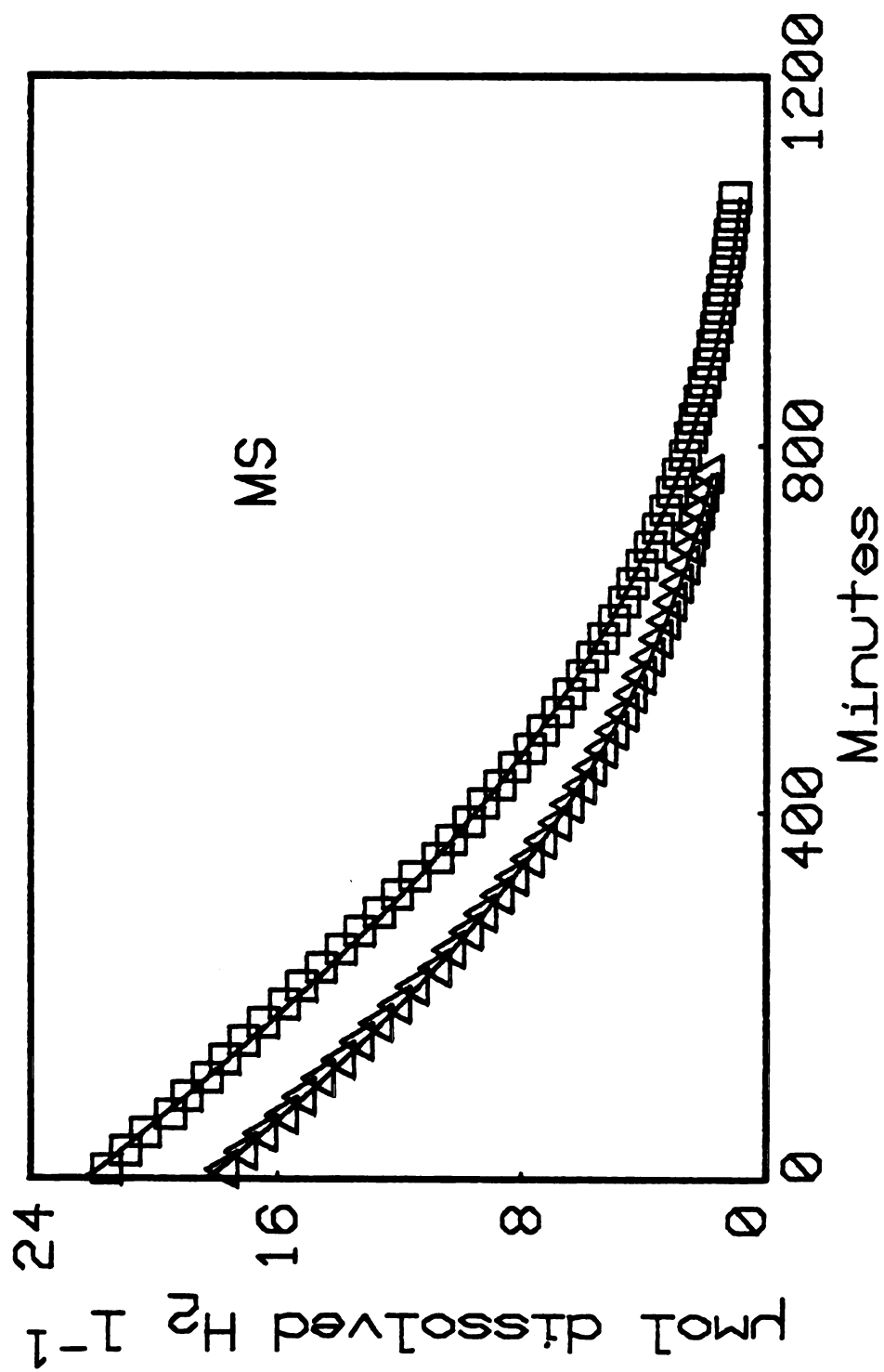


Figure 2

Figure 3. H<sub>2</sub> progress curve data for Methanospirillum PM1 (squares) and Methanobacterium PM2 (triangles) versus theoretical curves calculated from best-estimates of  $V_{\max}$ ,  $K_m$  and  $S_0$ .

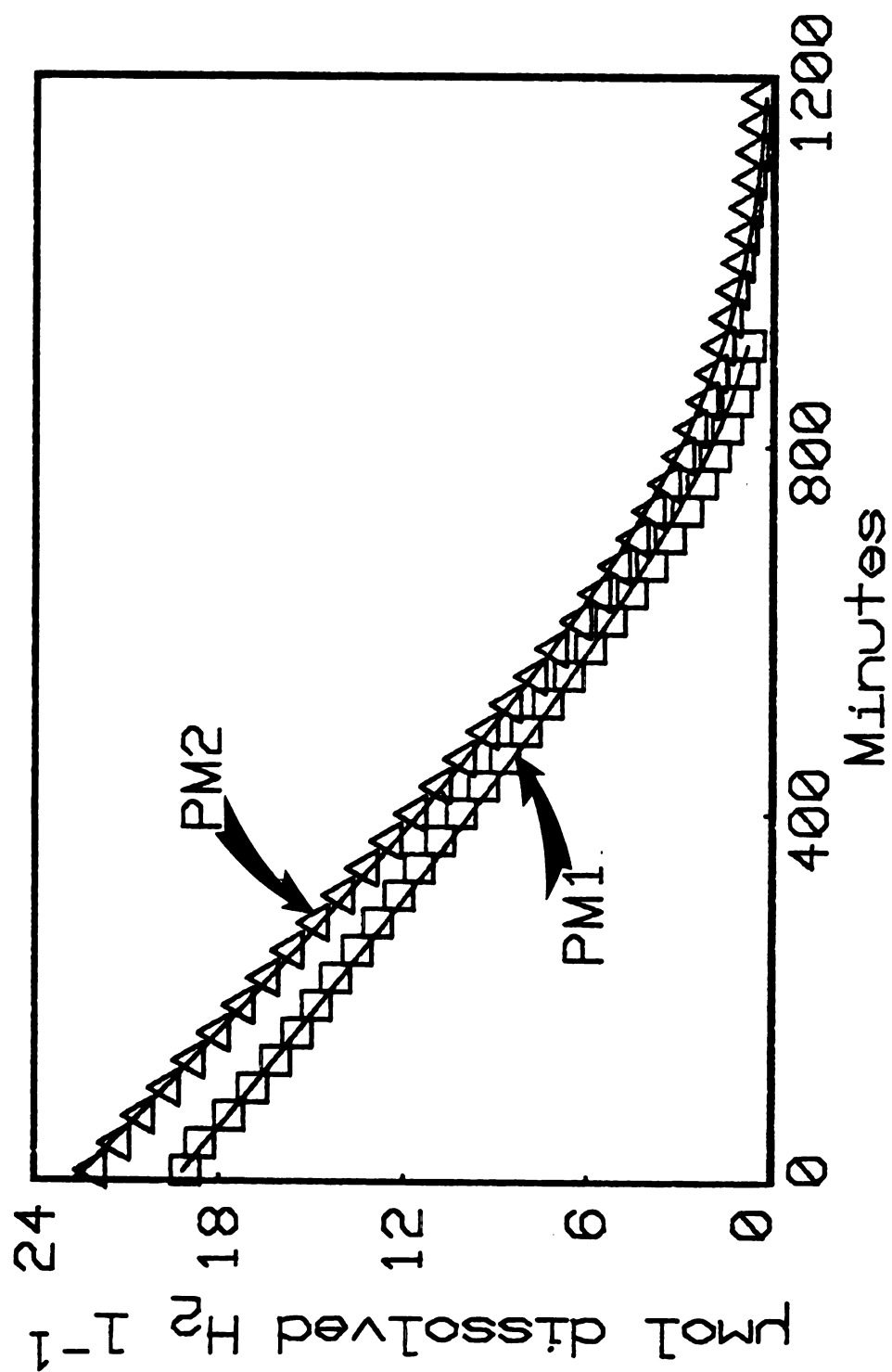


Figure 3

Figure 4.  $H_2$  progress curve data for Desulfovibrio G11 at two different initial concentrations of  $H_2$  plotted against theoretical curves.

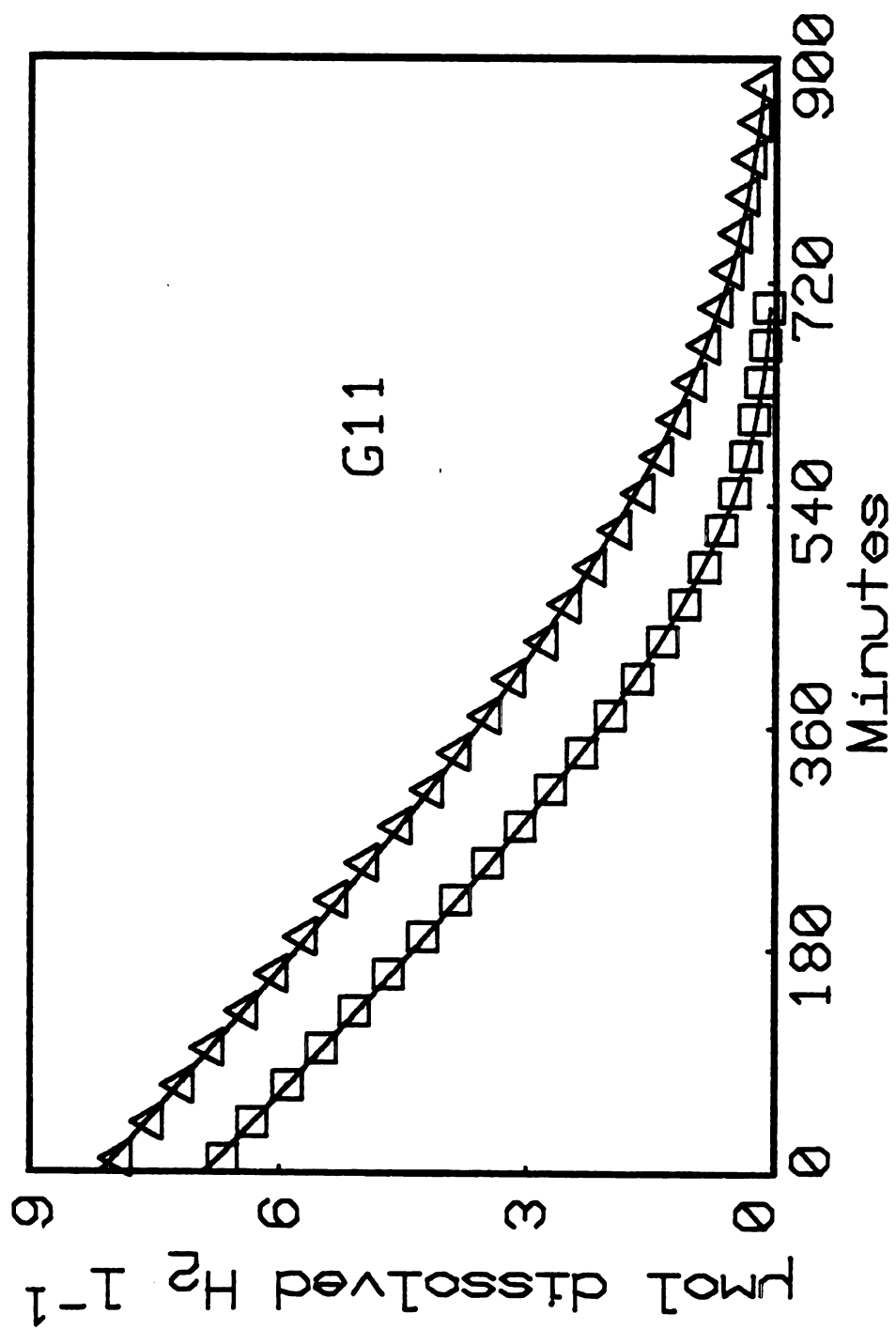


Figure 4



Figure 5.  $H_2$  progress curve data for Desulfovibrio PS1 plotted against theoretical Michaelis-Menten curves at two different initial  $H_2$  concentrations.

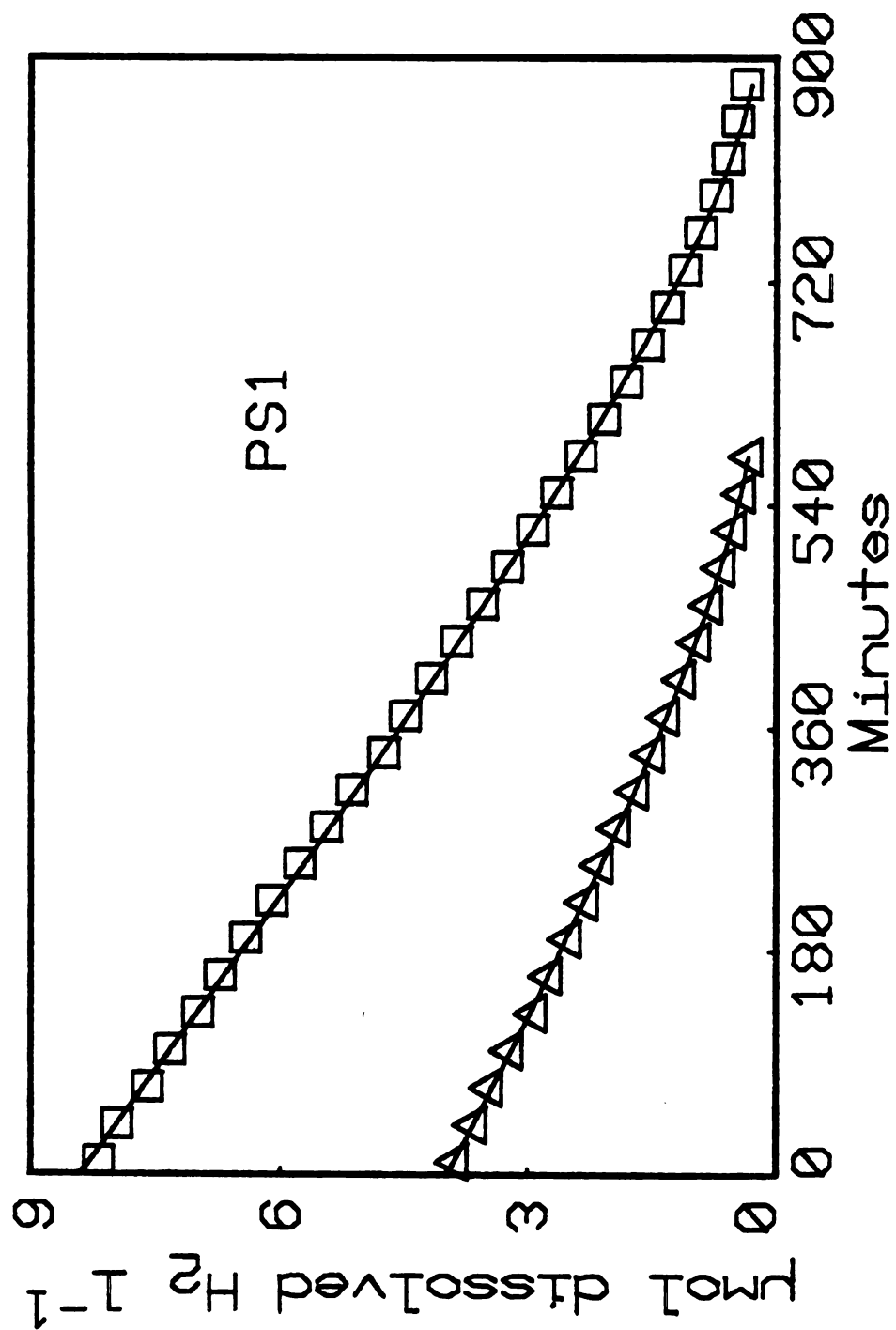


Figure 5

Table 1. Summary of H<sub>2</sub> kinetic parameters for methanogenic and sulfate-reducing bacteria.<sup>a</sup>

Organism	V <sub>max</sub> (uM min <sup>-1</sup> ) <sup>b</sup>	K <sub>m</sub> (uM) <sup>c</sup>
<u>Methanospirillum</u> JF-1	9.05	5.00
<u>hungatei</u>	12.5	4.94
	13.2	4.36
	16.3	5.51
<u>Methanospirillum</u> PM1	19.6	3.24
	16.5	1.75
<u>Methanobacterium</u> PM2	13.3	4.1
<u>Methanosarcina</u> MS	21.6	12.8
<u>barkeri</u>	22.6	12.5
<u>Desulfovibrio</u> G11	6.89	1.19
	6.29	1.01
	6.54	1.06
	6.75	1.03
<u>Desulfovibrio</u> PS1	4.53	0.69
	1.82	0.70
	3.46	0.65

<sup>a</sup>Michaelis-Menten parameters were estimated by fitting H<sub>2</sub> disappearance data directly to the integrated Michaelis-Menten equation, given initial K<sub>m</sub> and V<sub>max</sub> estimates obtained via linear analysis of transformed data.

<sup>b</sup>V<sub>max</sub> values are for total amount of H<sub>2</sub> consumed per volume of aqueous phase (300 or 500 ml) in which the bacteria were suspended. Protein content was 0.04–0.09 g/flask, except for MS progress curves where total g protein was about twice this value.

<sup>c</sup>K<sub>m</sub> estimates are for H<sub>2</sub> dissolved in the aqueous phase.

Table 2. H<sub>2</sub> K<sub>m</sub> estimates for Desulfovibrio strains G11 and PS1 at different initial H<sub>2</sub> concentrations.<sup>a</sup>

Organism	S <sub>0</sub> (uM) <sup>b</sup>	K <sub>m</sub> (uM) <sup>c</sup>
PS1	10.6	0.70
	9.69	1.50
	8.42	0.69
	2.92	1.18
G11	20.6	0.74
	16.1	1.31
	6.89	1.01

<sup>a</sup>S<sub>0</sub> and K<sub>m</sub> estimates were obtained by fitting the H<sub>2</sub> progress curve data to the integrated Michaelis-Menten equation using nonlinear least-squares analysis. Initial estimates of K<sub>m</sub> and S<sub>0</sub> for nonlinear analysis were calculated using a linearized version of the integrated Michaelis-Menten equation. Total protein content per flask was 0.08 g.

<sup>b</sup>Initial H<sub>2</sub> concentrations are mol H<sub>2</sub> dissolved in the aqueous phase at t = 0.

<sup>c</sup>K<sub>m</sub> estimates are for H<sub>2</sub> dissolved in the aqueous phase.

Figure 6.  $\text{CH}_4$  and dissolved sulfide appearance data versus theoretical curves calculated using best-estimates of  $V_{\text{max}}$  and  $K_m$ . The initial substrate concentration was not updated and taken as being equal to the final concentration of product, either sulfide or  $\text{CH}_4$ .

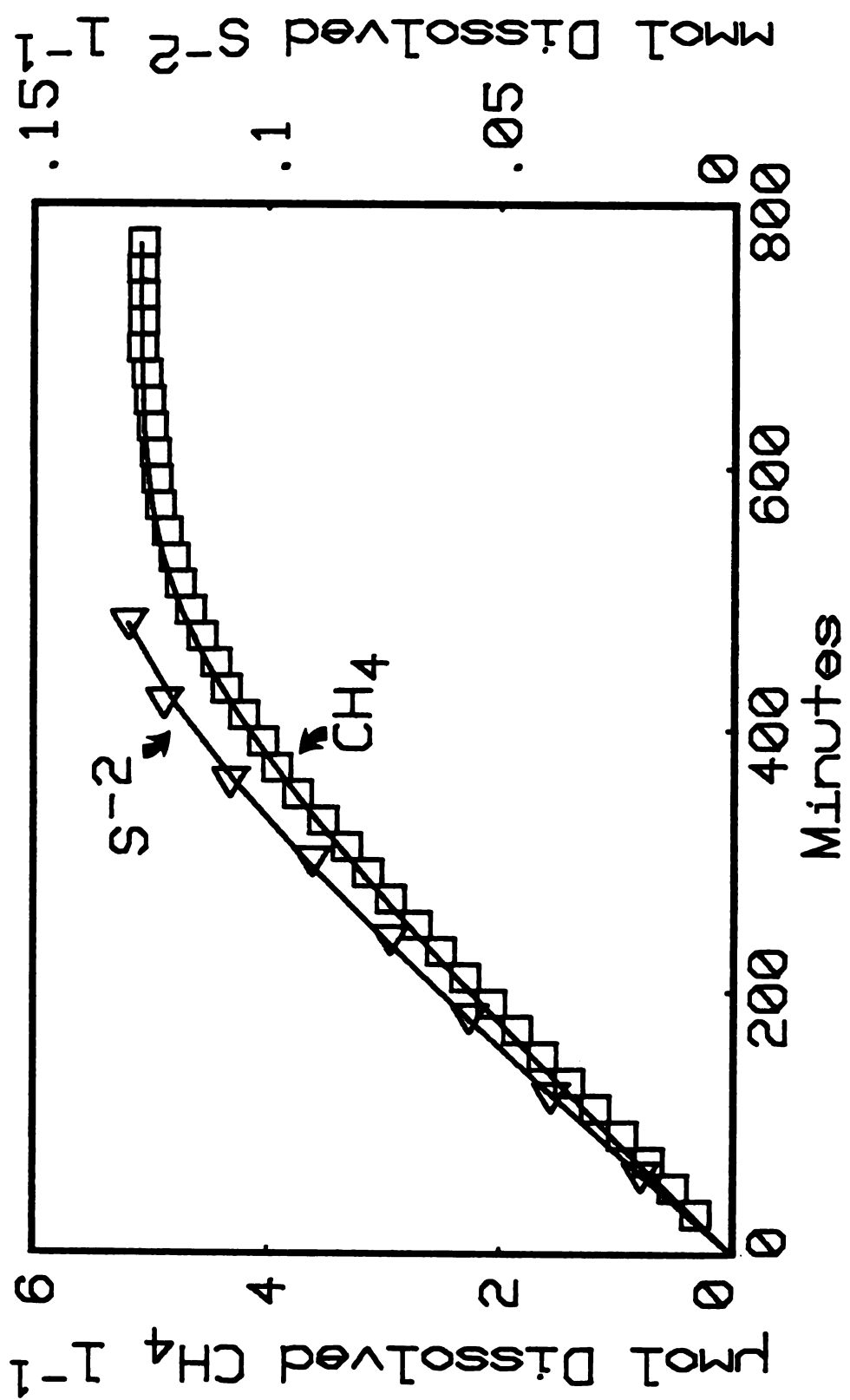


Figure 6

Table 3. Michaelis-Menten parameters for product appearance by methanogenic and sulfate-reducing bacteria.<sup>a</sup>

Organism	$V_{\max}$ ( $\mu\text{M min}^{-1}$ ) <sup>b</sup>	$K_m$ ( $\mu\text{M}$ ) <sup>c</sup>
<u>Methanosarcina</u> MS	5.52	4.37
<u>barkeri</u>		
<u>Methanospirillum</u> PM1	4.41	1.57
<u>Methanobacterium</u> PM2	2.97	1.15
<u>Desulfovibrio</u> G11 <sup>d</sup>	1	3
	1	8
	1.2	3

<sup>a</sup>Product (sulfide and  $\text{CH}_4$ ) appearance data were fitted to the integrated Michaelis-Menten equation for progress curves of unknown origin (8,19).

<sup>b</sup>Total mol  $\text{H}_2$  consumed within each flask, normalized to the volume of anaerobic diluent in which the bacteria were suspended. Protein content per flask ranged from 0.04–0.09 g.

<sup>c</sup> $K_m$  estimates are mol  $\text{H}_2 \text{ l}^{-1}$  dissolved in the aqueous phase.

<sup>d</sup>Parameter estimates were calculated from fits of transformed data to a linearized version of the integrated Michaelis-Menten equation describing progress curves of unknown origin (19).

similar results were observed for Methanospirillum JF-1.

Michaelis-Menten parameters for product appearance by methanogens and sulfate-reducers. The fit of  $\text{CH}_4$  and sulfide appearance data to the integrated Michaelis-Menten equation for product formation is illustrated in Figure 6.  $\text{CH}_4$  progress curve data generally fit the integrated Michaelis-Menten equation better than did sulfide appearance data. The  $K_m$  values for  $\text{CH}_4$  were about equal to or slightly less than those calculated from  $\text{H}_2$  progress curve data (Table 3). Sulfide  $K_m$  estimates for Desulfovibrio G11 were generally higher than those determined from  $\text{H}_2$  depletion data (Table 3).  $\text{H}_2$   $V_{\max}$  estimates determined from product appearance were approximately 1/4 of the  $\text{H}_2$   $V_{\max}$  values for the same suspension of cells.

Apparent  $\text{H}_2$   $K_m$  values for mixtures of G11 and JF-1. To examine the influence different ratios of Desulfovibrio G11 to total  $\text{H}_2$ -consuming activity have on the apparent  $K_m$  for  $\text{H}_2$  consumption, we performed  $\text{H}_2$  progress curves on bacterial suspensions containing various mixtures of G11 plus JF-1. In the absence of the other organism, the  $K_m$  for  $\text{H}_2$  uptake agreed with estimates for G11 and JF-1 in Table 1. In contrast, the apparent  $K_m$  was shifted in a nonlinear way from those values for the pure cultures when one organism (G11 versus JF-1) dominated total  $\text{H}_2$ -consuming activity (Figure 7). Qualitatively similar results were obtained with mixtures of G11 plus Methanosarcina MS.

The theoretical curve in Figure 7 was constructed by numerical integration of the two-term Michaelis-Menten equation shown above. All simulations were run using an initial substrate ( $\text{H}_2$ ) concentration of 4 x the  $K_m$  for the methanogenic population (viz., 5  $\mu\text{M}$ ). The resulting simulated data were fitted to the integrated Michaelis-Menten equation



Figure 7. Apparent  $H_2$   $K_m$  at different ratios of sulfate-reducing activity (organism 1) to total  $H_2$ -consuming capacity. See text for experimental details and how theoretical curve was constructed.

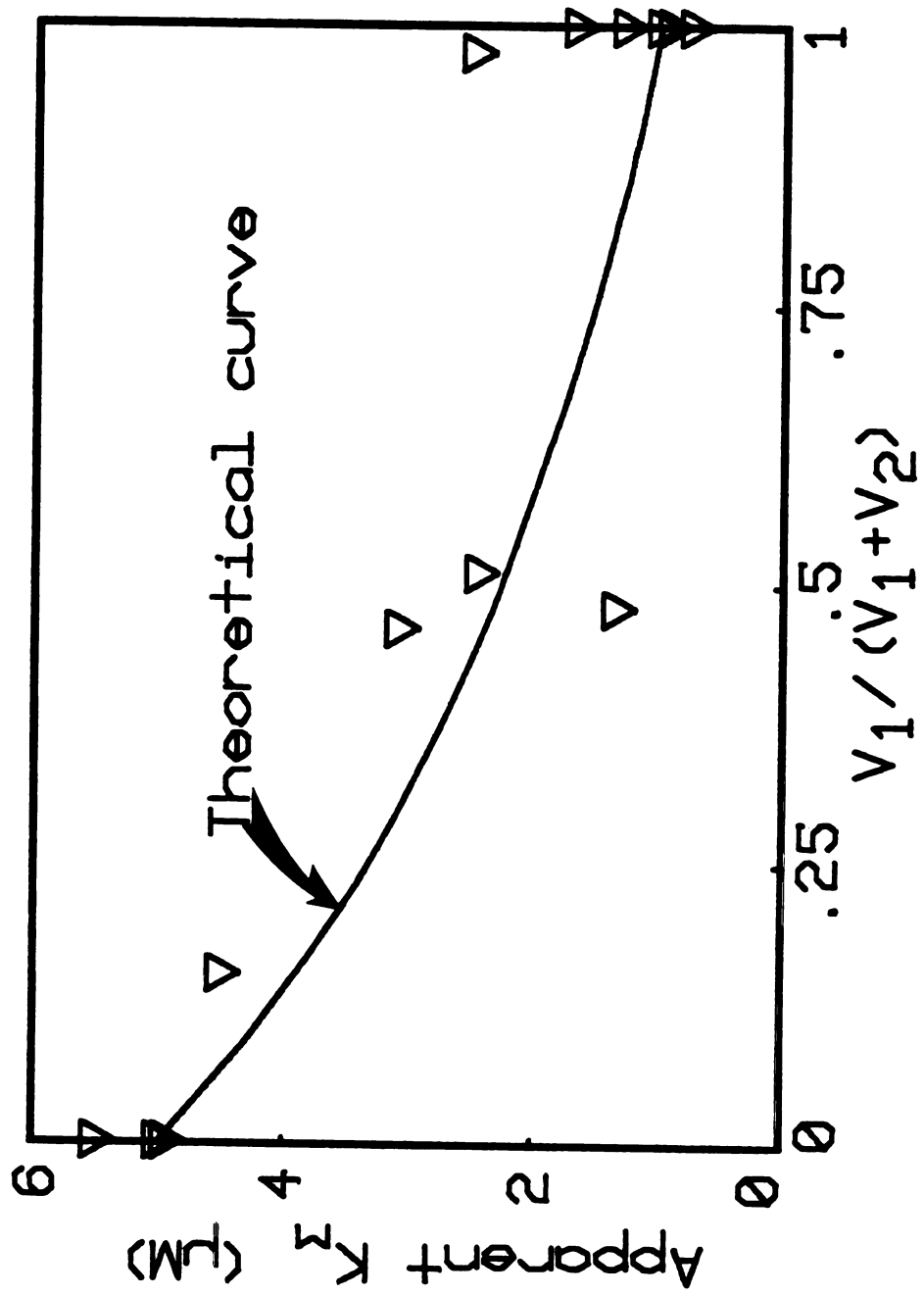


Figure 7

using nonlinear regression analysis to obtain apparent  $H_2$   $K_m$  values at different ratios of sulfate-reducing to total  $H_2$ -consuming activity.

Estimates of Monod growth kinetic parameters. Estimates of  $u_{max}$ ,  $K_s$  and  $Y_{H_2}$  for  $H_2$  consumption by Desulfovibrio G11 were obtained by fitting sigmoidal substrate depletion data to the integrated Monod relation, assuming constant yield. The fitting of sigmoidal  $H_2$  progress curve data obtained for this bacterium has been illustrated in another publication (Robinson and Tiedje, AEM submitted, ms no. 723). Estimates of Monod growth kinetic parameters for G11 are shown in Table 4. The half-saturation constant ( $K_s$ ) for  $H_2$ -limited growth of G11 was 2-4 times its half-saturation constant for uptake (Table 1). Preliminary experiments with Methanospirillum JF-1 indicate that its  $K_s$  for  $H_2$  is in the range 2-10  $\mu M$ .

Figure 8. Comparison of theoretical curve with measured  $H_2$  concentrations (squares) for growth of Desulfovibrio G11 growing on  $H_2$  as the sole electron donor. The initial substrate concentration ( $S_0$ ) was estimated by extrapolating back to  $t=0$  on the  $H_2$  concentration axis.

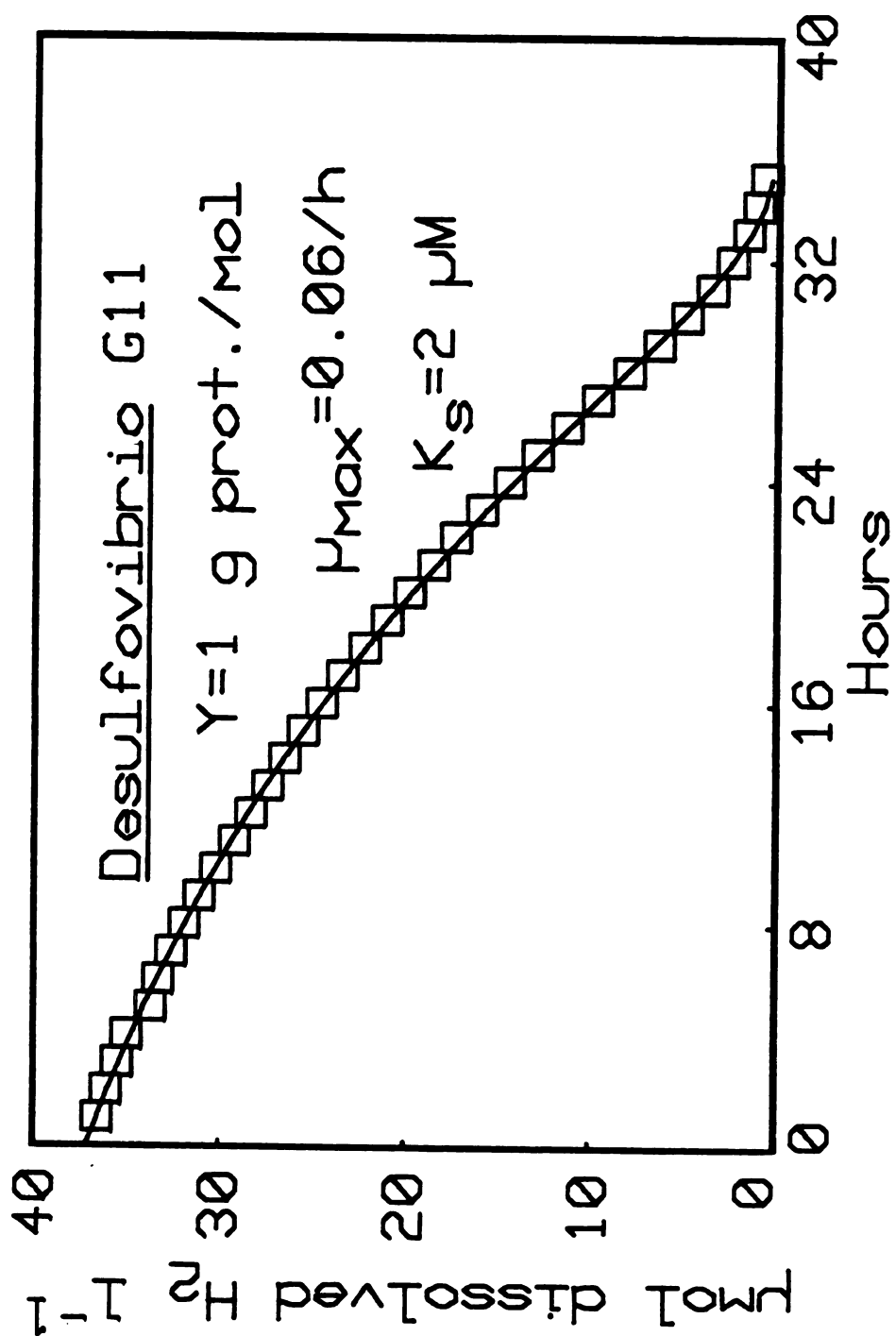


Figure 8

Table 4. Monod growth kinetic parameters for Desulfovibrio G11.<sup>a</sup>

$10^{-2} \times u_{\max}$ (h <sup>-1</sup> ) <sup>b</sup>	$K_s$ (uM) <sup>c</sup>	$Y_{H_2}$ (g prot. mol <sup>-1</sup> ) <sup>d</sup>
6.54	4.17	0.72
4.87	2.42	0.99

<sup>a</sup>Data were fitted to the integrated Monod equation according to procedures described by Robinson and Tiedje (AEM submitted, ms no. 723).

<sup>b</sup>Calculated from aqueous phase H<sub>2</sub> data.

<sup>c</sup>Half-saturation coefficients for growth are for mol H<sub>2</sub> l<sup>-1</sup> dissolved in the aqueous phase.

<sup>d</sup>Yield coefficients are expressed as g protein produced per total H<sub>2</sub> consumed in the flask.

## DISCUSSION

Our  $H_2$   $K_m$  estimates for sulfate-reducing bacteria agree with a value recently reported for Desulfovibrio vulgaris Marburg determined by Kristjansson et. al. (15). They estimated an  $H_2$   $K_m$  of 1.3  $\mu M$  from disappearance of  $H_2$  in the aqueous phase using an  $H_2$ -electrode. The agreement between this value and our  $H_2$   $K_m$  estimates for Desulfovibrio G11 and PS1 is noteworthy since ours were determined by following non-transfer limited  $H_2$  consumption in the gas phase, while theirs was calculated from direct measurements of aqueous phase  $H_2$  concentrations. This lends additional support to the validity of determining half-saturation coefficients by monitoring depletion of the substrate from the gas phase (25). Its interesting to note the close agreement between Kristjansson et. al.'s  $H_2$   $K_m$  estimate and our values given they estimated this parameter by calculating slopes at different points along a progress curve and using these as initial velocity estimates, a statistically questionable procedure (8).

The  $H_2$   $K_m$  estimates we obtained for the methanogens, with the exception of Methanosarcina barkeri MS are higher on average (mean = 5  $\mu M$ ) than previously determined estimates. Hungate et. al. (13) and Ferry et. al. (27) reported  $H_2$   $K_m$  values for Methanobrevibacter ruminantium and Methanobacterium formicicum of 1 and 2  $\mu M$ , respectively. Kristjansson et. al. (15) reported an  $H_2$   $K_m$  for Methanobrevibacter arboriphilus AZ of 6.6  $\mu M$ , similar to values we found for Methanospirillum hungatei JF-1 and Methanobacterium PM2. The two strains of Methanospirillum we studied--namely, JF-1 and G11--possessed different half-saturation constants for  $H_2$  uptake; PM1's  $H_2$   $K_m$  was about

2  $\mu\text{M}$  and similar to  $K_m$  estimates for the sulfate-reducers, whereas JF-1 had an average  $\text{H}_2$   $K_m$  of approximately 5  $\mu\text{M}$ . The uptake parameter estimates for PM1 correlated with the observation that it grew more rapidly than did JF-1; in fact, its growth rate was on a par with that of Desulfovibrio G11.

The  $K_m$  for  $\text{H}_2$  consumption by Methanosarcina MS was at least 2-fold greater than  $K_m$  estimates for the other methanogens. Two factors may potentially account for MS's apparently lower affinity for  $\text{H}_2$ : (i) a decrease in activity gradually over the course of the progress curve or (ii) mass-transport limitations between the aqueous phase and the surfaces of MS aggregates. A slight decline in  $\text{H}_2$ -consuming activity with time is the more likely of these two, since the initial  $\text{H}_2$  concentration and differences in stirring rates did not influence the apparent  $K_m$ , factors which are expected to alter apparent  $K_m$  values for gaseous substrate consumption if a mass-transport limitation exists (25).

Our  $\text{H}_2$   $K_m$  estimates for sulfate-reducers and methanogens are similar to values found by other workers for methanogenic habitats and sediments in which sulfate-reducers are the dominant  $\text{H}_2$  consumers. Robinson and Tiedje (25) determined  $\text{H}_2$   $K_m$  values for rumen fluid, anaerobic digester sludge and eutrophic sediment ranging from 4-9  $\mu\text{M}$ , overlapping the range we found for methanogenic bacteria. Additionally, Lovely et. al. (16) observed a shift in the apparent  $\text{H}_2$   $K_m$  when  $\text{FeSO}_4$ -amended sediments were treated with  $\text{CHCl}_3$  to inhibit methanogenesis comparable in magnitude to the difference between average  $K_m$  values for the methanogens and sulfate reducers studied by us. Estimates for rumen fluid of 1  $\mu\text{M}$  and eutrophic sediments of 2  $\mu\text{M}$



reported by Hungate et. al. (13) and Strayer and Tiedje (29), respectively, are low but comparable in magnitude to the  $H_2$   $K_m$  estimates in Table 1.

In addition to determining  $K_m$  values for  $H_2$  consumption, we also estimated Michaelis-Menten parameters for  $CH_4$  and sulfide appearance. This was done to (i) check if  $V_{max}$  estimates for product appearance were 1/4 of values for  $H_2$  consumption (the expected result) and (ii) determine whether uptake parameters for mixtures of bacteria with different substrate affinities can be estimated by following the individual products produced. Although the estimated uptake half-saturation constants for product appearance were similar to  $K_m$  values obtained for  $H_2$  depletion, they must be cautiously interpreted since the final concentration of either sulfide or  $CH_4$  was taken as equalling the initial substrate concentration. Its not possible to use the initial  $H_2$  concentration to estimate Michaelis-Menten parameters for sulfide or  $CH_4$  appearance because a one-to-one stoichiometry between  $H_2$  consumption and production of either product does not exist. An important result of the product appearance experiments is that  $V_{max}$  estimates for  $CH_4$  and sulfide production were about 1/4 of the  $H_2$   $V_{max}$  values obtained for a given flask experiment, in accordance with the stoichiometries for chemolithotrophic methanogenesis and sulfate-reduction. The more significant result, however, is the finding that uptake constants for mixtures of bacteria having different substrate affinities--such as sulfate-reducers and methanogens--cannot be estimated by following appearance of the individual products ( $CH_4$  and sulfide); significant underestimates of the half-saturation constant will be obtained depending on the fraction the organism producing the

product ( $\text{CH}_4$ , for example) comprises of total substrate-consuming activity.

A one-term Michaelis-Menten model cannot be used to accurately predict rates of substrate depletion by bacterial consortia in which individual populations possess different uptake parameters. One manifestation of the inadequacy of a one-term model for such cases is the dependence of the apparent  $\text{H}_2$   $K_m$  on the relative amounts of Desulfovibrio G11 and Methanospirillum hungatei JF-1 for mixtures of these organisms. On the other hand, a two-term Michaelis-Menten equation does predict accurately total  $\text{H}_2$  consumption by two resting bacterial populations and further, predicts (i) apparent  $\text{H}_2$  affinities for particular combinations of sulfate-reducing plus methanogenic activities and (ii) the partitioning of a given initial  $\text{H}_2$  concentration between these two anaerobic  $\text{H}_2$ -consumers. Lovely et. al. (16) observed that a two-term Michaelis-Menten model accurately predicted total  $\text{H}_2$  consumption by sulfate-reducers and methanogens in eutrophic sediments when Michaelis-Menten parameters independently determined for these two populations were plugged into a two-term Michaelis-Menten expression. We found apparent  $\text{H}_2$   $K_m$  values for several ratios of sulfate-reducing to total  $\text{H}_2$ -consuming activity agreed with values predicted from solutions of a two-term model, illustrating that apparent uptake constants for substrate consumption (or product appearance) depend on the respective densities of the organisms catalyzing this process when they possess dissimilar substrate affinities.

Michaelis-Menten parameters for the organisms we studied (assuming that no significant difference really exists among  $V_{\max}$  estimates normalized to protein) predict that sulfate-reducers will outcompete

methanogens (with the possible exception of Methanospirillum PM1) for  $H_2$  if sulfate is not limiting. Our results are corroborated by the finding that sulfate-reduction dominates total  $H_2$ -consuming activity in habitats where sulfate concentrations are high (14,21). On the other hand, methanogens may effectively compete for  $H_2$  under sulfate-limited conditions, a situation that presumably occurs in many eutrophic lake sediments.

Solutions to the two-term Michaelis-Menten equation predict that methanogenic bacteria may process more of an initially saturating  $H_2$  concentration even when sulfate-reducers are saturated for sulfate (Figure 9). Further, when the initial  $H_2$  concentration is in the saturating region ( $10 \times K_m$ ) with respect to methanogenic activity (also saturating for sulfate-reduction)  $K_m$  differences of 10-fold between competing bacterial populations influence little the partitioning of  $H_2$ . On the other hand, organisms like JF-1 must comprise a significantly greater fraction of total  $H_2$ -consuming activity when the initial substrate concentration is in the mixed- to first-order region in order for them to process an equal share of the  $H_2$  (Figure 9), in analogy with conclusions reached by Healey regarding competition among growing bacterial populations (11). Experiments performed with mixtures of JF-1 and G11 at different initial  $H_2$  concentrations corroborate predictions made by Figure 9; the difference in the half-saturation constant between sulfate-reducers and methanogens becomes important when the initial  $H_2$  concentration (or steady-state  $H_2$  pool in a habitat) does not saturate  $H_2$ -consuming activity. Thus, methanogens could compete well with sulfate-reducers in sulfate-rich natural habitats if their densities are relatively high and the steady-state  $H_2$  concentration is saturating.

Figure 9 . Fifty-percent partitioning curves for mixtures of sulfate-reducing and methanogenic bacteria. Each curve predicts what proportion of the total  $H_2$ -consuming activity an organism (2) with a lower uptake affinity for  $H_2$  (or any substrate) must comprise in order for it to process an equal share (50%) of a given initial substrate concentration. Curves were constructed by numerically integrating a two-term Michaelis-Menten expression at a given ratio of  $K_m$  values ( $K_{m,2}/K_{m,1}$ ) for various initial substrate concentrations and ratios of methanogenic to total  $H_2$ -consuming activity. Initial substrate concentrations were 100 (diamonds), 10 (circles), 1 (triangles) and 0.1 (squares).

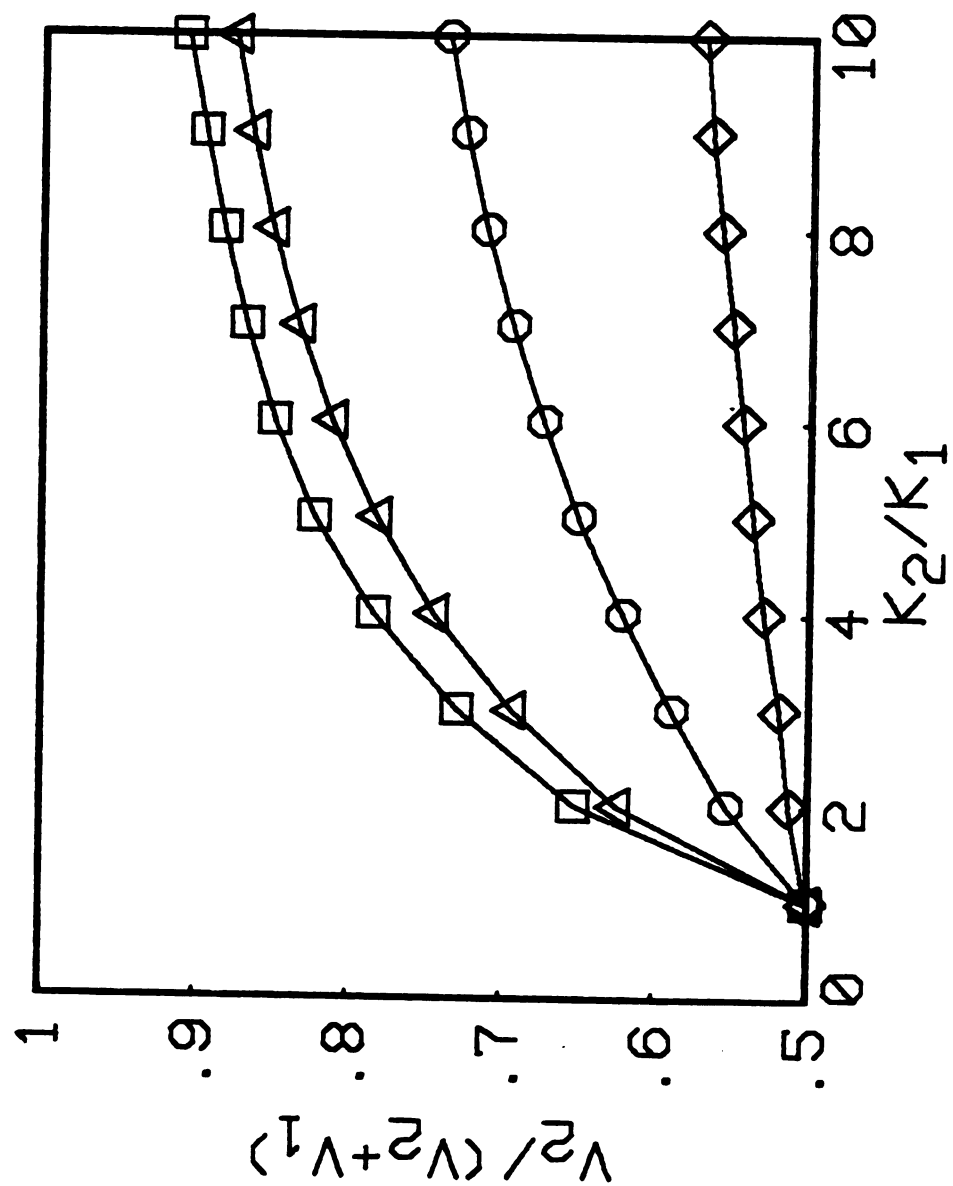


Figure 9

But in most anaerobic ecosystems in situ  $H_2$  concentrations are in the first- to mixed-order regions (26,29) and thus, sulfate-reducers would be expected to account for an appreciable proportion of total  $H_2$ -consuming activity due to their lower  $K_m$  for  $H_2$ , given comparable levels of methanogen and sulfate-reducer biomass.

When growth (or an increase in activity) occurs during a progress curve the resulting substrate depletion curve is sigmoidal (23,25), an observation inconsistent with Michaelis-Menten kinetics. Thus Michaelis-Menten kinetic parameters cannot be used to assess competition for  $H_2$  between sulfate-reducers and methanogens when growth occurs. In a natural habitat, Michaelis-Menten kinetics will predict the partitioning of a given substrate among competing bacterial populations only if the biomass levels are in steady-state or approximately so. If biomass levels of the competing populations increase (25% or greater) then Monod kinetics predicts the outcome of substrate partitioning. We estimated half-saturation constants ( $K_s$ ) for batch growth of Desulfovibrio G11 on  $H_2$  were 2-4  $\mu M$ , similar in magnitude to this bacterium's  $H_2$   $K_m$ . Our  $Y_{H_2}$  estimates (avg. = 0.86 g protein  $\text{mol}^{-1} H_2$ ), when converted into the equivalent of g cells produced per mol sulfate reduced, are similar in magnitude to those reported for Desulfovibrio Marburg and Madison strains reported by Badziong et. al. (3). Results of preliminary growth studies with Methanospirillum JF-1 suggest its  $K_s$  for  $H_2$  is 2-10  $\mu M$  [ $> 10$ -fold below a  $K_s$  value reported by Schonheit et. al. (28) for Methanobacterium thermoautotrophicum probably obtained under phase-transfer limited conditions], and that its  $u_{\max}$  and  $Y_{H_2}$  are lower than those for G11. Differences in  $Y_{H_2}$  for these two bacteria are expected since sulfate-reduction yields more energy than does

chemolithotrophic methanogenesis per mol of  $H_2$  consumed (30). In summary, Monod kinetic parameters predict, in analogy with uptake  $H_2$  parameters, that sulfate-reducers will outcompete methanogens  $H_2$  and in so doing, process a greater fraction of the  $H_2$  available to these two bacterial groups.

One final item must be considered in evaluating the competition for  $H_2$  among sulfate-reducers and methanogens. The latter group of  $H_2$ -consumers are metabolic specialists; that is, the number of different electron donors they may metabolize appears to be quite limited (4). In contrast, sulfate-reducers are generalists; they are capable of anaerobically respiring a diversity of electron donors including  $H_2$  and additionally, can ferment numerous organic compounds (24). Thus, sulfate-reducers not limited to growth on  $H_2$  would be expected to grow to significant cell densities in habitats where sulfate is limiting and then if sulfate is suddenly added (either naturally or artificially) they can effectively compete with chemautotrophic methanogens for limiting  $H_2$ . Lovely et. al. (16) observed that sulfate-reducers comprised 50% of the overall  $V_{max}$  for  $H_2$  consumption in eutrophic sediments amended with 20 mM sulfate. Typically these sediments are sulfate-depleted and the large population of sulfate-reducers capable of oxidizing  $H_2$  presumably developed as a result of their fermentative growth on the cadre of organic substrates occurring in eutrophic sediments.

#### ACKNOWLEDGMENTS

We thank Dr. Marvin P. Bryant and Dan R. Shelton for supplying cultures used in this study. We also thank Walter Smolenski and Marilyn

Boucher for expert technical assistance. This research was supported by National Science Foundation grants DEB 78-05321 and DEB 81-09994.



## LITERATURE CITED

1. Abram, J. W., and D. B. Nedwell. 1978. Hydrogen as a substrate for methanogenesis and sulfate reduction in anaerobic saltmarsh sediment. *Arch. Microbiol.* 117:93-97.
2. Abram, J. W., and D. B. Nedwell. 1978. Inhibition of methanogenesis by sulfate-reducing bacteria competing for transferred hydrogen. *Arch. Microbiol.* 117:89-92.
3. Badziong, W., R. K. Thauer, and J. G. Zeikus. 1978. Isolation and characterization of Desulfovibrio growing on hydrogen plus sulfate as the sole energy source. *Arch. Microbiol.* 116:41-49.
4. Balch, W. E., G. E. Fox, L. J. Magrum, C. R. Woese, and R. S. Wolfe. 1979. Methanogens: Reevaluation of a unique biological group. *Microbiologic. Revs.* 43: 260-296.
5. Beck, J. V., and K. J. Arnold. 1976. Parameter estimation in engineering and science. John Wiley and Sons, Inc., New York, New York. p. 334-350.
6. Bryant, M. P., L. L. Campbell, C. A. Reddy, and M. R. Crabill. 1977. Growth of Desulfovibrio in lactate or ethanol media low in sulfate in association with H<sub>2</sub>-utilizing methanogenic bacteria. *Appl. Environ. Microbiol.* 33:1162-1169.
7. Cappenberg, T. E. 1974. Interrelationships between sulfate-reducing and methane-producing bacteria in bottom deposits of a fresh-water lake. I. Field observations. *Antonie van Leeuwenhoek J. Microbiol. Serol.* 40:235-295.
8. Cornish-Bowden, A. 1976. Principles of enzyme kinetics. Butterworths, Inc., Boston, Mass. p. 200-210.
9. Duggleby, R. G., and J. F. Morrison. 1977. The analysis of progress curves for enzyme-catalyzed reactions by non-linear regression. *Biochem. Biophys. Acta.* 481:297-312.
10. Flett, R. J., R. D. Hamilton, and N. E. R. Campbell. 1976. Aquatic acetylene-reduction techniques: solutions to several problems. *Can. J. Microbiol.* 22:43-51.
11. Healey, F. P. 1980. Slope of Monod equation as an indicator of advantage in nutrient competition. *Microb. Ecol.* 5: 281-286.
12. Hungate, R. E. 1968. A roll tube method for cultivation of strict anaerobes, p. 117-132. In J. R. Norris and D. W. Ribbons (eds.), Vol. 3B. Academic Press Inc., New York.
13. Hungate, R. E., W. Smith, T. Bauchop, J. Yu, and J. C. Rabinowitz.

1970. Formate as an intermediate in the bovine rumen fermentation. *J. Bacteriol.* 102:389-397.
14. Jorgensen, B. B. 1980. Mineralization and the bacterial cycling of carbon, nitrogen and sulfur in marine sediments, p. 239-351. In D. C. Ellwood, J. N. Hedger, M. J. Latham, J. M. Lynch, J. H. Slater (eds.), *Contemporary microbial ecology*. Academic Press, London, New York, Toronto, Sydney, San Francisco.
  15. Kristjansson, J. R., P. Schonheit, and R. K. Thauer. 1982. Different  $K_s$  values for hydrogen of methanogenic bacteria and sulfate-reducing bacteria: An explanation for the apparent inhibition of methanogenesis by sulfate. *Arch. Microbiol.* 131:278-282.
  16. Lovely, D. R., D. Dwyer, and M. J. Klug. 1982. Kinetic analysis of competition between sulfate reducers and methanogens for hydrogen in sediments. *Appl. Environ. Microbiol.* 43: 1373-1379.
  17. McInerney, J. M., and M. P. Bryant. 1981. Anaerobic degradation of lactate by syntrophic association of *Methanosarcina barkeri* and *Desulfovibrio* species and effect of  $H_2$  on acetate degradation. *Appl. Environ. Microbiol.* 41:346-354.
  18. McInerney, M. J., M. P. Bryant, and N. Pfennig. 1979. Anaerobic bacterium that degrades fatty acids in syntrophic association with methanogens. *Arch. Microbiol.* 122: 129-135.
  19. Mountfort, D. O., R. A. Asher, E. L. Mays, and J. M. Tiedje. 1980. Carbon and electron flow in mud and sandflat intertidal sediments of Delaware inlet, Nelson, New Zealand. *Appl. Environ. Microbiol.* 39:686-694.
  20. Nimmo, I. A., and G. L. Atkins. 1974. A comparison of two methods for fitting the integrated Michaelis-Menten equation. *Biochem. J.* 141:913-914.
  21. Oremland, R. S., and B. F. Taylor. 1978. Sulfate reduction and methanogenesis in marine sediments. *Geochim. Cosmochim. Acta* 42:209-214.
  22. Pachmayr, F. 1960. Vorkommen und bestimmung von schwefelverbindungen in mineralwasser. Ph. D. thesis, Univ. Munich.
  23. Pirt, S. J. 1975. Principles of microbe and cell cultivation. John Wiley and Sons, Inc., New York, New York. p. 22-28.
  24. Postgate, J. R. 1982. The sulphate-reducing bacteria. Cambridge Univ. Press, Cambridge, Great Britain. p. 46-81.
  25. Robinson, J. A., and J. M. Tiedje. 1982. Kinetics of hydrogen consumption by rumen fluid, anaerobic digester sludge and

- sediment. Appl. Environ. Microbiol. in press (AEM no. 364).
26. Robinson, J. A., R. F. Strayer, and J. M. Tiedje. 1981. Method for measuring dissolved hydrogen in anaerobic ecosystems: Application to the rumen. Appl. Environ. Microbiol. 41: 545-548.
  27. Schauer, N. L., and J. G. Ferry. 1980. Metabolism of formate in Methanobacterium formicicum. J. Bacteriol. 142:800-807.
  28. Schonheit, P., J. Moll, and R. K. Thauer. 1980. Growth parameters ( $K_s$ ,  $\mu_{max}$ ,  $Y_s$ ) of Methanobacterium thermoautotrophicum. Arch. Microbiol. 127:59-65.
  29. Strayer, R. F., and J. M. Tiedje. 1978. Kinetic parameters of the conversion of methane precursors to methane in hypereutrophic lake sediment. Appl. Environ. Microbiol. 36:330-340.
  30. Thauer, R. K., K. Jungermann, and K. Decker. 1977. Energy conservation in chemotrophic anaerobic bacteria. Bact. Revs. 41: 100-180.
  31. Wilhelm, E., R. Battino, and R. J. Wilcock. 1977. Low-pressure solubility of gases in liquid water. Chem. Rev. 77:219-262.
  32. Winfrey, M. R., and J. G. Zeikus. 1977. Effect of sulfate on carbon and electron flow during microbial methanogenesis in freshwater sediments. Appl. Environ. Microbiol. 33:275-281.
  33. Wood, W. A. 1981. Physical methods, p. 358. In P. Gerhardt (ed.), Manual of methods for general bacteriology. American Society for Microbiology, Washington, D.C.
  34. Zehnder, A. J. B. 1978. Ecology of methane formation. In R. Mitchell (ed.), Water pollution microbiology. Vol. 2. John Wiley and Sons, Inc., New York. p. 349-376.

## **APPENDICES**

## APPENDIX A

### PHASE-TRANSFER KINETICS

Phase-boundaries commonly occur in the natural habitats of microorganisms. They are regions where dissimilar phases (e.g., gas, solid, liquid) come together and examples can be found in terrestrial as well as aquatic ecosystems. Any boundary between phases potentially limits microbial activity when substrates required for metabolism must pass from one phase (gas or solid) into the phase where the microorganisms reside (liquid). Mass-transport across these interfaces dominates the overall kinetic pattern if the rate of phase-transfer cannot supply the biological demand (2). But if phase-transfer exceeds the rate of microbial substrate consumption, then mathematical relations defining the nature of this consumption can be discerned, and the parameters in these equations estimated (3,7). Thus, any kinetic investigation of microbial activity in situations where phase-boundaries occur must first assess whether mass-transport is limiting apparent rates of microbial activity or not.

The majority of the work presented in this thesis involved estimating kinetic parameters for  $H_2$  consumption by suspensions of bacteria and samples obtained from methanogenic habitats. I wanted to estimate  $H_2$  kinetic parameters by monitoring substrate depletion in the gaseous phase, since this is generally easier than following substrate consumption in the aqueous phase. But concentrations of a gaseous substrate in the gas phase may be multiplied by a partition coefficient to obtain aqueous phase concentrations only when a mass-transport

limitation does not exist (5). Thus, it was essential to understand the influence transport of  $H_2$  from the gaseous into the aqueous phase exerts on the kinetic pattern of  $H_2$  consumption. In accord with this, I constructed a model (PHASIM) to predict conditions leading to mass-transport limitations and more importantly, how these limitations influence apparent  $H_2$  kinetic parameters. In this appendix I not only include the PHASIM model found in chapter I, but also additional systems of differential equations that describe (i) gaseous substrate consumption by growing cells and (ii) gaseous product formation from gaseous and nongaseous substrates. This appendix concludes with recommendations on how mass-transport limitations may be experimentally detected and the consequences for kinetic investigations if they are ignored.

The systems of equations that appear below are nonlinear and lack analytical solutions. Thus, solution curves (viz., substrate or product concentration versus time) for these equations must be approximated using numerical integration. There are many techniques available to solve these types of initial-value problems, but I chose the Runge-Kutta procedure since its self-starting and provides good approximations to even 'stiff' nonlinear equations (1).

Gaseous substrate consumption by resting cells. Gaseous substrate consumption by cells in the aqueous phase of a two-component system, comprised of gaseous and aqueous phases, may be described by the two equations shown below. These expressions are identical to those in the PHASIM model (chapter I) and are presented here again for the sake of completeness.

$$dS_g/dt = -K_{1a}(BS_g - S_a) \quad [A.1]$$

$$dS_a/dt = K_{1a}(BS_g - S_a) - V_{max}S_a/(K_m + S_a) \quad [A.2]$$

The variables  $S_g$  and  $S_a$  equal the gaseous and aqueous phase concentrations of the gaseous substrate, respectively. The parameters  $K_{1a}$ ,  $B$ ,  $V_{max}$  and  $K_m$  are the volumetric transfer coefficient, the Bunsen absorption coefficient, the maximum rate of gaseous substrate consumption, and the  $S_a$  at which the rate of consumption is half-maximal.

Solutions to the above system of equations predict that gaseous substrate consumption follows Michaelis-Menten kinetics when the  $K_{1a}$  is greater than  $V_{max}$  and that further increases in the  $K_{1a}$  do not alter substrate depletion (Figure 1). In contrast, the mass-transport term in [A.2] controls substrate consumption when  $V_{max}$  is greater than the  $K_{1a}$ . In this case, the kinetic pattern is approximately first-order and increases in the  $K_{1a}$  increase rates of substrate depletion (Figure 2). In addition to these, solutions to [A.1] and [A.2] predict that apparent  $K_m$ 's for gaseous substrate consumption are markedly dependent on  $V_{max}$  and the initial substrate concentration under mass-transport limited conditions. Thus, only when a phase-transfer limitation does not exist do apparent saturation kinetic parameters have biological meaning, and this holds whether gaseous substrate depletion is monitored in the gaseous or aqueous phase.

Gaseous substrate consumption by growing cells. When gaseous substrate consumption results in microbial growth, then the Michaelis-Menten model no longer applies. This is particularly evident when the initial substrate concentration is greater than the

Figure 1. Influence of  $K_{1a}$  on gaseous substrate consumption not limited by phase-transfer. Equations [A.1] and [A.2] were numerically integrated for the following parameter values and initial conditions:  $B=0.02$ ,  $V_{\max}=0.1$ ,  $K_m=5$ ,  $S_{a,0}=20$ , and  $S_{g,0}=0$ .  $K_{1a}$  equalled 10 (squares), 5 (circles) and 2 (triangles).



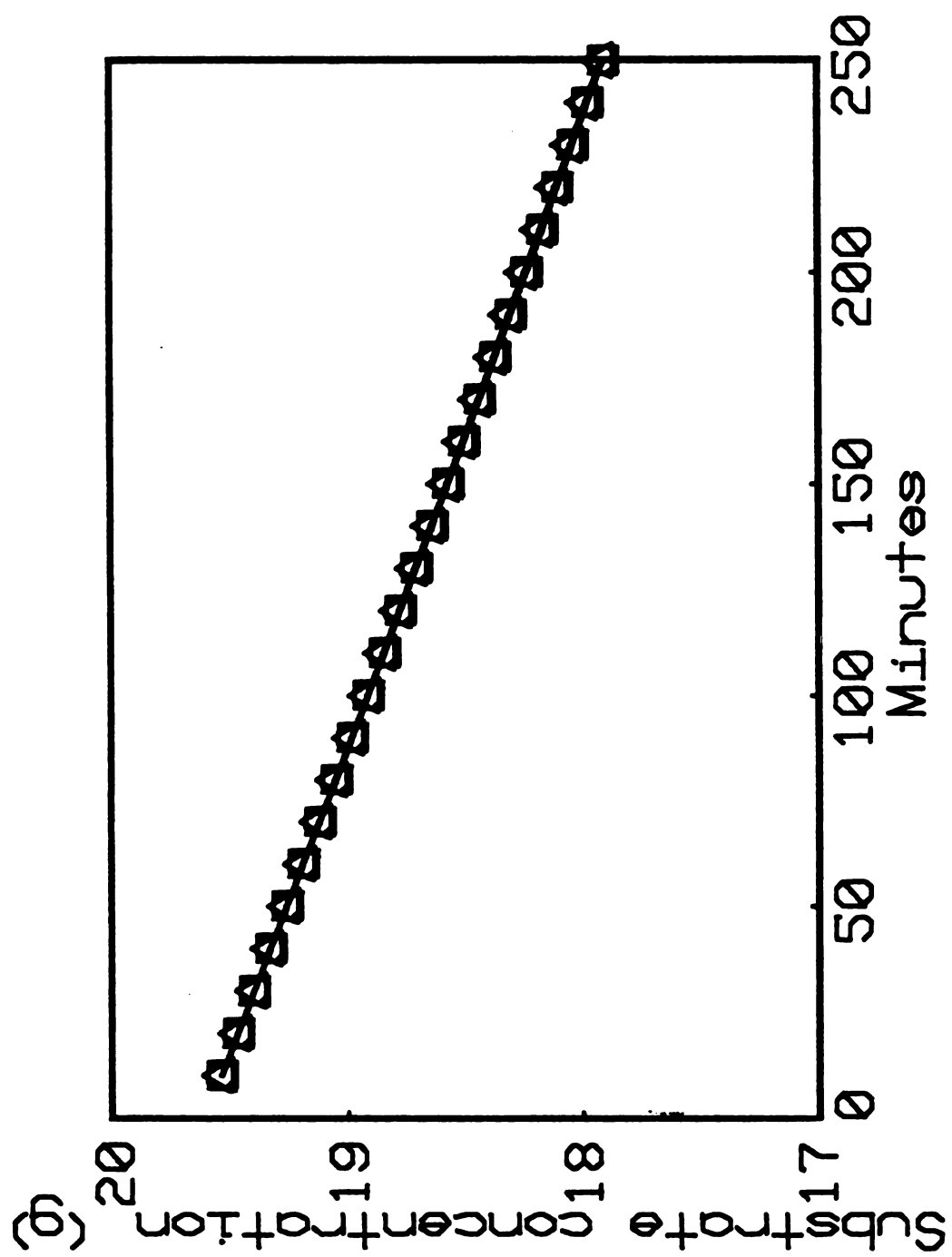


Figure 1

Figure 2. Influence of  $K_{1a}$  on gaseous substrate consumption limited by mass-transport. All parameter values and initial conditions are identical with those used for Figure 1, except  $V_{\max}$  was increased to 10.

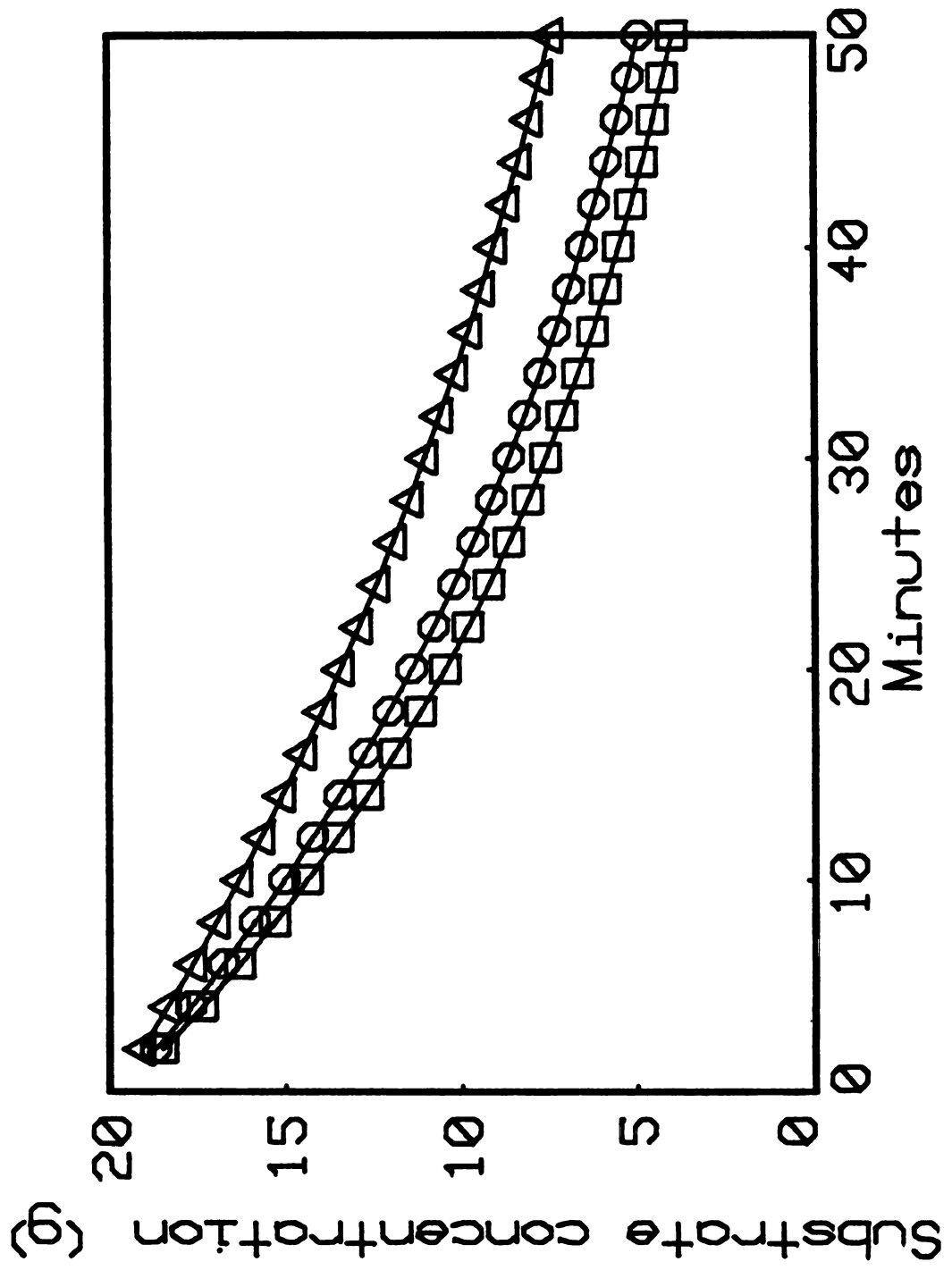


Figure 2

half-saturation constant ( $K_s$ ) for growth, since this results in sigmoidal substrate depletion (4,5). This type of kinetic pattern never occurs if Michaelis-Menten kinetics controls the rate of gaseous substrate consumption. To account for growth [A.2] can be changed to

$$dS_a/dt = -K_1 a(BS_g - S_a) - [u_{max} S_a / (K_s + S_a)] X / Y \quad [A.3]$$

where  $u_{max}$ ,  $K_s$  and  $Y$  equal the maximum growth rate, the  $S_a$  at which the growth rate is half-maximal and the yield coefficient, respectively. In order to simultaneously solve [A.3] and [A.1] using numerical integration a third equation for updating the biomass concentration ( $X$ ) is needed. This equation has the form

$$dX/dt = [u_{max} S_a / (K_s + S_a)] X \quad [A.4]$$

The gaseous substrate depletion curve for growing cells is approximately first-order when mass-transport is severely limiting, even when  $S_0$  is greater than  $K_s$  (Figure 3). This is reminiscent of gaseous substrate consumption by resting cells (5) and substantial overestimates of  $K_s$  would probably result if apparent growth rates were used together with [A.4] under steady-state conditions to estimate this parameter. This probably accounts for the unrealistically high  $H_2$   $K_s$ 's for methanogenic bacteria grown in continuous culture appearing in the literature (6). When gaseous substrate depletion by growing cells is moderately mass-transport limited, it becomes difficult to qualitatively discern this situation from gaseous substrate consumption affected by phase-transfer (Figure 4 versus Figure 5). But if  $S_a/S_g$  ratios are calculated and plotted versus time, the difference between these two simulations becomes obvious. When gaseous substrate consumption is not phase-transfer limited,  $S_a/S_g$  ratios equal the partition coefficient and do not change during substrate depletion (Figure 5). In contrast,  $S_a/S_g$

Figure 3. Gaseous substrate consumption by growing cells severely limited by mass-transport. Equations [A.1], [A.3] and [A.4] were numerically integrated for the following parameter values and initial conditions:  $K_{1a}=0.1$ ,  $u_{\max}=0.2$ ,  $K_s=1$ ,  $Y=0.05$ ,  $B=0.02$ ,  $S_{g,0}=200$ ,  $S_{a,0}=0$  and  $X_0=1$ . Note the ratio of  $S_a/S_g$  should equal  $B$  if phase-transfer is not rate-limiting.

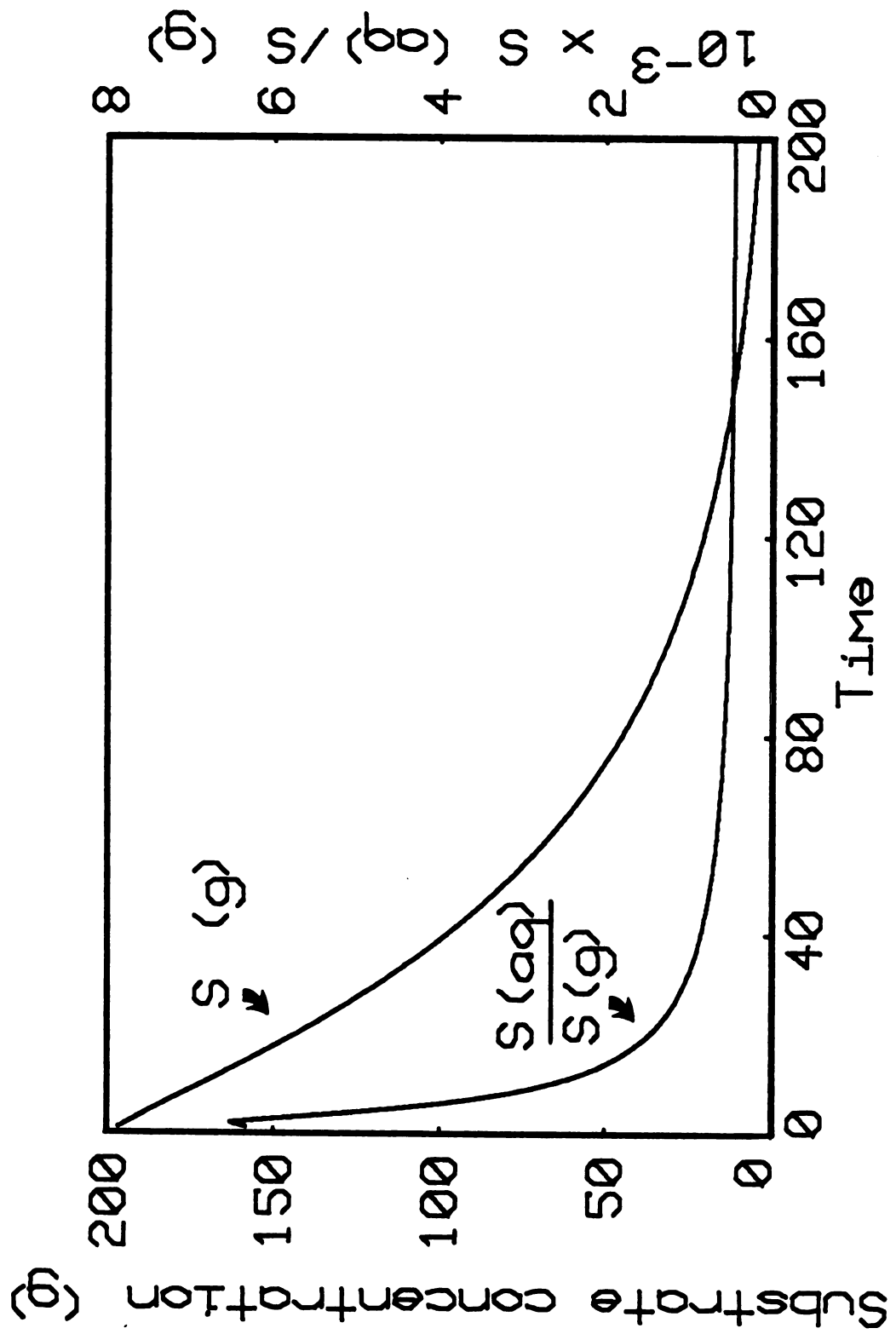


Figure 3

Figure 4. Gaseous substrate consumption by growing cells moderately limited by phase-transfer. Parameter values and initial conditions are the same as those used for Figure 3, except  $K_{1a}=0.5$ .

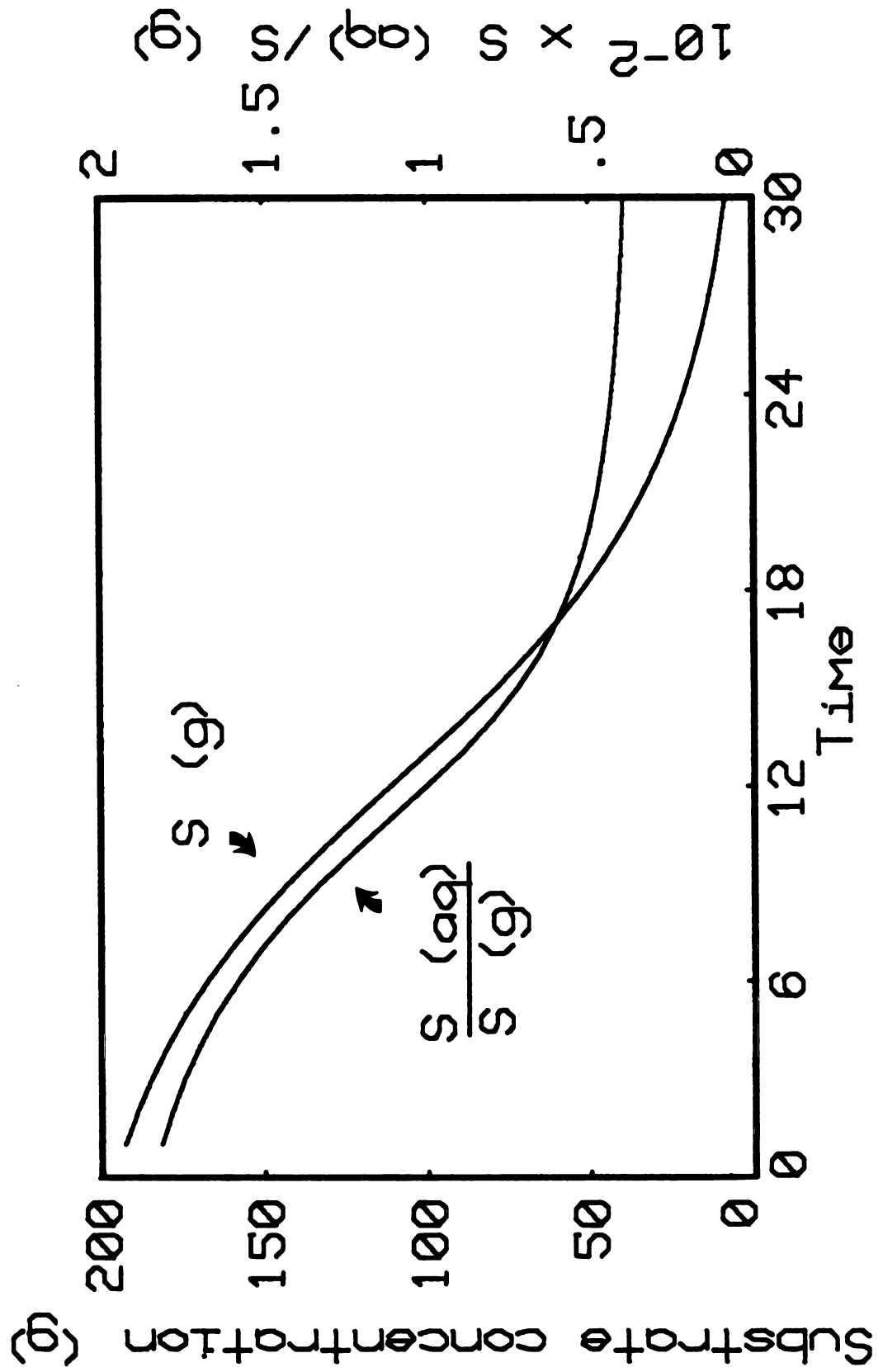


Figure 4



Figure 5. Gaseous substrate consumption by growing cells not limited by mass-transport. Same parameter values and initial conditions as those used for Figures 3-4, except  $K_{1a}=1000$ .

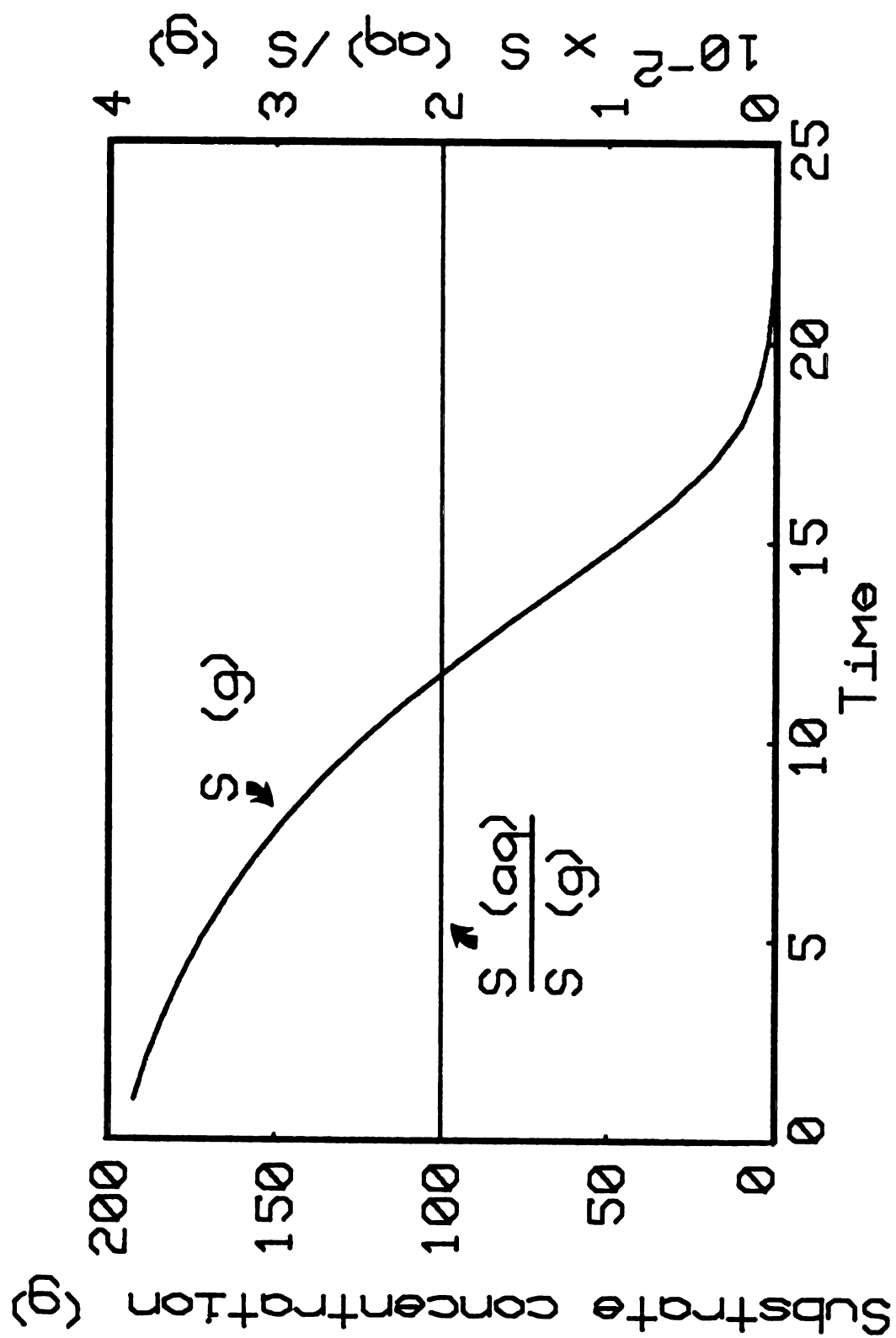


Figure 5

ratios decrease with time for mass-transport limited substrate consumption and equal B only at the start of the simulation, when mass-transfer still exceeds microbial demand (Figure 4). These ratios fluctuate widely when transfer of the gaseous substrate into the aqueous phase is severely rate-limiting (Figure 3). Solutions to [A.1], [A.3] and [A.4] for various combinations of parameters and initial conditions suggest that a mass-transport limitation will not arise if  $-dS_a/dt_{\max}$  (the slope of the substrate depletion curve at the inflection point) is less than the  $K_{1a}$ . As was true for the situation described by [A.1] and [A.2], gaseous substrate progress curves for growing cells may be used to estimate  $K_s$ ,  $U_{\max}$  and Y only in the absence of a phase-transfer limitation.

Production of a gaseous product from a gaseous substrate. The production of a gaseous product from a gaseous substrate mirrors the kinetic pattern of substrate depletion. If a phase-transfer limitation exists then obviously gaseous product formation data, like gaseous substrate consumption data, cannot be used to estimate microbial kinetic parameters. To simulate this situation the equations

$$dP_a/dt = V_{\max} S_a / (K_m + S_a) - K_{1a}' (P_a - B' P_g) \quad [A.5]$$

and

$$dP_g/dt = K_{1a}' (P_a - B' P_g) \quad [A.6]$$

need to be simultaneously solved along with [A.1] and [A.2]. The variables  $P_a$  and  $P_g$  equal the aqueous and gaseous phase concentrations of the gaseous product, respectively. The parameters  $K_{1a}'$  and  $B'$  are the volumetric transfer and Bunsen absorption coefficients for the product, respectively.

Production of a gaseous product from a non-gaseous substrate. A

phase-transfer limitation can also occur for the production of a gaseous product from a non-gaseous substrate. If the rate of non-gaseous substrate depletion is greater than the mass-transport rate, then the gaseous and aqueous phases will not be equilibrium. The aqueous phase will become supersaturated with the gaseous product (Figure 6) and estimates of microbial kinetic parameters from product appearance data will be erroneous. The system of expressions that simulate this situation are

$$dS/dt = -V_{\max}S/(K_m + S) \quad [A.7]$$

$$dP_a/dt = V_{\max}S/(K_m + S) - K_1a'(P_a - B'P_g) \quad [A.8]$$

and

$$dP_g/dt = K_1a'(P_a - B'P_g) \quad [A.9]$$

In [A.7], S equals the concentration of the non-gaseous substrate.

#### Experimental detection of phase-transfer limitations. A

mass-transport limitation influences apparent saturation kinetic parameters in a number of predictable ways. How this limitation influences the  $K_m$  for gaseous substrate consumption has been extensively discussed elsewhere (3,5,7). In summary, apparent  $K_m$ 's for gaseous substrate consumption depend on the (i) initial substrate concentration, (ii) magnitude of the biological sink in the aqueous phase, and (iii)  $K_1a$  under phase-transfer limited conditions. Most significantly, the biological activity cannot be saturated if phase-transfer rates are less than the microbial demand. Similarly, the production of a gaseous product reflects the kinetics of gaseous substrate consumption and hence, kinetic parameters for product appearance will be erroneous if the mass-transport rate is less than  $V_{\max}$ . Experiments should be designed to check for these behaviors before biological significance can

Figure 6. Influence of  $K_{1a}$  on ratio of aqueous to gaseous phase concentrations of a gaseous product produced from a non-gaseous substrate. Parameter values and initial conditions were  $V_{\max}=1$ ,  $K_m=5$ ,  $B=0.02$ ,  $S_0=20$ ,  $P_{a,0}=0$  and  $P_{g,0}=0$ . For curves A, B and C the  $K_{1a}$  respectively was 100, 0.5 and 0.1. Note the aqueous phase becomes supersaturated with the gaseous product when the  $K_{1a}$  is less than  $V_{\max}$ .

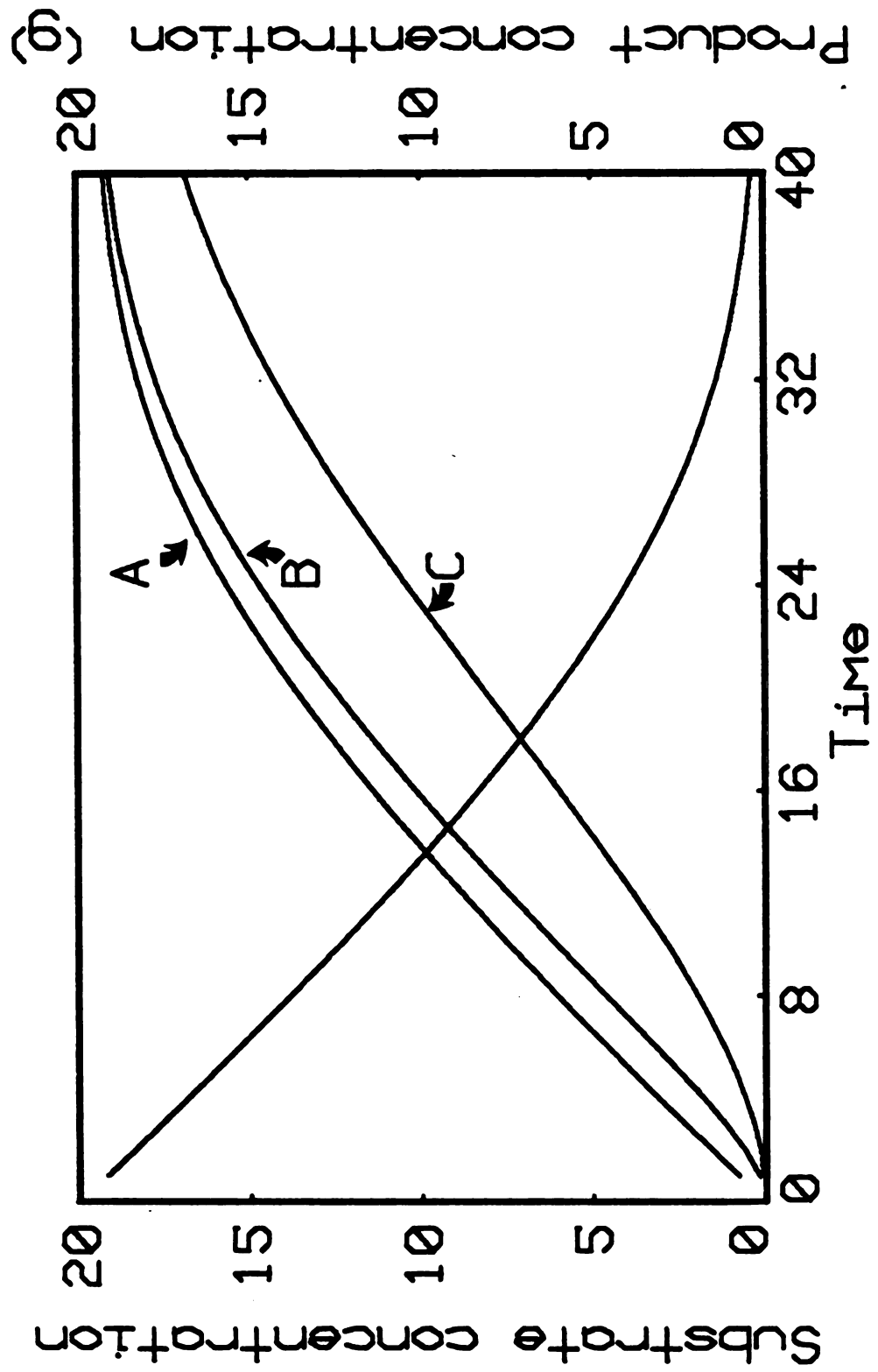


Figure 6

be ascribed to the estimated  $K_m$ 's.

Ascertaining whether or not mass-transport limits gaseous product appearance in the gas phase, when this product is derived from a non-gaseous substrate, is complicated because sigmoidal product appearance may result from (i) substrate depletion under phase-transfer limited conditions and (ii) growth-linked product formation. As for the cases mentioned above, kinetic parameters for product formation will depend on  $S_0$  and  $V_{max}$  under mass-transport limitations. But the only way to check for the obfuscating influence of growth is by following substrate depletion. If substrate consumption is non-sigmoidal and product appearance is sigmoidal, then chances are a mass-transport limitation exists (Figure 7). This assumes that no lag occurs before Michaelis-Menten substrate depletion commences. In summary, both the non-gaseous substrate and gaseous product should be monitored in order to verify that gaseous product formation is not limited by its movement from the aqueous into the gaseous phase. Only then may estimates of microbial kinetic parameters be obtained that are independent of physical parameters that affect the  $K_{La}$ , such as stirring speed and inter-facial area.

Should only aqueous phase data be used to calculate saturation kinetic parameters for gaseous substrate consumption? After extensively simulating gaseous substrate consumption using the PHASIM model, I found apparent  $V_{max}$ 's for substrate depletion depend on the partition coefficient ( $B$ ) when aqueous phase data are used to estimate this kinetic parameter. In contrast, the estimated  $K_m$  equals the  $K_m$  used for a given simulation when this parameter is calculated from aqueous phase substrate concentrations (Figure 8). PHASIM also predicts that  $V_{max}$

Figure 7. Gaseous product formation from a non-gaseous substrate for different values of  $K_{1a}$ . Same parameter values and initial conditions used for Figure 6.



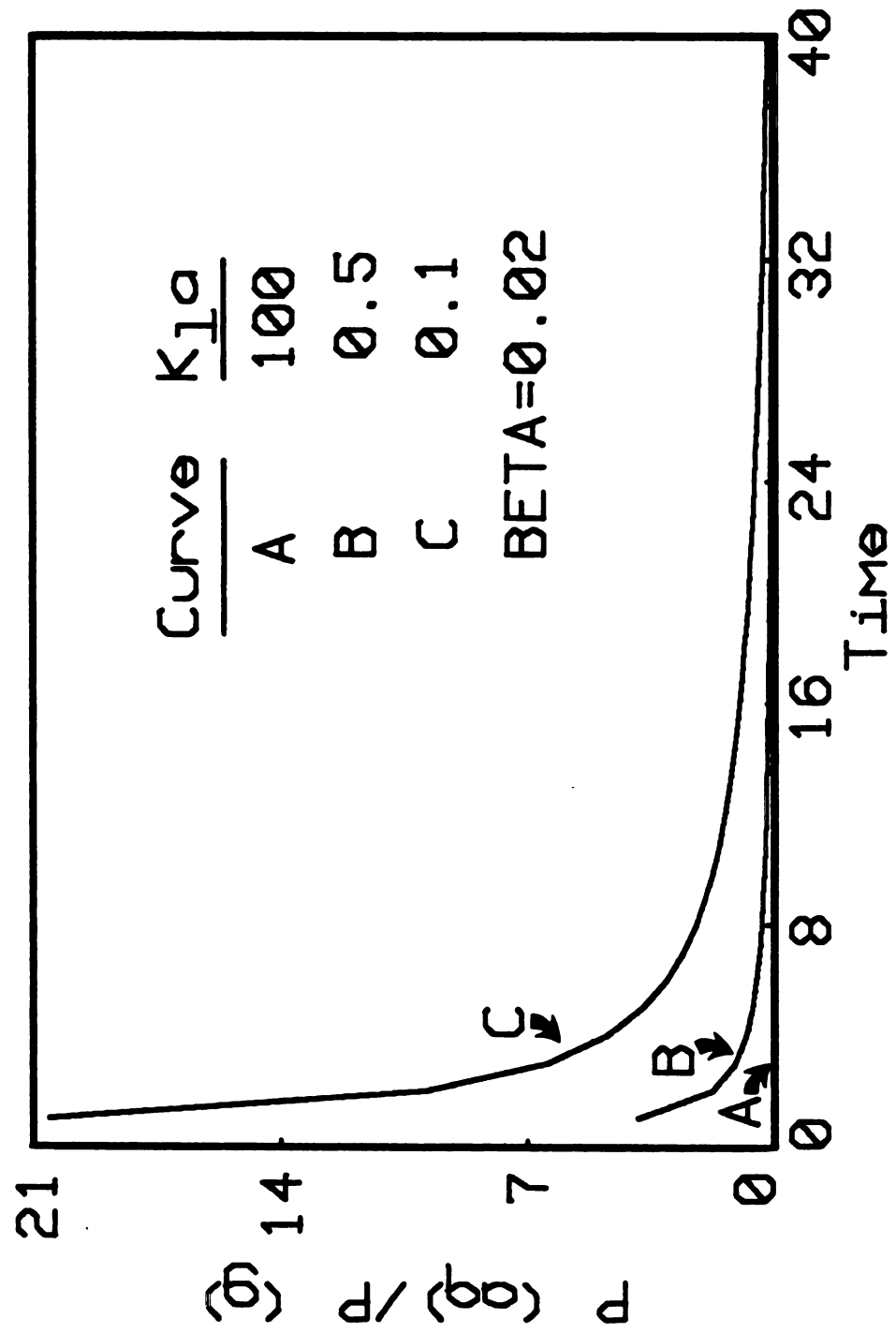


Figure 7

Figure 8. Influence of gaseous substrate solubility on  $K_{m,app}$  and  $V_{max,app}$  estimated from aqueous phase data.  $V_{max}$  and  $K_m$  values were each 5, and the  $K_{1a}$  was 50 for all simulations. Note  $K_{m,app} (aq)$  equals  $K_m$  and  $V_{max,app} (aq)$  does not equal  $V_{max}$ .

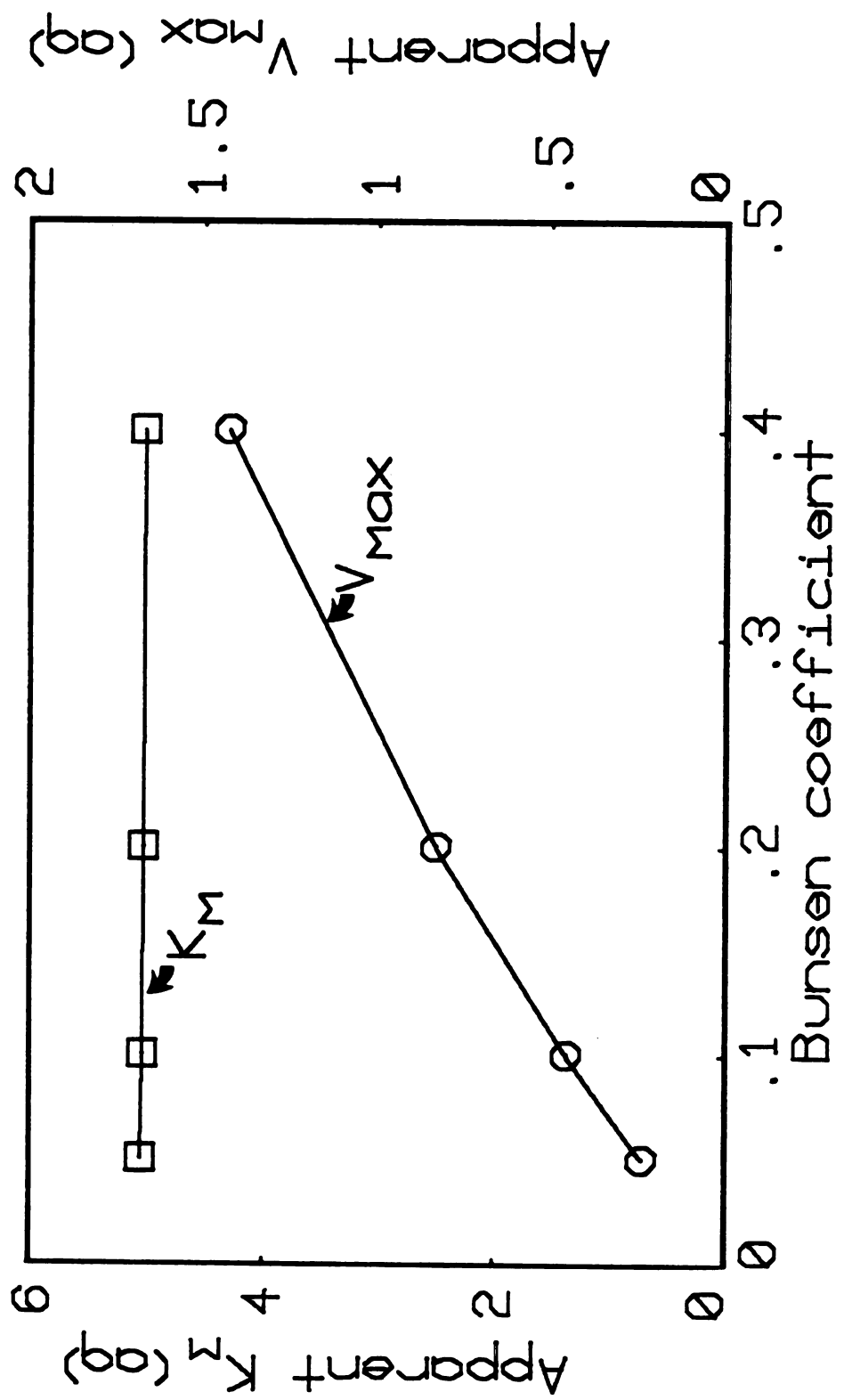


Figure 8

Figure 9. Influence of gaseous substrate solubility on  $K_{m,app}$  and  $V_{max,app}$  estimated from for total mass (mol) of gaseous substrate being consumed with time. Same parameter values used for Figure 8. Note that  $V_{max,app} (tot)$  equals  $V_{max}$ , whereas  $K_{m,app} (tot)$  does not equal  $K_m$ .

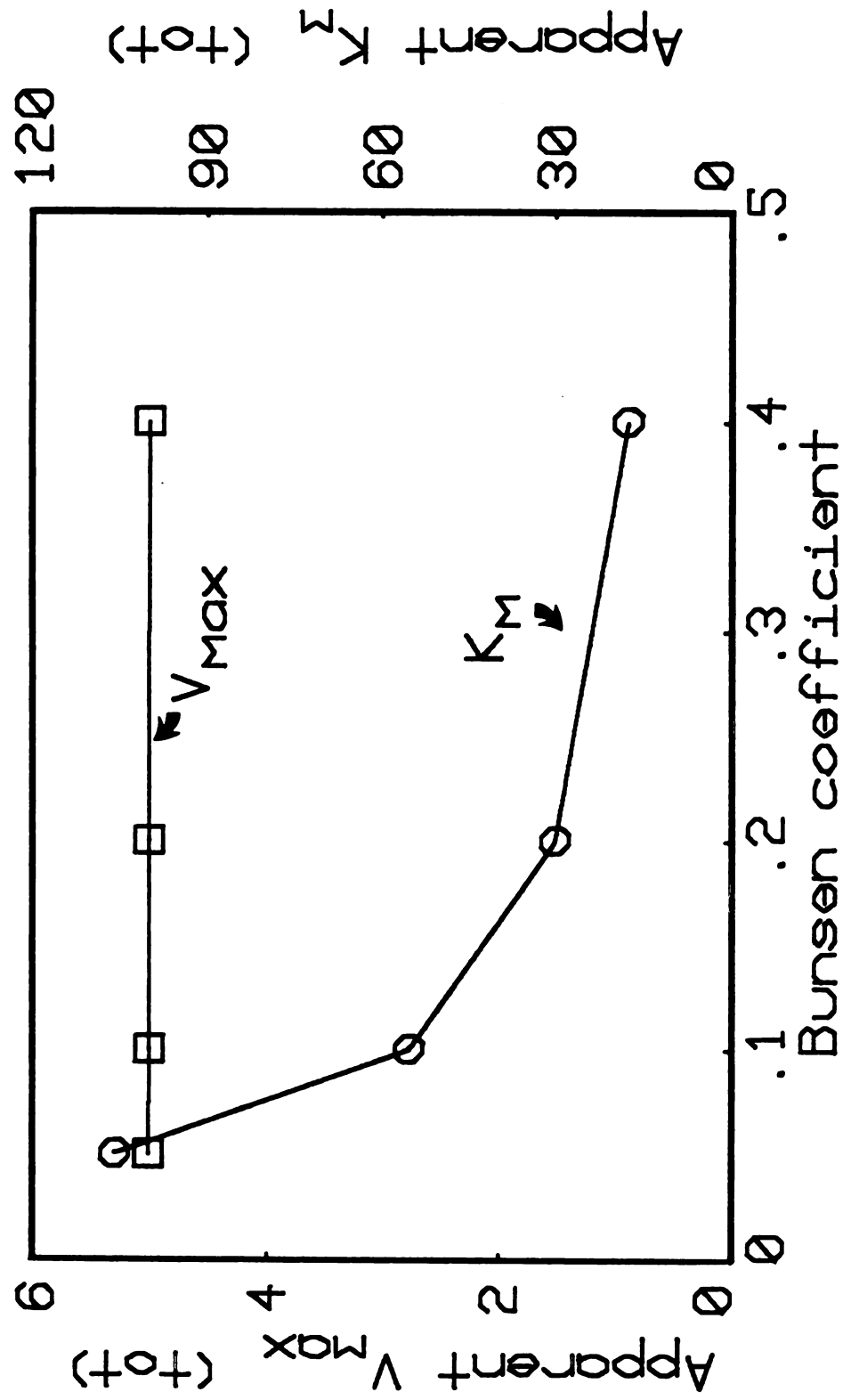


Figure 9

should be calculated from the sum,  $S_a$  plus  $S_g$ , since only when this is done do apparent  $V_{\max}$ 's equal the  $V_{\max}$ 's used to simulate the data (Figure 9). These predictions are supported by the observation that theoretical  $S_g$  curves approximate actual  $H_2$  progress curves only when  $K_m$ 's calculated from aqueous phase data and  $V_{\max}$ 's estimated from total quantities of  $H_2$  consumed are plugged into PHASIM. Using the  $V_{\max}$  estimated from aqueous  $H_2$  consumption data yields theoretical progress curves far too long compared to  $H_2$  depletion curves presented in chapters I and III. The above findings may be generalized as follows: half-saturation kinetic parameters should be estimated from substrate concentrations occurring in the phase containing the microorganisms, while  $V_{\max}$  estimates should be calculated from the total amount of the partitioning substrate consumed in the closed system. Of course, this assumes that a mass-transport limitation is absent.

A preliminary analysis of gaseous substrate consumption for growing cells suggest that (i) like  $K_m$ ,  $K_s$  should be estimated from aqueous phase data, (ii) in analogy with  $V_{\max}$ ,  $Y$  should be calculated from the total quantity of partitioning substrate being consumed, and (iii)  $u_{\max}$  may be estimated from gaseous or aqueous phases substrate concentrations, or the sum of these two. These statements need some explanation. The  $K_s$  is computed using only aqueous phase data because it's the liquid phase concentration of the growth-limiting substrate that determines to what extent the bacteria are saturated. Since biomass-C (or electrons) may be derived from the gaseous substrate present in either of the 2 phases, then  $Y$  should be estimated using data for the total amount of the substrate present in the closed system. Finally, the cells do not partition and estimation of their growth rate requires

no knowledge of the partitioning substrates' fate therefore,  $u_{\max}$  will be identical no matter which phase (or both) substrate depletion is monitored in.

#### LITERATURE CITED

1. Burden, R. L., J. D. Faires, and A. C. Reynolds. 1978. Numerical analysis. Prindle, Weber and Schmidt. Boston, Massachusetts. p. 239-245.
2. Charles, M. 1980. Technical aspects of the rheological properties of microbial cultures. Advances in biochemical engineering. 8: 1-62.
3. Ngian, R. F., S. H. Lin, and W. R. B. Martin. 1977. Effect of mass transfer resistance on the Lineweaver-Burk plots for flocculating microorganisms. Biotech. Bioeng. 19: 1773-1784.
4. Pirt, S. J. 1975. Principles of cell and microbe cultivation. John Wiley and Sons, Inc., New York, New York. p. 22-28.
5. Robinson, J. A., and J. M. Tiedje. Kinetics of hydrogen consumption by rumen fluid, anaerobic digester sludge and sediment. Appl. Environ. Microbiol. in press.
6. Schonheit, P. J., J. Moll, and R. K. Thauer. 1980. Growth parameters ( $K_s$ ,  $u_{max}$  and  $Y_s$ ) of Methanobacterium thermoautotrophicum. Arch. Microbiol. 127: 59-65.
7. Shieh, W. K. 1979. Theoretical analysis of the effect of mass-transfer resistances on the Lineweaver-Burk plot. Biotech. Bioeng. 21: 503-504.



## APPENDIX B

## PROGRESS CURVE ANALYSIS

Michaelis-Menten kinetics. Either the derivative or integrated forms of the Michaelis-Menten equation can be used to estimate  $K_m$  and  $V_{max}$ . Both of these forms are examples of nonlinear models that may be algebraically transformed into linear models. Linearized versions of the derivative form of the Michaelis-Menten equation, most typically the Lineweaver-Burk equation, have received widespread use for estimation of the above two kinetic parameters from initial velocity data (4). To a lesser extent, product appearance data obtained from progress curve experiments have been fitted to a linearized version of the integrated Michaelis-Menten equation to estimate  $K_m$  and  $V_{max}$  (11). Use of the integrated form has the advantage that estimates of  $K_m$  and  $V_{max}$  can be obtained from a single experiment in which substrate depletion or product formation is monitored, assuming that product inhibition is absent. In contrast, multiple experiments are required if the derivative form of the equation is employed and thus, the integrated Michaelis-Menten equation is preferable when routine estimates of these parameters are needed.

Notwithstanding use of linearized versions of Michaelis-Menten equations, its always preferable to directly fit data to nonlinear models since transforming data for fitting to linearized versions of these models concomitantly transforms the measurement errors (4). The inappropriateness of using ordinary least-squares analysis to fit data to linearized forms of Michaelis-Menten expressions has been previously pointed out (4). This practice should only be used to obtain

provisional estimates of the Michaelis-Menten parameters for subsequent improvement via nonlinear regression analysis. But a disadvantage to using nonlinear extremization techniques is these are iterative procedures (2), which can require appreciable computing power. The dramatic increase in availability of inexpensive microcomputers now makes it possible to take full advantage of these parameter estimation techniques when fitting data to integrated and derivative forms of equations describing enzyme-catalyzed reactions. Thus, linearized versions of these nonlinear models may be relegated to providing initial estimates of parameters and for illustrative purposes only.

After integration, the Michaelis-Menten expression for product appearance is

$$V_{\max}t = P + K_m \ln[S_0/(S_0 - P)] \quad [B.1]$$

where,  $V_{\max}$ =the maximum rate of product appearance (or substrate consumption),  $t$ =time,  $P$ =product concentration at time  $t$ ,  $K_m$ =substrate concentration at which rate of product appearance is half-maximal, and  $S_0$ =the initial substrate concentration. Since the rate of product formation equals the rate of substrate consumption, [B.1] can be rewritten to give

$$V_{\max}t = S_0 - S + K_m \ln(S_0/S) \quad [B.2]$$

in which  $S$ =the substrate concentration at time  $t$ . The integrated Michaelis-Menten equation cannot be explicitly solved for either  $P$  or  $S$ , but solutions to it can be approximated using either (i) Newton's method for finding roots to implicit functions or by (ii) numerically integrating the derivative form of this expression (3).

Linear analysis. As alluded to previously, the integrated Michaelis-Menten equation can be linearized. Three different

linearizations, taken from a monograph by Cornish-Bowden (4), are shown below.

$$t/\ln(S_0/S) = (1/V_{\max})[(S_0 - S)/\ln(S_0/S)] + K_m/V_{\max} \quad [B.3]$$

$$(S_0 - S)/t = V_{\max} - K_m \ln(S_0/S)/t \quad [B.4]$$

$$t/(S_0 - S) = (K_m/V_{\max}) \ln[(S_0/S)/(S_0 - S)] + 1/V_{\max} \quad [B.5]$$

In theory, any of the above three expressions can be used to estimate  $K_m$  and  $V_{\max}$  when substrate disappearance data are appropriately transformed. But in practice [B.3], [B.4] and [B.5] yield different estimates of these parameters because each transforms the measurement errors differently. Additionally, goodness-of-fit (using  $r^2$  as the criterion) of the transformed data to [B.3], [B.4] and [B.5] will be dissimilar for the same reason. The simulated progress curve data plotted in Figure 1 illustrate these points. The lines are error-free substrate concentrations transformed and plotted according to [B.3], [B.4] and [B.5]. These data were generated by solving [B.2] for a  $K_m$  and  $V_{\max}$  of 1 and an  $S_0$  of 2. With these are plotted error curves for the three different linearizations, derived by either adding or subtracting a constant error of 0.01 units to the data before they were transformed. Linearization [B.4], which has received the most use (11), is the least statistically acceptable of the three. Equation [B.5] gives the best fit for linearized data, while the influence of measurement error on data transformed for fitting to [B.3] is intermediate between [B.4] and [B.5]. Analogous results are found for linearized data having a constant relative error of 0.005 units (Figure 2). Similar conclusions hold for product formation, with

$$t/P = (K_m/V_{\max}) \ln[S_0/(S_0 - P)/P] + 1/V_{\max} \quad [B.6]$$

providing the best estimates of  $K_m$  and  $V_{\max}$  for transformed data.

Figure 1. Plots of Michaelis-Menten progress curve data transformed according to [B.3] (A), [B.4] (B) and [B.5] (C) with simple error bars of  $\pm 0.01$  units.  $K_m=1$ ,  $V_{max}=1$  and  $S_0=2$ .

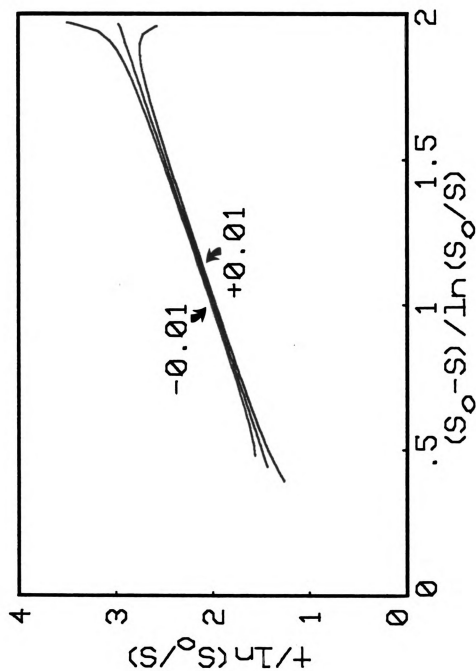


Figure 1

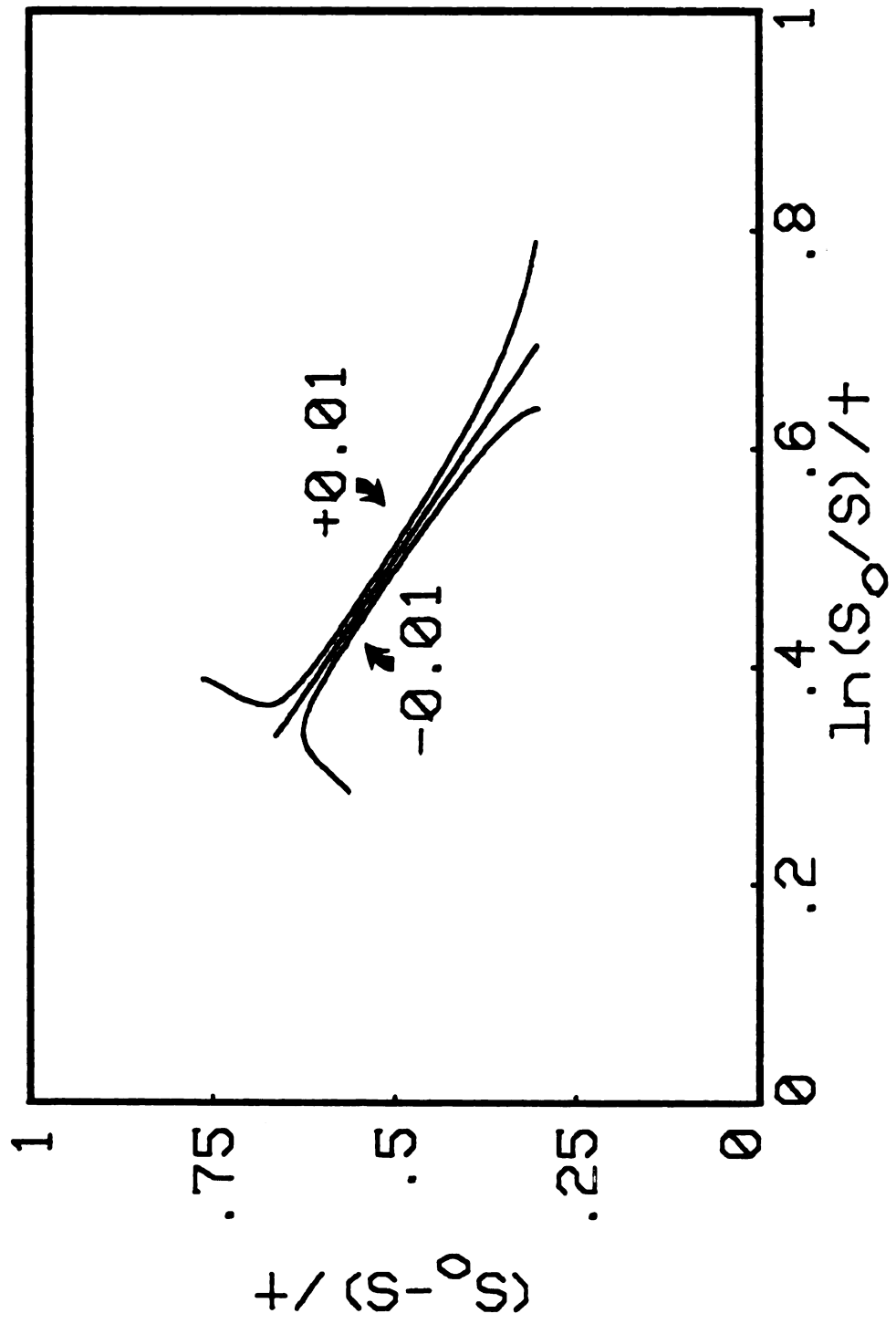


Figure 1 continued

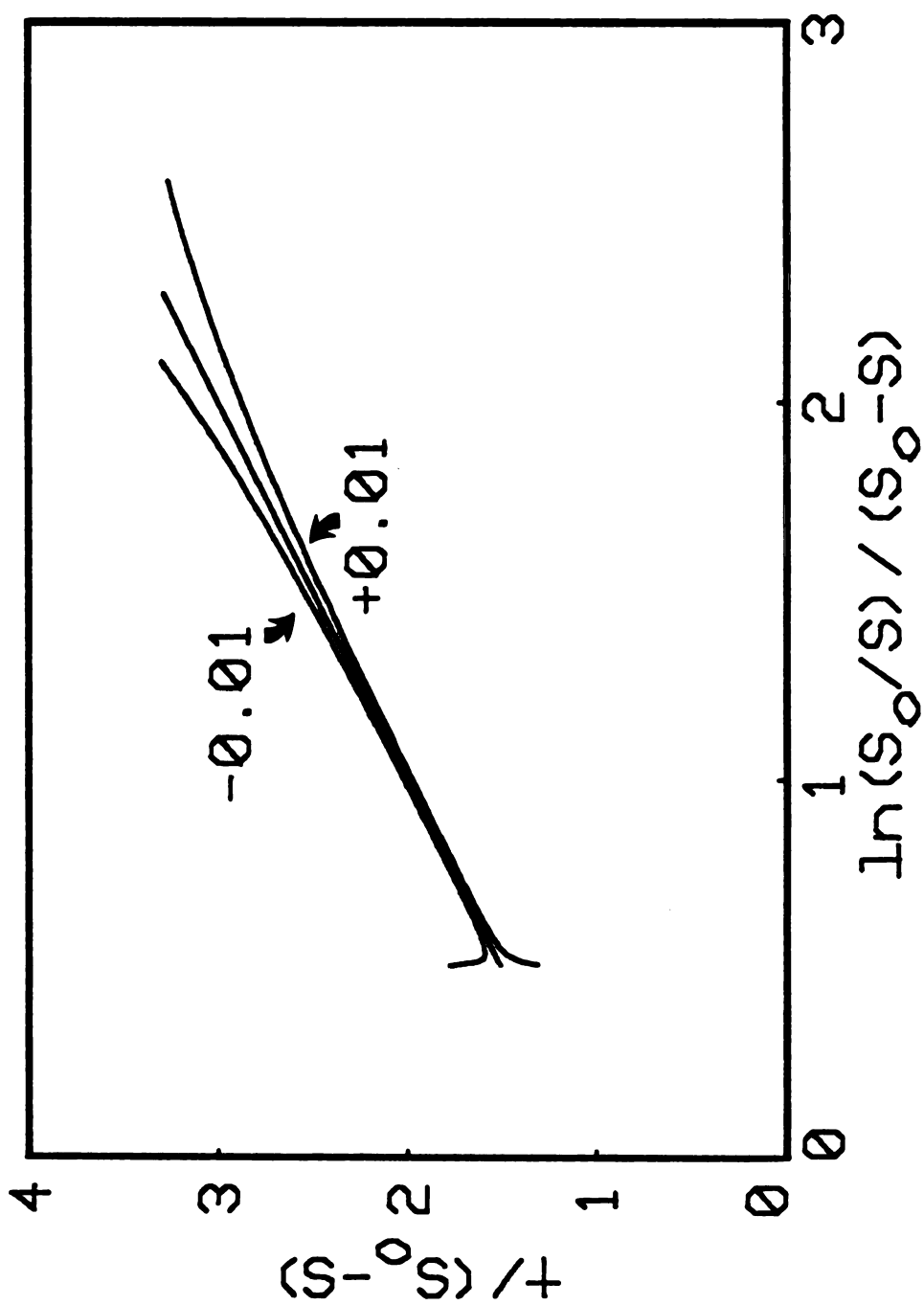


Figure 1 continued

Figure 2. Plots of Michaelis-Menten progress curve data transformed according to [B.3] (A), [B.4] (B) and [B.5] (C) with relative error bars of  $\pm 0.005$  units. Same  $K_m$ ,  $V_{max}$  and  $S_0$  used for Figure 1.



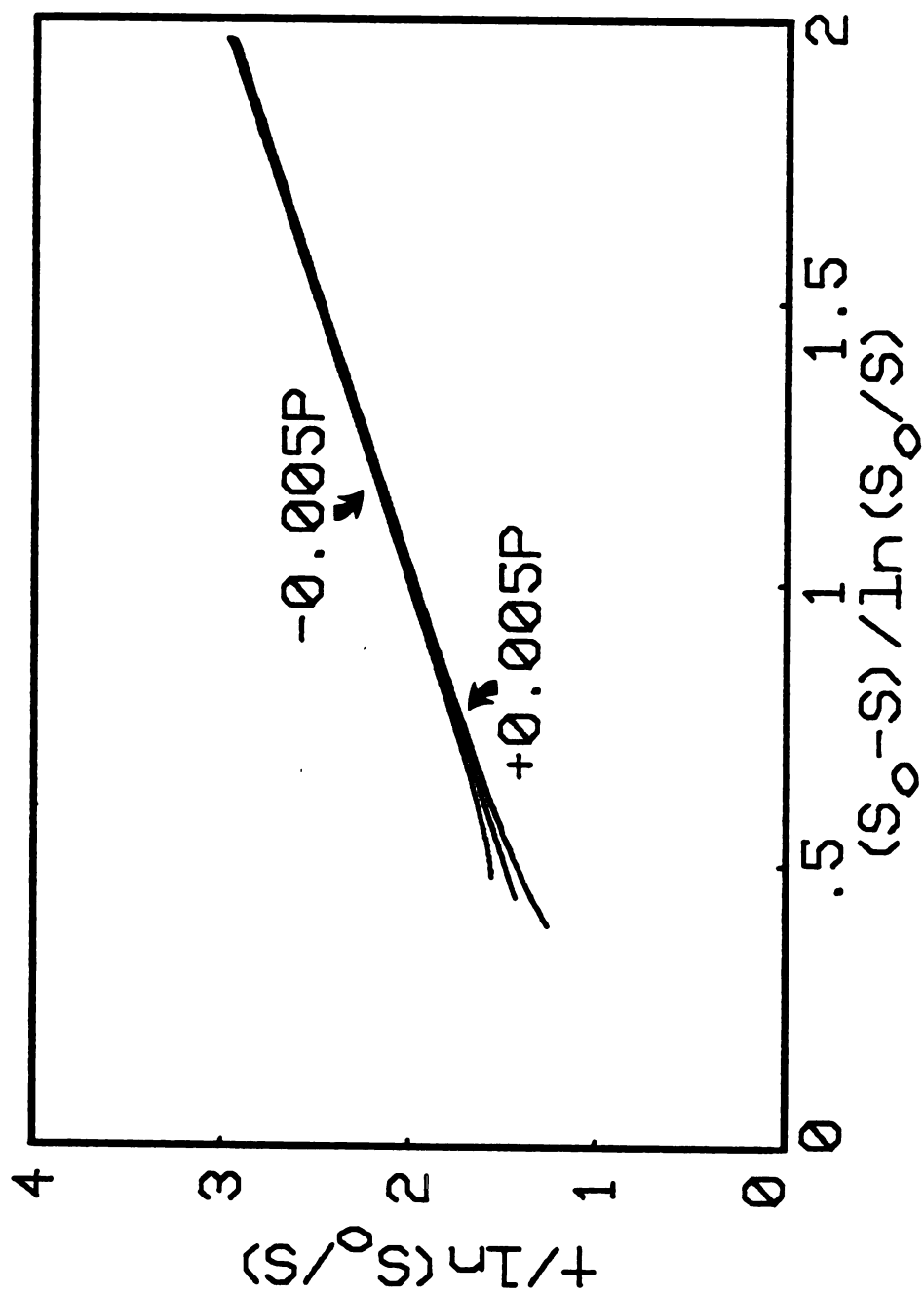


Figure 2

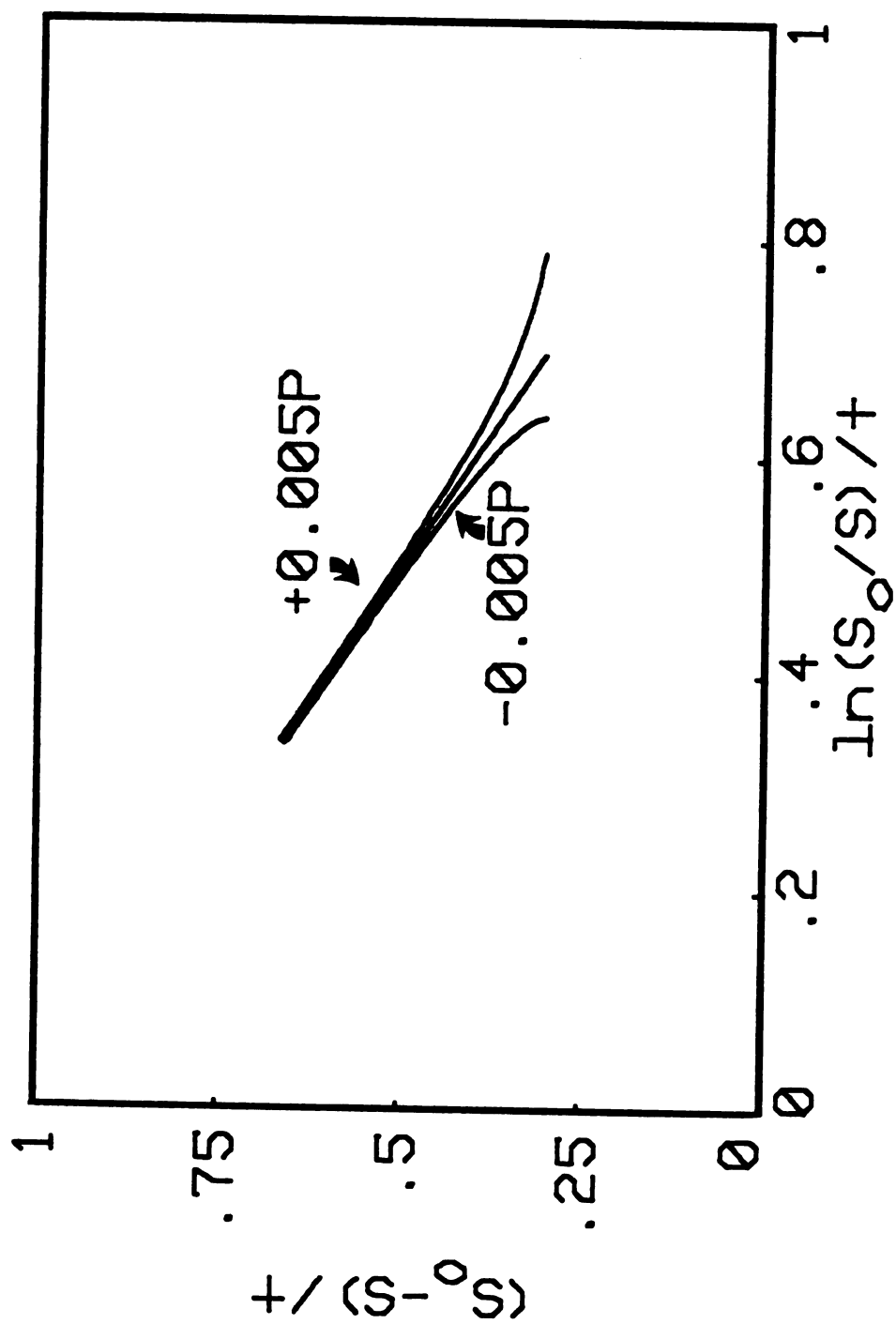


Figure 2 continued

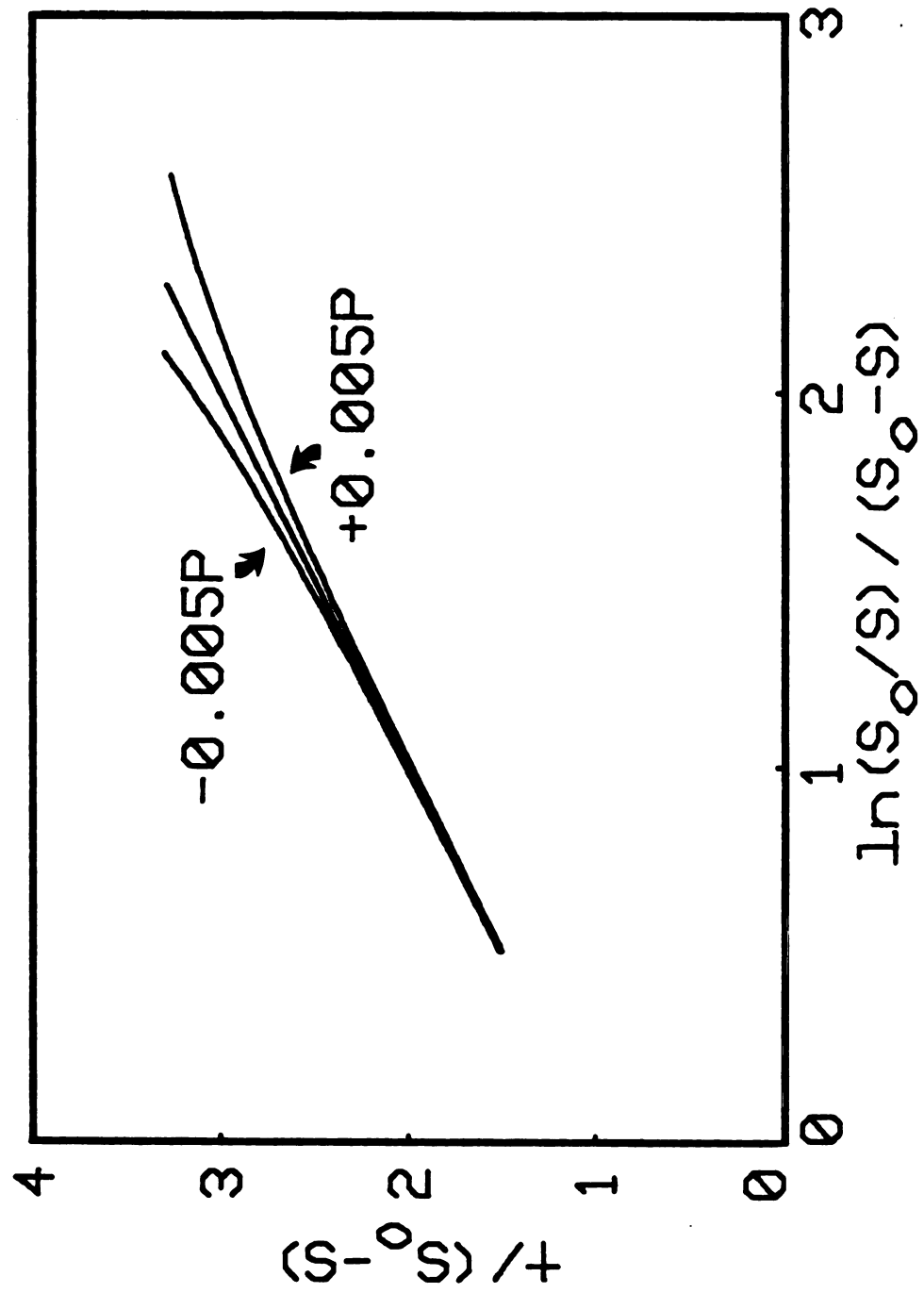


Figure 2 continued

Nonlinear analysis. The use of iterative techniques for fitting data to nonlinear equations requires that the sensitivity of the dependent variable to changes in each of the parameters be calculable. The first derivatives of P or S with respect to  $K_m$  and  $V_{max}$  satisfy this requirement and these expressions may be derived from [B.1] or [B.2] using implicit differentiation (14). The sensitivity equations for  $K_m$  and  $V_{max}$  are only different in sign when derived from [B.1] versus [B.2]. The sensitivity of S to changes in  $V_{max}$  is described by

$$dS/dV_{max} = -t/(1+K_m/S) \quad [B.7]$$

and the sensitivity of S to  $K_m$  is given by

$$dS/dK_m = \ln(S_0/S)/(1+K_m/S) \quad [B.8]$$

Note that [B.7] and [B.8] are both functions of  $K_m$ . By definition then, the integrated Michaelis-Menten equation is a nonlinear model since its sensitivity equations are not independent of the parameters. Linear models have sensitivity equations that are functions of only the independent variable or equal unity (2).

In addition to their being required for nonlinear regression, the sensitivity equations predict (i) whether the parameters may be uniquely estimated or not, (ii) the relative precision of the estimated parameters, and (iii) the range of the independent variable over which the model is most sensitive to changes in the parameters. The last item is useful in designing optimal experiments for parameter estimation (2). If the sensitivity equations are proportional, then its impossible to obtain unique estimates of the paramters from the data using least-squares analysis (2). Unique parameter estimates may be obtained when the sensitivity equations are very similar, but they are highly correlated. This situation is undesirable since it implies that several

combinations of parameter estimates may describe the same data set and is somewhat true for the integrated Michaelis-Menten equation, depending on  $S_0$ . The sensitivity equations for  $K_m$  [B.8] and  $V_{max}$  [B.7] yield similar curves with the former being numerically dominated by the latter (Figure 3). These facts explain the strong correlation among errors in these 2 parameters and the tendency of standard error estimates for  $V_{max}$  to be less than those for  $K_m$  (4,13). Lower standard errors for  $V_{max}$  versus  $K_m$  run contrary to intuition since the optimal initial substrate concentration for progress curve experiments is in the mixed-order region ( $2-4 \times K_m$ ). But the explanation lies in the behavior of the integrated Michaelis-Menten equation itself and the sensitivity equations derived from it.

There exist a number of techniques that may be used to fit S-t data pairs to [B.2] in the least-squares sense. I used the Gaussian method (2) to fit the  $H_2$  consumption data presented in chapters I and III to this nonlinear model. This technique uses the equation

$$S - S_0 = \Delta V_{max} dS/dV_{max} + \Delta K_m dS/dK_m \quad [B.9]$$

where,  $S_0$  = theoretically predicted substrate concentration at time  $t$  given current parameter estimates, and  $\Delta K_m$  plus  $\Delta V_{max}$  are correction terms for these parameters. Equation [B.9] is similar to one that has previously appeared for analysis of product formation data (1,11). Application of [B.9] proceeds by first evaluating the sensitivity equations [B.7] and [B.8] for the measured substrate concentrations and the residual errors ( $S_0 - S$ ) using the initial parameter estimates. Initial estimates may be obtained from [B.3], [B.4] or [B.5]. The correction terms are then calculated using multiple linear regression and are added (they may be positive or negative) to the initial

Figure 3. Sensitivity coefficients for  $K_m$  and  $V_{max}$ . Same parameter values and  $S_0$  used for Figure 1. Note sensitivity coefficients for  $K_m$  and  $V_{max}$  differ only in sign when derived from [B.1] versus [B.2].

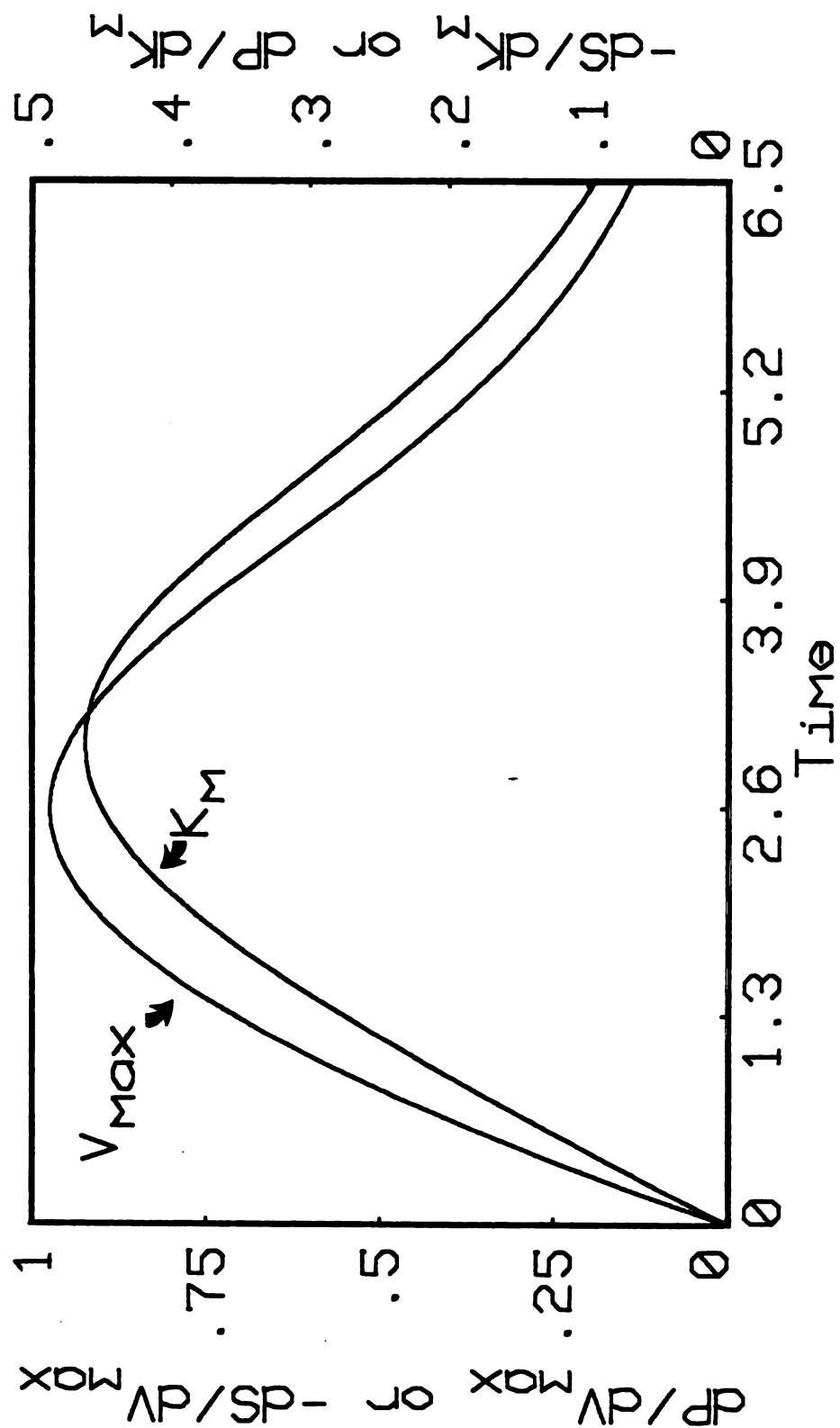


Figure 3

estimates of  $K_m$  and  $V_{max}$ . These then serve as the 'initial estimates' for the next iteration and this process continues until the correction terms are less than some small value (e.g., 0.0001). Once the solution has converged, estimates of the standard errors of  $K_m$  and  $V_{max}$  are calculated from the variances of their respective correction terms (6).

Monte Carlo simulation. The superiority of nonlinear regression analysis for [B.2] over linear least-squares analysis of transformed progress curve data fitted to [B.3], [B.4] or [B.5] can be demonstrated by analyzing simulated data containing known measurement errors. I simulated progress curve experiments by solving [B.2] with values for  $K_m$ ,  $V_{max}$  and  $S_0$  of 1, 1, and 2, respectively. Measurement errors of either the simple (constant standard deviation) or relative (constant coefficient of variation) type were introduced into these error-free data using a pseudo-random number generator, according to the procedure of Harbaugh and Bonham-Carter (8). For simple errors a standard deviation of 0.01 units was used, whereas relative errors were created for a coefficient of variation of 0.005 units. The simulated data were analyzed using (i) equations [B.4] and [B.5] and (ii) by fitting the  $S-t$  data pairs directly to [B.2] using [B.9]. Nonlinear analysis of the simulated data yielded the best estimates of  $K_m$  and  $V_{max}$  as well as giving consistently lower values for the residual sum-of-squares (Table 1).

Nonlinear analysis when  $S_0$  is unknown. In the progress curve experiments described in chapters I and III the initial substrate concentration had to be estimated. It could not be directly measured because of the time required (ca., 5 min) for  $H_2$  injected into the recirculating gas stream to become homogeneously distributed. For these



Table 1. Comparison of nonlinear versus linear analysis of Michaelis-Menten progress curve data containing simple or relative errors.<sup>a</sup>

Mean (n = 16) <sup>b</sup>	Simple errors			Relative errors		
	SD = 0.01	SD = 0.02	SD = 0.04	CV = 0.05	CV = 0.01	CV = 0.02
$K_m, i^e$	0.90	0.92	0.88	0.88	0.96	0.96
$K_m, f^d$	1.03	1.07	1.15	1.00	1.08	0.98
$V_{max, i}^c$	0.94	0.95	0.91	0.94	0.99	0.90
$V_{max, f}^d$	1.01	1.02	1.07	1.00	1.02	0.99
$RSS_i/RSS_f^e$	1.51	1.51	1.77	2.75	2.75	2.08

<sup>a</sup>Progress curves were generated by solving [B.2] for a  $K_m$  and  $V_{max}$  of 1 and an  $S_0$  of 2. Simple (constant standard deviation) and relative (constant coefficient of variation) errors were generated using an equation derived from the central limit theorem (8).

<sup>b</sup>Parameter values are means of 16 progress curve replicates. Each progress curve contained 50 equally spaced data points and were run until 95% complete. Initial estimates were calculated from linear regression analysis of data transformed according to [B.5].

<sup>c</sup>Final estimates were obtained by directly fitting the substrate depletion data to [B.2] using PROGCVR 1 (Appendix C), given the initial estimates.

<sup>d</sup>Ratio of residual sum-of-squares for initial parameters estimates to residual sum-of-squares for final parameter estimates.

Figure 4. Sensitivity coefficients for  $S_0$  derived from [B.1] versus [B.2]. Same  $K_m$ ,  $V_{\max}$  and  $S_0$  used for Figure 1.

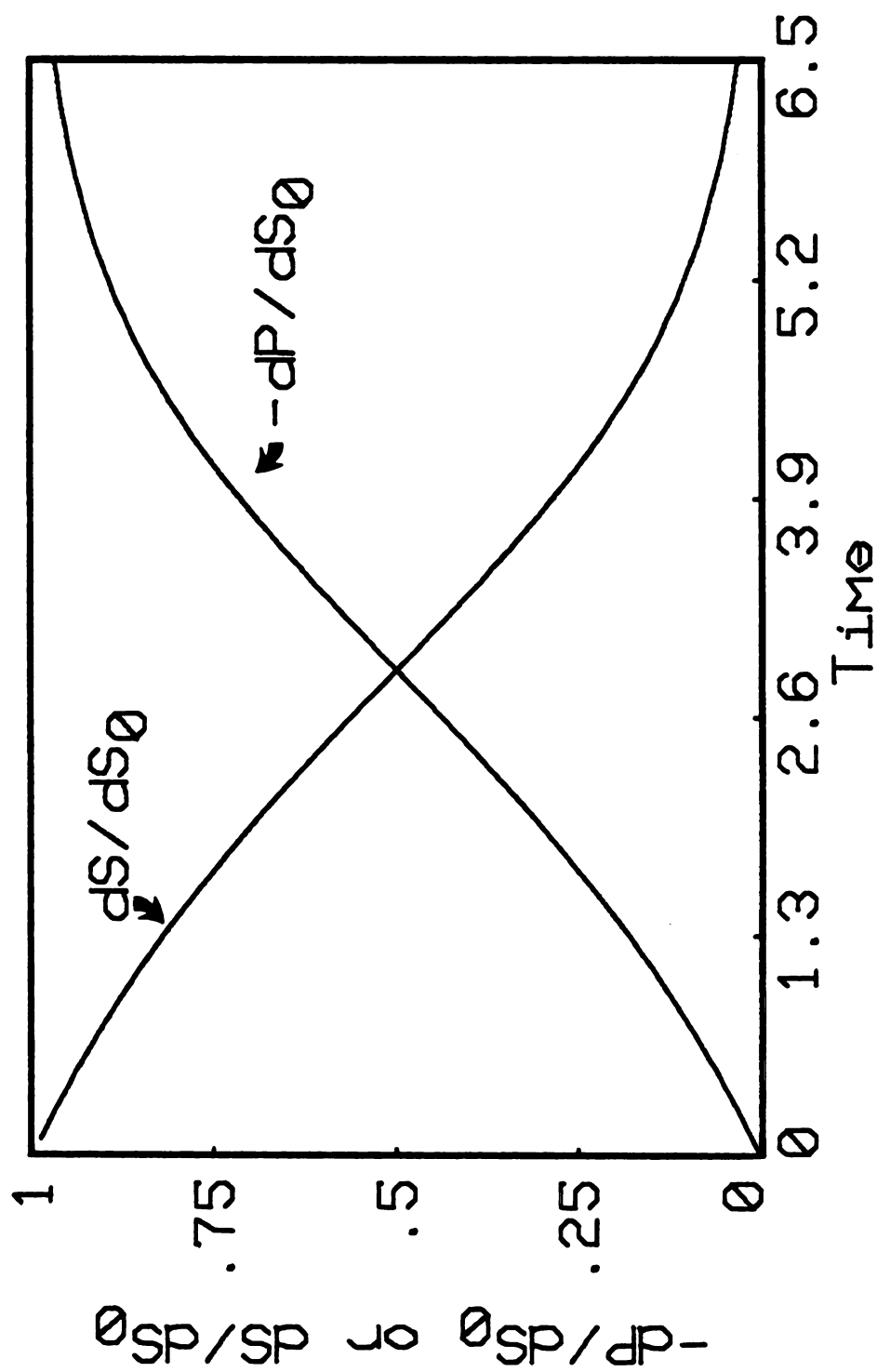


Figure 4

experiments,  $S_0$  was estimated by fitting a straight line to the first 3-6 data points and extrapolating back to the S axis.

Its possible to treat an initial state, such as  $S_0$ , as another 'parameter' to be estimated using nonlinear regression analysis (2). But a sensitivity equation for  $S_0$  is required before this can be done. The sensitivity of S to changes in  $S_0$ , derived from [B.2], is given by

$$dS/dS_0 = (1 + K_m/S_0) / (1 + K_m/S) \quad [B.10]$$

An equation for the sensitivity of P to  $S_0$  may be derived from [B.1] and is

$$dP/dS_0 = K_m [1/S_0 - 1/(S_0 - P)] / [1 + K_m/(S_0 - P)] \quad [B.11]$$

Equation [B.10] and [B.11] describe curves that are mirror images of one another (Figure 4). I have found its not possible to update  $S_0$  when data is fitted to [B.1]. This holds for product data ( $CH_4$ ,  $H_2S$ ) and substrate data ( $H_2$ ) when the latter is converted into the equivalent of the former using the relation,  $P = S_0 - S$ . This likely results from the best information on  $S_0$  being at the end of a progress curve in which product is followed, whereas the opposite holds when substrate depletion is monitored (Figure 4).

In Appendix C is are listed two computer programs that fit data to integrated Michaelis-Menten equations. The first (PROGCRV1) is for substrate disappearance data and estimates  $K_m$  and  $V_{max}$  when  $S_0$  is unknown. It employs equation [B.9] amended with a third term ( $\Delta S_0 dS/dS_0$ ) to fit S-t data pairs to [B.2]. The second program PROGCRV2 also fits data to a 3-parameter model, but its for product appearance when the origin of the progress curve is unknown. An equation similar to [B.9] is used to fit a version of [B.1] that includes the displacement parameter,  $P_0$  (1,6). Both of these programs also estimate the standard

errors of the parameters assuming no correlation among the measurement errors.

Monod kinetics. Michaelis-Menten kinetics describes substrate consumption where the amount of catalytic units present is constant. Indeed it makes little sense to estimate  $V_{\max}$  when this parameter changes over the course of a progress curve experiment. In chapter III, I show data in which growth occurred during the course of  $H_2$  consumption. These data are inconsistent with the integrated Michaelis-Menten model, but may be fitted to a version of the Monod growth model. The rate of substrate consumption for a growing bacterial culture in a closed environment may be described by

$$dS/dt = -\{u_{\max}S/(K_s+S)\}X/Y \quad [B.12]$$

where,  $u_{\max}$ =the maximum specific growth rate,  $K_s$ =the half-saturation constant for growth and  $Y$ =the yield coefficient. The variable  $X$  equals the biomass concentration and may be eliminated from [B.12] using

$$X=Y(S_0-S)+X_0 \quad [B.13]$$

which relates the biomass concentration at time  $t$  to the substrate concentration  $S$ . After elimination of  $X$ , [B.12] becomes

$$dS/dt = -[u_{\max}S/(K_s+S)][Y(S_0-S)+X_0]/Y \quad [B.14]$$

which may be integrated to give

$$C_1 \ln\{[Y(S_0-S)+X_0]/X_0\} - C_2 \ln(S/S_0) = u_{\max}t \quad [B.15]$$

where,  $C_1=(K_sY+S_0Y+X_0)/(YS_0+X_0)$  and  $C_2=K_sY/(YS_0+X_0)$ . Equation [B.15] gives the familiar S-shaped curve for substrate depletion during batch growth. A relation similar to [B.15] describing the increase of biomass during batch growth has been derived by integrating the expression obtained after eliminating  $S$  from [B.12] using the mass-balance relation [B.13] (10,12).

Equation [B.15] like [B.2] is implicit in S and its solution must be numerically approximated. Though Newton's method works for approximating solutions to [B.2], I have been unable to solve [B.15] using this technique. But solution curves may be estimated by solving [B.12] simultaneously with

$$dX/dt=[u_{\max}S/(K_s+S)]X \quad [B.16]$$

using numerical integration. An example of a solution is depicted in Figure 5, which was solved for the following initial conditions and parameter values:  $u_{\max}=0.1$ ,  $K_s=5$ ,  $Y=0.2$ ,  $X_0=1$  and  $S_0=20$ .

Linear analysis. Its not possible to linearize the integrated Monod equation for the purpose of obtaining provisional  $K_s$ ,  $U_{\max}$  and Y estimates from transformed S-t data pairs. But initial estimates of these paramters may be obtained using

$$-\Delta S/\Delta t=[u_{\max}S/(K_s+S)]X/Y \quad [B.17]$$

and

$$\Delta X/\Delta t=[u_{\max}S/(K_s+S)]X \quad [B.18]$$

Equations [B.17] and [B.18] are derived by replacing infinitesimal time (dt) with finite time ( $\Delta t$ ) and are approximately correct if  $\Delta t$  is relatively small (14). These finite-difference equations are nonlinear, but may be linearized by taking the reciprocals of both sides giving

$$-\Delta t/\Delta S=(K_s Y/u_{\max})X/S+YX/u_{\max} \quad [B.19]$$

and

$$\Delta t/\Delta X=(K_s/u_{\max})X/S+X/u_{\max} \quad [B.20]$$

If both sides of [B.19] and [B.20] are multiplied by X then these equations become

Figure 5. Sigmoidal substrate consumption (S) and biomass formation (X) for cells growing in batch. Equation [B.14] was numerically integrated for the following parameter values and initial conditions:  $u_{\max}=0.1$ ,  $K_s=5$ ,  $Y=0.2$ ,  $S_0=20$  and  $X_0=1$ .

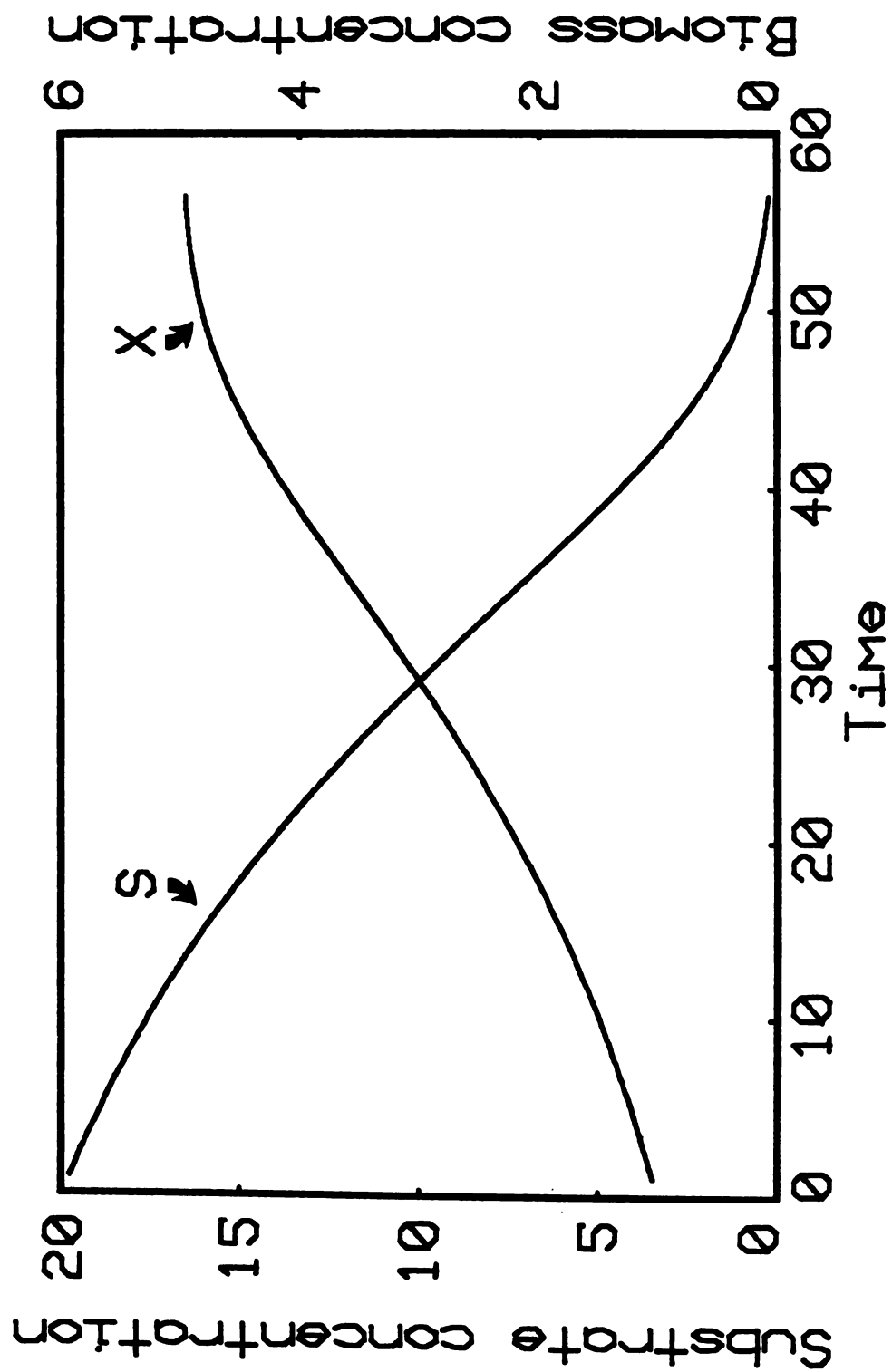


Figure 5



$$-\Delta tX/\Delta S = (K_s Y/u_{\max})1/S + Y/u_{\max} \quad [B.21]$$

and

$$\Delta tX/\Delta X = (K_s/u_{\max})1/S + 1/u_{\max} \quad [B.22]$$

which yield straight lines when  $\Delta tX/\Delta S$  and  $\Delta tX/\Delta X$  are plotted against  $1/S$  (Figure 6). Thus, [B.21] and [B.22] may be used to estimate  $K_s$ ,  $u_{\max}$  and  $Y$  given  $S$ - and  $X$ - $t$  data pairs.

Nonlinear analysis. As was the case for [B.2],  $S$ - $t$  data pairs may be fitted to [B.15] using the Gaussian technique. The required sensitivity equations for the parameters of this nonlinear model are

$$dS/du_{\max} = -t/C_6 \quad [B.23]$$

$$dS/dK_s = (Y/C_5)[\ln(X/X_0) - \ln(S/S_0)]/C_6 \quad [B.24]$$

$$dS/dY = \{C_3(S_0 - S)/X + \ln(X/X_0)/C_5[K_s + (1 - C_3)S_0] - \ln(S/S_0)/C_5(K_s - C_4S_0)\}/C_6 \quad [B.25]$$

In the above three equations the terms  $C_3$ ,  $C_4$ ,  $C_5$  and  $C_6$  equal  $(K_s Y + YS_0 + X_0)/(YS_0 + X_0)$ ,  $K_s Y/(YS_0 + X_0)$ ,  $YS_0 + X_0$  and  $C_3 Y/X + C_4/S$ , respectively. Although nonlinear analysis is possible for [B.15] and superior to analysis of linearized data, the graphical similarity among [B.23], [B.24] and [B.25] (Figure 7) predicts that estimates of  $u_{\max}$ ,  $K_s$  and  $Y$  will be highly correlated.

The integrated form of the Monod relation {[B.15]} is superior to the derivative forms {[B.12] and [B.16]} for estimating  $K_s$ ,  $u_{\max}$  and  $Y$  from gaseous substrate consumption data. A sensitivity analysis of derivative forms of Monod equations (like those used for continuous culture) predict that the best information about  $u_{\max}$  is achieved at the highest rates of substrate consumption. But mass-transport can easily limit gaseous substrate consumption by cells reproducing at high growth

Figure 6. Linearized discretized Monod data. Simulated data plotted in Figure 5 were linearized according to [B.21] and [B.22]. -  $S/t$  and  $X/t$  values were calculated by fitting cubic splines to the  $S$ - and  $X$ - $t$  data pairs and then evaluating the first derivatives of the cubic polynomials.

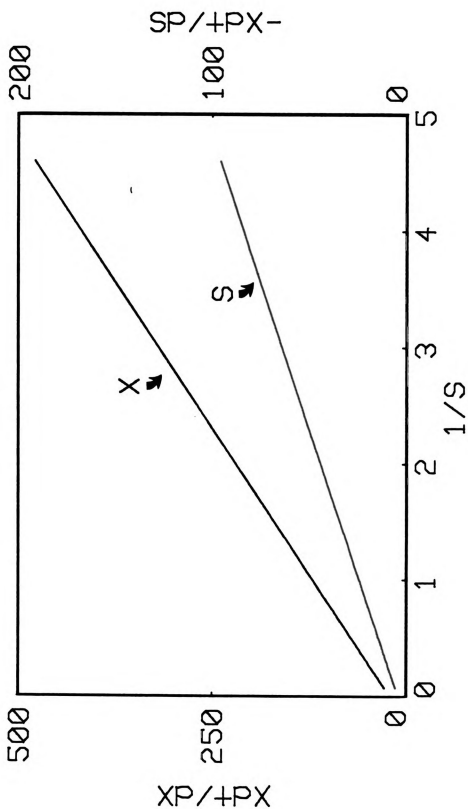


Figure 6

Figure 7. Sensitivity coefficients for  $u_{\max}$ ,  $K_s$  and  $Y$ . Same parameter values and initial conditions used for Figure 5.

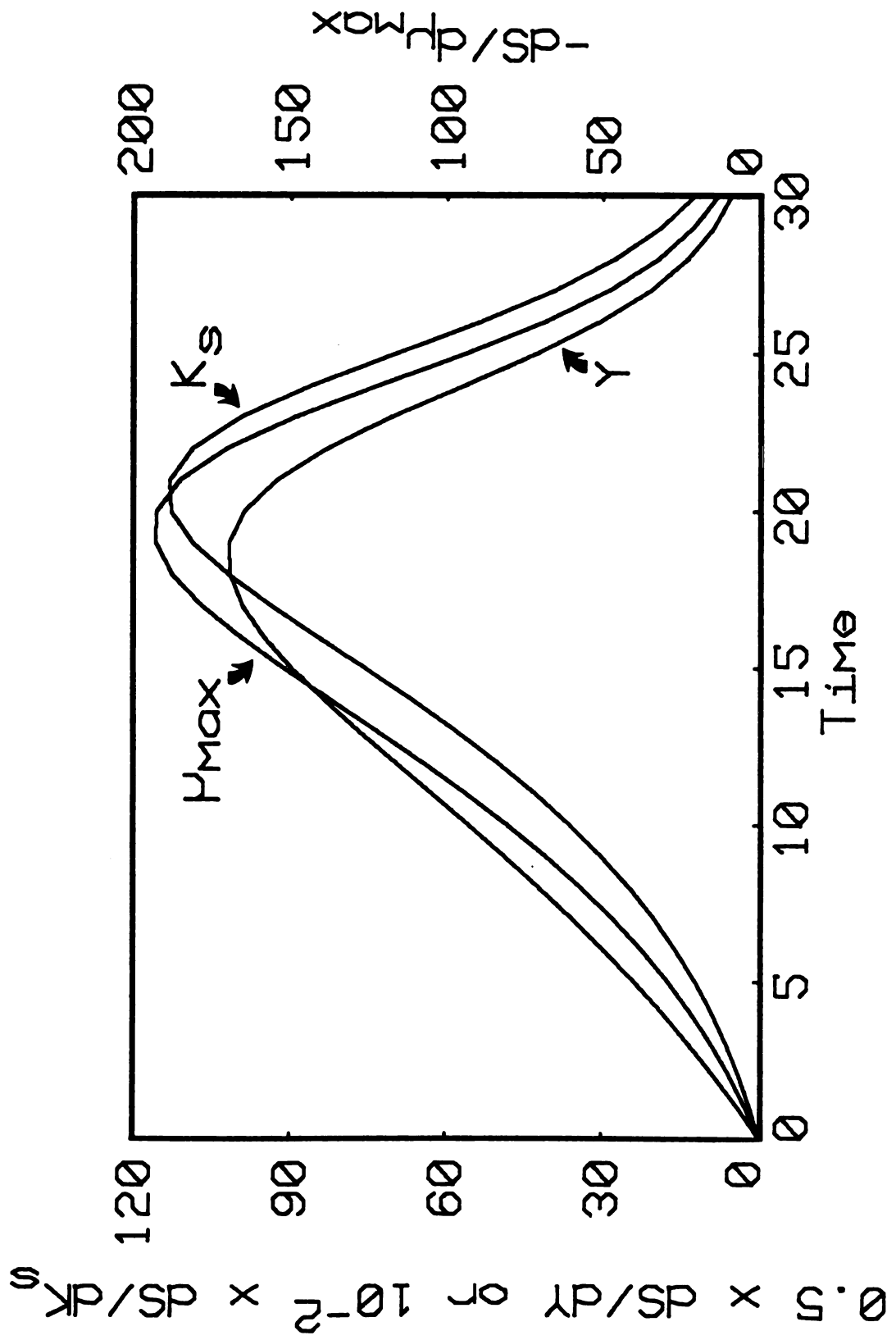


Figure 7

rates, thus preventing the estimation of biological kinetic parameters (Appendix A). This holds for cells growing in continuous culture or batch. In contrast, good information about  $u_{\max}$  is obtainable using [B.15] at substrate concentrations in the mixed-order region, where mass-transport influences estimates of this parameter to a lesser extent. Indeed the sensitivity equations for [B.15] predict that (i) the optimal substrate concentration for estimation of  $K_s$ ,  $u_{\max}$  and  $Y$  using [B.15] is no greater than four times  $K_s$  and (ii) the precision of the estimated growth parameters is greatest for  $u_{\max}$  and least for  $K_s$  (Figure 7). These predictions intuitively seem incorrect, but a similar situation holds for substrate consumption controlled by Michaelis-Menten kinetics. Although one expects a Michaelis-Menten progress curve to yield better estimates of  $K_m$  than  $V_{\max}$ , since optimal initial substrate concentrations lie in the mixed-order region, the opposite is true in practice (compare the estimated standard errors of  $K_m$  with those of  $V_{\max}$  in chapters I and III).

In Appendix C is listed MONODCRV which is a program that uses

$$S-S_0 = \Delta K_s dS/dK_s + \Delta u_{\max} dS/du_{\max} + \Delta Y dS/dY \quad (\text{B.26})$$

to fit substrate disappearance data to [B.15]. It requires initial estimates of  $K_s$ ,  $u_{\max}$  and  $Y$  plus initial substrate ( $S_0$ ) and biomass ( $X_0$ ) concentrations. MONODCRV does not calculate provisional values for these parameters and must be supplied with independently determined estimates. In order to obtain these for data shown in chapter III, I fitted cubic splines (3) to the  $S$ - and  $X$ - $t$  data pairs using a computer program (SPLINE) written by David D. Myrold which calculates the spline interpolants plus their respective first-derivatives. This information can be used in conjunction with [B.22] and [B.23] to estimate  $K_s$ ,  $u_{\max}$

and  $Y$ . MONODCRV does not update  $S_0$  nor  $X_0$ .  $S_0$  could not be directly measured because of the previously stated reasons and had to be estimated by extrapolating back to the  $S$  axis. It is possible to derive a sensitivity equation for updating  $S_0$ , but this was not done because I wanted to restrict the number of estimated parameters to 3. As with PROGCRV1 and PROGCRV2, MONODCRV estimates the standard errors of the parameters assuming no correlation among measurement errors.

Correlated measurement errors. Underestimates of standard errors for parameters are obtained if least-squares analysis is applied to data that lack statistical independence (i.e., possess correlated measurement errors). This situation worsens as the number of data points increases and has been shown to be true for linear (2,7) as well as nonlinear models (2).

The easiest means of checking for lack or presence of correlated measurement errors is by examining the residuals (2,5,7). These equal the observed values of the dependent variable minus values predicted using the fitted equation and contain all of the information not explained after fitting data to a given model {e.g., [B.2], [B.15]}. In Figure 8 are shown the residuals for  $H_2$  consumption by Desulfovibrio G11. Ideally these should be random and give the impression of a horizontal band. But it is obvious they do not and in fact all the residuals calculated after fitting [B.2] to the Michaelis-Menten progress curves shown in chapters I and III exhibit essentially the same pattern. Thus, the measurement errors are correlated and the standard errors estimated for  $K_m$  and  $V_{max}$  by PROGCRV1 are too low. Notwithstanding the presence of correlated measurement errors, I was able to reduce their influence on standard error estimates for  $K_m$  and

Figure 8. Residuals for H<sub>2</sub> progress curve data fitted to [B.2] using nonlinear least-squares analysis. Residuals were calculated by subtracting predicted H<sub>2</sub> concentrations (calculated from the best parameter estimates) from the observed H<sub>2</sub> concentrations. Residuals are all expressed as percentages of the predicted H<sub>2</sub> values.



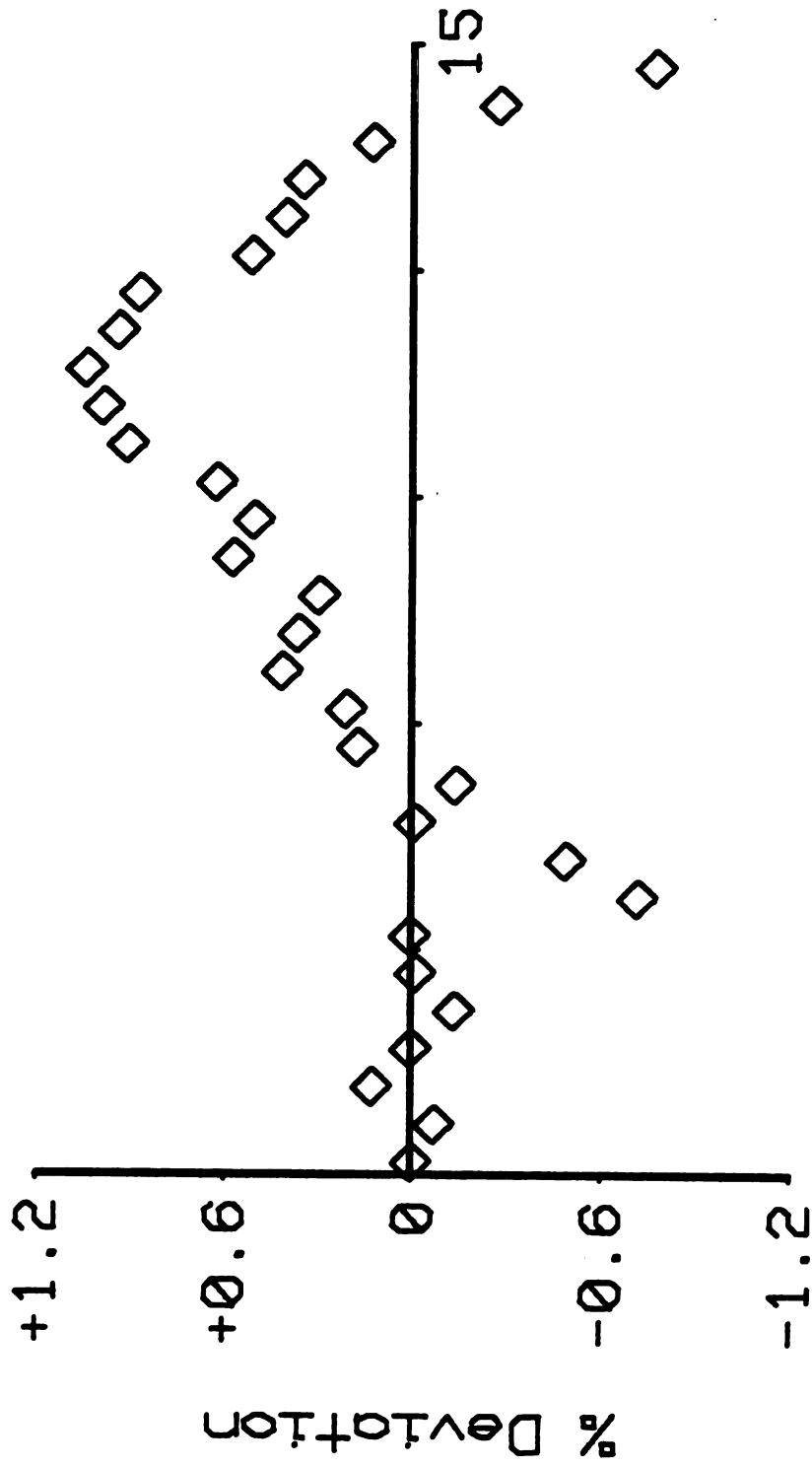


Figure 8

$V_{\max}$  by increasing the sampling interval from 10 to 30 min. This reduced the degree to which the standard errors for  $K_m$  and  $V_{\max}$  were underestimated since the magnitude of this error is proportional to the number of measurements (7).

The correlated measurement errors observed for  $H_2$  consumption by resting cells could have resulted from (i) fitting data to the wrong model for biological  $H_2$  consumption or (ii) the influence of physical factors on the circulation of gas through the sampling loop of the  $H_2$  GC. The first cause is serious since it questions the significance of the  $K_m$  estimates presented in chapters I and III. If  $S_0$  is less (e.g., 2- to 5-fold) than  $K_s$ , then [B.15] yields substrate depletion data very similar to what is expected for [B.2], regardless of the values of  $u_{\max}$  and  $Y$  (Figure 9). When the simulated data in Fig. 9 are fitted to [B.2] using PROGCRV1, the residuals exhibit a pattern similar to that seen in Figure 8. But the apparent  $K_m$  bears no relation to the  $K_s$  and depends upon  $S_0$ . The  $K_m$ 's for  $H_2$  consumption by rumen fluid, anaerobic sludge, eutrophic lake sediment, Desulfovibrio strains and the methanogenic bacteria were independent of  $S_0$  and thus, the correlated measurement errors are probably not a result of incorrectly fitting the  $H_2$  consumption data to [B.2] instead of an integrated Monod-type equation. This is supported by the pattern of residuals obtained after fitting a straight line to  $H_2$  disappearance data that resulted from sampling an empty flask containing  $H_2$  (Figure 10). These systematic residuals were not a result of adsorption occurring within the sampling loop, as has been previously observed for volatile organics (9), since repeated injections of  $H_2$  standards exhibited no statistical dependence (Figure 11), but likely resulted from incomplete mixing of  $H_2$  in the

Figure 9. Simulated Monod progress curve data containing simple errors (standard deviation=0.01 units) fitted to the integrated form of the Michaelis-Menten equation [B.2] . Parameter values and initial conditions were  $u_{\max}=0.1$ ,  $K_s=5$ ,  $Y=0.2$ ,  $S_0=4$  and  $X_0=1$ . Inset shows residuals calculated for data fitted to [B.2]. Note that although theoretical curve passes smoothly through all the data points, the residuals exhibit systematicity indicating the data have actually been fitted to the wrong model.

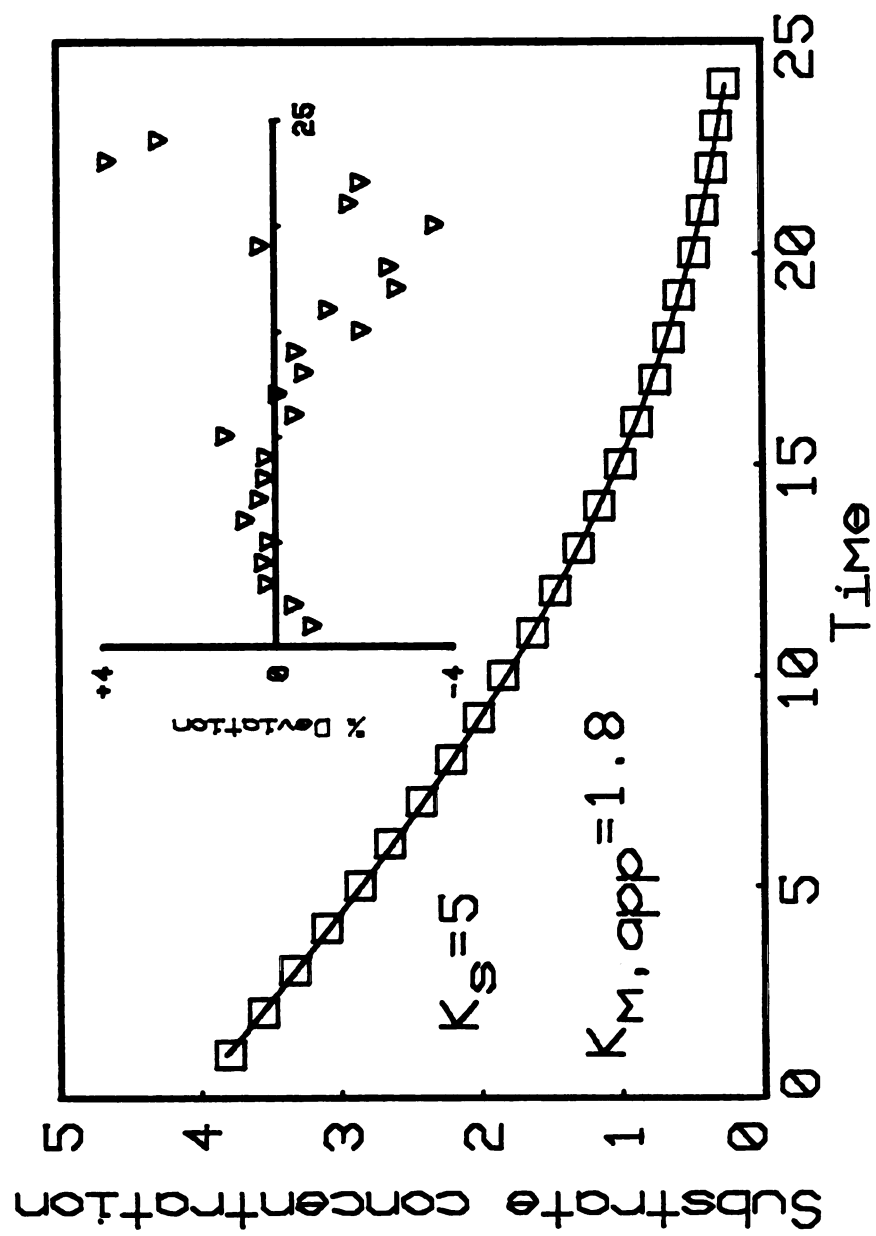


Figure 9

Figure 10. Residuals for H<sub>2</sub> removal from an empty flask containing H<sub>2</sub> due to sampling. The raw data were fitted to a linear model and this used to estimate predicted values which were in turn subtracted from the observed H<sub>2</sub> concentrations. The percentage deviation of each residual is plotted versus injection number. Note the systematicity exhibited by the residuals reminiscent of that seen in Figure 8.

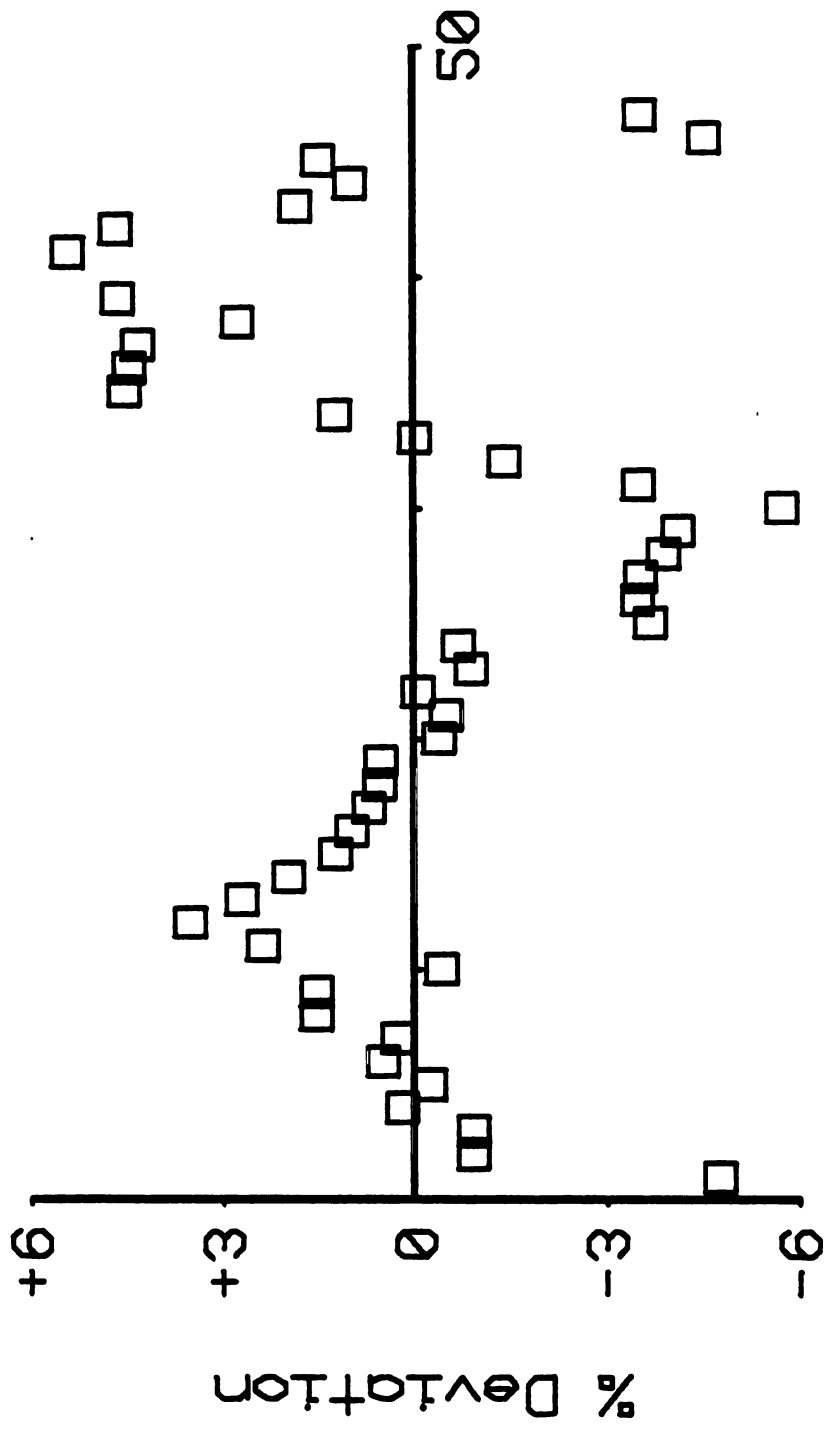


Figure 11. Residuals for H<sub>2</sub> standard tank sampled with time. A  $5.98 \times 10^{-5}$  atm (6.05 Pa) was sampled with time and residuals calculated by subtracting the mean H<sub>2</sub> concentration from all measured values. Residuals are plotted versus injection number. Note the lack of a systematic trend among the residuals indicating statistical independence of the H<sub>2</sub> measurements.

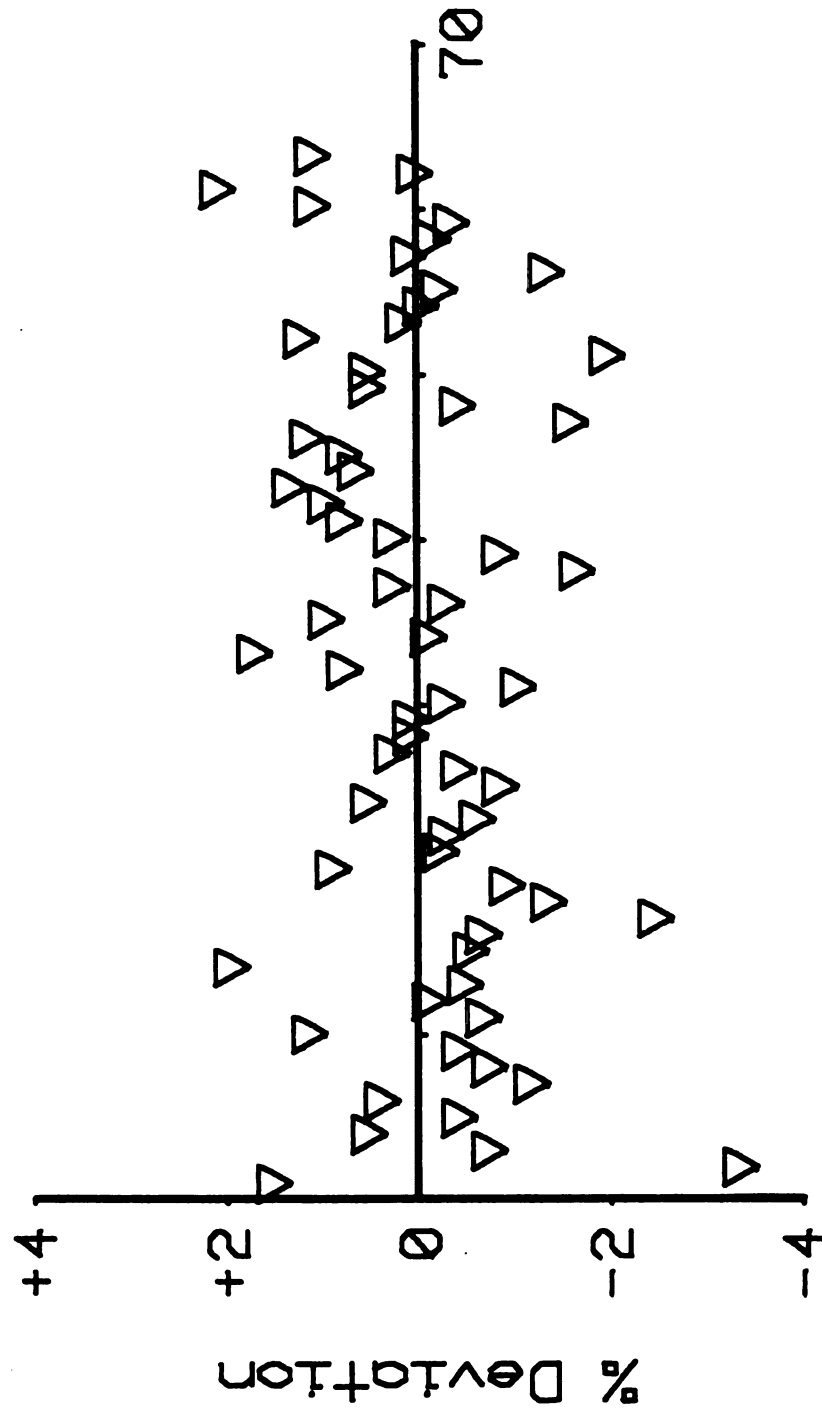


Figure 11



recirculating gas stream. In summary, the correlated measurement errors observed for the  $H_2$  progress curves were caused by slight heterogeneities in the recirculating  $H_2$  gas and not by inappropriate use of the integrated Michaelis-Menten equation.

## LITERATURE CITED

1. Atkins, G. L., and I. A. Nimmo. 1973. The reliability of Michaelis constants and maximum velocities estimated by using the integrated Michaelis-Menten equation. *Biochem. J.* 135: 779-784.
2. Beck, J. V., and K. J. Arnold. 1976. Parameter estimation in engineering and science. John Wiley and Sons, Inc., New York, New York. p. 334-350.
3. Burden, R. L., J. D. Faires, and A. C. Reynolds. 1978. Numerical analysis Prindle, Weber and Schmidt. Boston, Massachusetts. p. 116-128 and 239-245.
4. Cornish-Bowden, A. 1979. Fundamentals of enzyme kinetics. Butterworth, Inc., Boston, Massachusetts. p. 200-210.
5. Draper, N. R., and H. Smith. 1981. Applied regression analysis. John Wiley and Sons, Inc., New York, New York. p. 459.
6. Duggleby, R. G., and J. F. Morrison. 1977. The analysis of progress curves for enzyme-catalyzed reactions by nonlinear regression. *Biochem. Biophys. Acta.* 481: 297-312.
7. Esener, A. A., I. A. Roels, and N. F. W. Kossen. 1981. On the statistical analysis of batch data. *Biotech. Bioeng.* 23:2391-2396.
8. Harbaugh, J., and G. Bonham-Carter. 1970. Computer simulation in geology. John Wiley and Sons, Inc., New York, New York. p. 61-97.
9. Jonsson, J. A., J. Vejrosta, and J. Novak. 1982. Systematic errors occurring with the use of gas-sampling loop injectors in gas chromatography. *J. Chromatogr.* 236: 307-312.
10. Knowles, G., A. L. Downing, and M. J. Barrett. 1965. Determination of kinetic constants for nitrifying bacteria in mixed culture, with the aid of an electronic computer. *J. Gen. Microbiol.* 38: 263-278.
11. Nimmo, I. A., and G. L. Atkins. 1974. A comparison of two methods for fitting the integrated Michaelis-Menten equation. *Biochem. J.* 141: 913-914.
12. Pirt, S. J. 1975. Principles of microbe and cell cultivation. John Wiley and Sons, Inc., New York, New York. p. 22-28.
13. Robinson, J. A., and J. M. Tiedje. Kinetics of hydrogen consumption by rumen fluid, anaerobic digester sludge and sediment. *Appl.*

Environ. Microbiol. in press.

14. Thomas, G. B., Jr. 1972. Calculus and analytical geometry. Addison-Wesley, Inc., Reading, Massachusetts. p. 76-81.

## APPENDIX C

### COMPUTER PROGRAMS FOR DATA ANALYSIS

Five computer programs (FILEMAN, PROGCRV1, PROGCRV2, MONODCRV and PHASIM) are contained within this appendix and were written during the course of my graduate studies. All 5 are in North Star BASIC (North Star Computers Inc., CA) and were written for an IMSAI 8080 microcomputer, linked to 2 minifloppy diskette drives (North Star disk operating system), a black-and-white monitor (Sanyo Electric Inc., CA), Decwriter II (Digital Equipment Corp., MA) and digital plotter (Houston Instrument, TX). FILEMAN and the progress curve analysis programs (PROGCRV1, PROGCRV2 and MONODCRV) were written to facilitate data reduction and analysis, whereas PHASIM was written to simulate the kinetic behavior of substrate consumption by cells in a liquid phase.

Data filing system. FILEMAN serves as the main link in a chain of programs that include PROGCRV1, PROGCRV2 and MONODCRV, as well as other programs not included in this appendix [e.g., REGRESS1 (regression routine for fitting data to one-term linear, exponential, logarithmic or power models), AUTOPLOT (routine for plotting data using digital plotter)]. I wrote all of FILEMAN except for the VIDPLOT subroutine (lines 3070-3910) which was written by Russell M. Edwards and Timothy B. Parkin. FILEMAN is used to create data arrays that are stored on minifloppy diskettes, using the North Star random access filing system, and can be retrieved later using FILEMAN or read into other programs (e.g., PROGCRV1, REGRESS1) for analysis. All the programs listed in this appendix were written so that they may read arrays created by

FILEMAN (PROGCRV1, PROGCRV2 and MONODCRV) or create simulated data arrays (PHASIM) that may be scanned and transformed using FILEMAN.

There are 2 levels of control in FILEMAN, with the following commands available to the user at the highest level: (1) GEN, (2) SCAN, (3) PROOF, (4) MODIFY, (5) FILE, (6) DESTROY, (7) CHAIN, (8) MERGE, (9) PLOT and (10) QUIT. GEN and SCAN are the only 2 commands encountered when FILEMAN is first run (lines 30-70). Thus, the user may initially create a new data array (lines 150-330) or scan an already existing one (lines 1070-1220 and 340-540). After this, the user has access to these 2 commands plus the additional 8 listed above (lines 80-140). The maximum size an array may be is 250 rows by 7 columns. But this may be increased or decreased, depending on the amount of computer memory available, by changing the dimensions of the doubly subscripted variable  $X(i,j)$  in line 20. The PROOF command allows the data file to be viewed on either the monitor or Decwriter (lines 340-540) and if the user is satisfied with its contents, the array can be stored on minifloppy diskettes using the FILE command (lines 720-1060). Before a data array can be stored, a filename and identification string having no more than 8 and 80 alphanumeric characters, respectively, must be specified. The identification string is stored along with the elements of the data array under the specified file name on the diskette. Erasure of unwanted data files on diskettes is accomplished via the DESTROY command (lines 1230-1290). The CHAIN command allows the user to load and execute other programs for analysis of arrays created and stored using FILEMAN (lines 1300-1410). Concatenation of data arrays having the same number of columns can be done using the MERGE command (lines 2280-2500). Again, the array generated using this command must have no more than 250 rows,

otherwise a 'dimension error' will result. In addition to outputting the array to either the monitor or Decwriter, it may be graphically displayed on these devices via the PLOT command (lines 3070-3910). The PLOT subroutine uses low-resolution graphics and scales the x-y axes to the largest elements in the two columns plotted. Only data in the first quadrant of the Cartesian co-ordinate system (i.e., positive x and y values) may be plotted. Finally, the QUIT command terminates execution of FILEMAN.

The second level of control in FILEMAN is linked to the first through the MODIFY and RETURN commands. The former provides the user with the following options: (1) CORRECT, (2) ADD, (3) DELETE, (4) TRANSFORM and (5) RETURN. The CORRECT command allows elements of the data array, including the identification string, to be corrected (lines 580-710). Secondly, data arrays may have elements added (lines 2510-2700) or deleted (lines 2710-3060) using the ADD and DELETE commands, respectively. They also may be mathematically transformed in various ways (delineated below) using the TRANSFORM command (lines 1420-2270). Lastly, the RETURN command permits the user to return to the first or highest command level.

When the TRANSFORM command is executed the user is first faced with 2 options, either a column within the data array may be mathematically transformed (lines 1760-2270) or 1 column of numbers can be used to transform a second (lines 1480-1750). If the first option is chosen the user may add, subtract, multiply or divide the specified column of numbers by a constant. Additionally, the natural logarithm of the numbers may be taken or they may be raised to a particular power. Lastly, the user may operate on the specified column of numbers with a

user-defined function entered at line 3940 before program execution. If the user chooses option 2 instead then 1 column may be added to or subtracted from, or multiplied or divided by, a second column of numbers. After each of the above transformations, control passes back to the highest level and combinations of the above commands may once more be executed. The above commands encountered by the user when FILEMAN is executed are generally self-explanatory and the entire data analysis package, with FILEMAN as its core, is designed to be 'user-friendly'.

#### FILEMAN LISTING

```

10 !CHR$(26)
20 DIM X(250,7),I$(80)
30 INPUT "GEN(1),SCAN(2)? ",C
40 IF C<1 OR C>2 THEN 30
50 INPUT "OUTPUT DEVICE (TYPE '0' FOR CRT OR '1' FOR DECWRITER)? ",D
60 IF O<>0 AND O<>1 THEN 50
70 ON C GOTO 150,1070
80 PRINT
"GEN(1),SCAN(2),PROOF(3),MODIFY(4),FILE(5),DESTROY(6),CHAIN(7)"
90 INPUT "MERGE(8),PLOT(9),QUIT(10) ",C
100 IF C<1 OR C>10 THEN 80
110 IF C>2 THEN 140
120 INPUT "OUTPUT DEVICE (TYPE '0" FOR CRT OR '1' FOR DECWRITER)? ",D
130 IF O<>0 AND O<>1 THEN 120
140 ON C GOTO 150,1070,340,550,720,1230,1300,2280,3070,3920
150 INPUT "ENTER THE NUMBER OF ROWS OF DATA YOU WISH TO STORE ",N
160 IF N<=190 THEN 190
170 PRINT#0 "MAXIMUM NO. OF ROWS ALLOWED IS 250; SEE LINE 10"
180 GOTO 3770
190 INPUT "ENTER THE NUMBER OF COLUMNS OF DATA YOU WISH TO STORE ",M
200 IF M<=7 THEN 230
210 PRINT#0 "MAXIMUM NO. OF COLUMNS ALLOWED IS 7; SEE LINE 10"
220 GOTO 3770
230 PRINT#0 CHR$(26)240 FOR I=1 TO N
250 PRINT "ROW #",Z3I,I,
260 FOR J=1 TO M
270 PRINT#0 TAB(J*10),
280 INPUT I X(I,J)
290 IF J<>M THEN 310

```

```

300 PRINT#0
310 NEXT J
320 NEXT I
330 GOTO 80
335 REM ':' = North Star BASIC's 'backslash'
340 PRINT#0:PRINT#0:PRINT#0 I$, " N= ",Z3I,N," M= ",Z3I,M:PRINT#0
350 I1=1
360 FOR K=1 TO M
370 PRINT#0,TAB(10*K-2),Z2I,K,
380 NEXT K:PRINT#0
390 FOR I=1 TO N
400 PRINT#0 Z3I,I,
410 FOR J=1 TO M
420 IF X(I,J)=-99 THEN 430 ELSE 450
430 PRINT#0 " ",
440 GOTO 460
450 PRINT#0 %10E2,X(I,J),
460 IF J<>M THEN 480
470 PRINT#0
480 NEXT J
490 IF O=1 THEN 530
500 IF I<>I1*15 THEN 530
510 INPUT "PRESS 'RETURN' TO CONTINUE ",Z7$
520 I1=I1+1
530 NEXT I
540 GOTO 80
550 INPUT "CORRECT(1),ADD(2),DELETE(3),TRANSFORM(4),RETURN(5)? ",C1
560 IF C1<1 OR C1>5 THEN 550
570 ON C1 GOTO 580,2510,2710,1420,80
580 INPUT "ENTER THE NO. OF ENTRIES TO BE CORRECTED ",N3
590 FOR L=1 TO N3
600 PRINT "ENTER MATRIX NOTATION OF ENTRY NO. ",L
610 INPUT I,J
620 IF I>N OR J>M THEN 580
630 IF I<>0 AND J<>0 THEN 680
640 PRINT "INCORRECT IDENTIFICATION STRING IS ",I$
650 PRINT "CORRECT IDENTIFICATION STRING?"
660 INPUT I$
670 GOTO 700
680 PRINT "INCORRECT VALUE IS ",%12E4,X(I,J)
690 INPUT "CORRECT VALUE? ",X(I,J)
700 NEXT L
710 GOTO 80
720 INPUT "DO YOU TO OVERWRITE AN EXISTING DATAFILE(1=YES;0=NO)? ",A2
730 IF A2=0 THEN 820
740 IF A2<>1 THEN 720
750 INPUT "ENTER THE NAME OF THE DATAFILE TO BE OVERWRITTEN ",N$
760 Q8=FILE(N$)
770 IF Q8=3 THEN 800
780 PRINT "THIS FILE DOES NOT EXIST ON THE DISK"
790 GOTO 750
800 DESTROY N$
810 GOTO 870

```



```

820 INPUT "ENTER THE NAME OF THE DATAFILE YOU WISH TO CREATE ",N$
830 L8=LEN(N$)
840 IF L8<=8 THEN 870
850 PRINT "FILENAMES MAY CONSIST OF 8 ALPHANUMERIC CHARCATERS OR LESS"
860 GOTO 820
870 Q1=FILE(N$)
880 IF Q1=-1 THEN 910
890 PRINT "THIS FILE ALREADY EXISTS ON THE DISK"
900 GOTO 820
910 IF A2=1 THEN 940
920 PRINT "ENTER IDENTIFICATION STRING FOR YOUR DATAFILES(80 CHRS. OR
LESS)"
930 INPUT I$
940 B=INT((7*M*N+100)/256)+1
950 CREATE N$,B,3
960 OPEN#0,N$
970 WRITE#0%0,I$,N,M,NOENDMARK
980 Z=0
990 FOR I=1 TO N
1000 FOR J=1 TO M
1010 WRITE#0%(Z*7+95),X(I,J),NOENDMARK
1020 Z=Z+1
1030 NEXT J
1040 NEXT I
1050 CLOSE#0
1060 GOTO 80
1070 INPUT "ENTER THE FILENAME YOU WISH TO SCAN ",N$
1080 Q4=FILE(N$)
1090 IF Q4=3 THEN 1120
1100 PRINT "THIS FILE DOES NOT EXIST ON THE DISK"
1110 GOTO 1070
1120 OPEN#0,N$
1130 READ#0%0,I$,N,M
1140 Z=0
1150 FOR I=1 TO N
1160 FOR J=1 TO M
1170 READ#0%(Z*7+95),X(I,J)
1180 Z=Z+1
1190 NEXT J
1200 NEXT I
1210 CLOSE#0
1220 GOTO 340
1230 INPUT "ENTER THE NAME OF THE FILE YOU WISH TO DESTROY ",N$
1240 Q6=FILE(N$)
1250 IF Q6=3 THEN 1280
1260 PRINT "THIS FILE DOES NOT EXIST ON THE DISK"
1270 GOTO 1230
1280 DESTROY N$
1290 GOTO 80
1300 PRINT "YOU MAY CHAIN THE FOLLOWING
PROGRAMS:REGRESS(1),PROGCURV(2),"
1310 PRINT "VIDPLOT(3),AUTOPLOT(4),REGANOV(5),NONLIN(6),DTLNPT(7)"
1320 INPUT "ENTER THE NUMBER OF THE PROGRAM YOU WISH TO CHAIN TO ",H1

```

```

1330 IF H1=1 THEN H$="REGRESS1"
1340 IF H1=2 THEN H$="PROG CURV"
1350 IF H1=3 THEN H$="VIDPLOT"
1360 IF H1=4 THEN H$="AUTO PLOT"
1370 IF H1=5 THEN H$="REGANOV"
1380 IF H1=6 THEN H$="NONLIN"
1390 IF H1=7 THEN H$="DTLNPT"
1400 IF H1<1 OR H1>7 THEN 1300
1410 CHAIN H$+",2"
1420 PRINT "YOU MAY TRANSFORM A SINGLE COLUMN OF NUMBERS(OPTION 1) OR"
1430 PRINT "YOU MAY TRANSFORM ONE COLUMN OF NUMBERS USING A SECOND
COL-"
1440 PRINT "UMN OF NUMBERS(OPTION 2)"
1450 INPUT "OPTION? ",P
1460 IF P<>1 AND P<>2 THEN 1420
1470 IF P=1 THEN 1760
1480 PRINT "THE FOLLOWING TRANSFORMATIONS MAY BE PERFORMED: ADD(1),"
1490 PRINT "SUBTRACT(2),MULTIPLY(3),DIVIDE(4)"
1500 INPUT "WHICH TRANSFORMATION DO YOU WISH TO USE? ",T1
1510 IF T1<1 OR T1>4 THEN 1480
1520 INPUT "ENTER THE FIRST AND SECOND COLUMNS ",C1,C2
1530 IF C1>M OR C2>M THEN 1520
1540 INPUT "SHOULD THE TRANSFORMED NUMBERS FORM A NEW
COLUMN(1=YES;0=NO)? ",A3
1550 IF A3<>1 AND A3<>0 THEN 1540
1560 IF A3=1 THEN M1=M+1 ELSE M1=C3
1570 FOR I=1 TO N
1580 IF X(I,C3)=-99 OR X(I,C4)=-99 THEN 1590 ELSE 1610
1590 X(I,M1)=-99
1600 GOTO 1720
1610 IF T1<>1 THEN 1640
1620 X(I,M1)=X(I,C3)+X(I,C4)
1630 GOTO 1720
1640 IF T1<>2 THEN 1670
1650 X(I,M1)=X(I,C3)-X(I,C4)
1660 GOTO 1720
1670 IF T1<>3 THEN 1710
1680 X(I,M1)=X(I,C3)*X(I,C4)
1690 GOTO 1720
1700 IF T1<>4 THEN 1720
1710 X(I,M1)=X(I,C3)/X(I,C4)
1720 NEXT I
1730 IF A3=0 THEN 1750
1740 M=M1
1750 GOTO 80
1760 PRINT "THE FOLLOWING TRANSFORMATIONS MAY BE PERFORMED: ADD(1),"
1770 PRINT
"SUBTRACT(2),MULTIPLY(3),DIVIDE(4),POWER(5),LN(6),OPERATE(7)"
1780 INPUT "WHICH TRANSFORMATION DO YOU WISH TO USE? ",T2
1790 IF T2<1 OR T2>7 THEN 1760
1800 INPUT "WHICH COLUMN OF NUMBERS DO YOU WISH TO TRANSFORM? ",C
1810 IF C>M THEN 1800
1820 INPUT "SHOULD THE TRANSFORMED NUMBERS FORM A NEW

```

```

COLUMN(1=YES;0=NO)? ",A3
1830 IF A3<>1 AND A3<>0 THEN 1820
1840 IF A3=1 THEN M1=M+1 ELSE M1=C
1850 A=0:S=0:L=1:D=1:I1=1:N1=N
1860 INPUT "DO YOU WISH TO TRANSFORM THE ENTIRE COLUMN?(1=YES;0=NO)?
",A4
1870 IF A4=1 THEN 1930
1880 IF A4<>0 THEN 1860
1890 PRINT "ENTER THE FIRST AND LAST ELEMENTS OF THE COULMN YOU WISH TO
TRANSFORM"
1900 INPUT I1,N1
1910 IF I1>N1 THEN 1890
1920 IF I1>N OR N1>N THEN 1890
1930 IF T2<>1 THEN 1950
1940 INPUT "HOW MUCH DO YOU WISH TO ADD TO EACH ENTRY? ",A
1950 IF T2<>2 THEN 1970
1960 INPUT "HOW MUCH DO YOU WISH TO SUBTRACT FROM EACH ENTRY? ",S
1970 IF T2<>3 THEN 1990
1980 INPUT "BY WHAT DO YOU WISH TO MULTIPLY EACH ENTRY? ",L
1990 IF T2<>4 THEN 2010
2000 INPUT "BY WHAT DO YOU WISH TO DIVIDE EACH ENTRY? ",D
2010 IF T2<>5 THEN 2030
2020 INPUT "BY WHAT POWER DO YOU WISH TO RAISE EACH ENTRY TO? ",P9
2030 FOR I=I1 TO N1
2040 IF X(I,C)=-99 THEN 2050 ELSE 2070
2050 X(I,M1)=-99
2060 GOTO 2170
2070 IF T2<>5 THEN 2100
2080 X(I,M1)=X(I,C)P9
2090 GOTO 2170
2100 IF T2<>6 THEN 2130
2110 X(I,M1)=LOG(X(I,C))
2120 GOTO 2170
2130 IF T2<>7 THEN 2160
2140 X(I,M1)=FNA(X(I,C))
2150 GOTO 2170
2160 X(I,M1)=L*X(I,C)/D+A-S
2170 NEXT I
2180 IF A3=0 OR A4=1 THEN 2550
2190 FOR I=1 TO I1-1
2200 X(I,M1)=X(I,C)
2210 NEXT I
2220 FOR I=N1+1 TO N
2230 X(I,M1)=X(I,C)
2240 NEXT I
2250 IF A3=0 THEN 2270
2260 M=M1
2270 GOTO 80
2280 INPUT "HOW MANY FILES DO YOU WISH TO MERGE? ",F
2290 Z9=0
2300 FOR I=1 TO F
2310 PRINT "ENTER THE NAME OF DATAFILE NO. ",I
2320 INPUT N$

```

```

2330 Q7=FILE(N$)
2340 IF Q7=3 THEN 2370
2350 PRINT "THIS FILE DOES NOT EXIST ON THE DISK"
2360 GOTO 2310
2370 OPEN#0,N$
2380 READ#0%0,I$,N,M
2390 Z=0
2400 FOR J=1+Z9 TO N+79
2410 FOR K=1 TO M
2420 READ #0%(Z*7+95),X(J,K)
2430 Z=Z+1
2440 NEXT K
2450 NEXT J
2460 CLOSE#0
2470 Z9=N+Z9
2480 NEXT I
2490 N=Z9
2500 GOTO 80
2510 INPUT "DO YOU WISH TO ADD ROW(S)(1) OR COLUMN(S)(2)? ",A5
2515 IF A5<1 OR A5>2 THEN 2510
2520 IF A5=1 THEN 2530 ELSE 2620
2530 INPUT "ENTER NO. OF ROW(S) TO BE ADDED ",R
2540 FOR I=N+1 TO N+R
2550 FOR J=1 TO M
2560 PRINT "DATUM(",I,"",",J,"")?"
2570 INPUT X(I,J)
2580 NEXT J
2590 NEXT I
2600 N=N+R
2610 GOTO 80
2620 INPUT "ENTER NO. OF COLUMN(S) TO BE ADDED? ",C1
2630 FOR I=1 TO N
2640 FOR J=M+1 TO M+C1
2650 PRINT "DATUM(",I,"",",J,"")?"
2660 INPUT X(I,J)
2670 NEXT J
2680 NEXT I
2690 M=M+C1
2700 GOTO 80
2710 INPUT "DELETE ROW(S)(1),COLUMN(S)(2) OR ENTRIES(3)? ",C2
2720 IF C2<1 OR C2>3 THEN 2710
2730 ON C2 GOTO 2740,2860,2980
2740 INPUT "ENTER FIRST AND LAST ROW(S) TO BE DELETED ",R1,R2
2750 N1=N-(R2-R1+1)
2760 IF N1>0 THEN 2790
2770 PRINT "ARE YOU SURE YOU WANT TO DELETE ALL OF THE ROWS?"
2780 GOTO 2740
2790 FOR I=R1 TO N1
2800 FOR J=1 TO M
2810 X(I,J)=X(I+N-N1,J)
2820 NEXT J
2830 NEXT I
2840 N=N1

```

```

2850 GOTO 80
2860 INPUT "ENTER FIRST AND LAST COLUMN(S) TO BE DELETED ",C1,C2
2870 M1=M-(C2-C1+1)
2880 IF M1>0 THEN 2910
2890 PRINT "ARE YOU SURE YOU WANT TO DELETE ALL OF THE COULMNS?"
2900 GOTO 2860
2910 FOR I=1 TO N
2920 FOR J=C1 TO M1
2930 X(I,J)=X(I,J+M-M1)
2940 NEXT J
2950 NEXT I
2960 M=M1
2970 GOTO 80
2980 INPUT "ENTER NO. OF ENTRY(S) TO BE DELETED ",N2
2990 IF N2>N*M THEN 2980
3000 FOR K=1 TO N2
3010 PRINT "MATRIX NOTATION OF ENTRY NO. ",K
3020 INPUT I,J
3030 IF I>N OR J>M THEN 3010
3040 X(I,J)=-99
3050 NEXT K
3060 GOTO 80
3070 FILL 63487,8:PRINT CHR$(26)
3080 PRINT CHR$(16):PRINT CHR$(30)
3090 FILL 63487,12
3100 Z=1:P=1.74532E-2
3110 FOR I9=61608 TO 63178 STEP 80:FILL I9,197
3120 NEXT I9
3130 FILL 63208,195
3140 FOR I9=63209 TO 63276:FILL I9,202
3150 NEXT I9
3160 IF U3=1 THEN 3170
3170 GOSUB 3320
3180 GOSUB 3230
3190 IF T>60 THEN 3230:IF E>145 THEN 3230
3200 NEXT E:STOP
3210 IF E<10 OR E>145 THEN 3290:IF T<4 OR T>70 THEN 3300
3220 IF Z<0 THEN Z=0:IF Z>0 THEN Z=1
3230 L1=(23-INT(T/3))*80+61284+INT(E/2+320
3240 M1=26((1-E+INT(E/2)*2)*3+T-INT(T/3)*3)
3250 V1=128
3260 V5=INT(V1/M1/2)*2*M1+V1-INT(V1*2/M1)*M1/2+M1*Z
3270 FILL L1,V5
3280 RETURN
3290 PRINT "X OUT OF RANGE: ",X:RETURN
3300 PRINT "Y OUT OF RANGE: ",Y:RETURN
3310 FILL 93487,8:STOP
3320 INPUT "COLUMN # PLOTTED ON X-AXIS,Y-AXIS? ",V2,V3
3330 IF V2>N THEN 3320 ELSE 3340
3340 IF V3>M THEN 3320
3350 PRINT CHR$(30)
3360 PRINT CHR$(26),CHR$(11),
3370 PRINT "FILE ",N$, " ", "COLUMN ",V2," VS. COLUMN ",V3

```

```

3380 PRINT CHR$(10),
3390 F1=X(1,V2)
3400 F3=X(1,V2)
3410 FOR A=2 TO N
3420 F2=X(A,V2)
3430 IF F2>F1 THEN F1=F2
3440 IF F2<F3 THEN F3=F2
3450 NEXT A
3460 G1=X(1,V3):G3=X(1,V3)
3470 FOR A=2 TO N
3480 G2=X(A,V3)
3490 IF G2>G1 THEN G1=G2
3500 IF G2<G3 THEN G3=G2
3510 NEXT A
3520 F2=135/F1:G2=56/G1
3530 FOR A=1 TO N
3540 IF X(A,V3)=-99 THEN 3590
3550 E=INT(X(A,V2)*F2)+10
3560 T=INT(X(A,V3)*G2)+14
3570 Z=1
3580 GOSUB 3210
3590 NEXT A
3600 PRINT %8E1,G1,
3610 PRINT CHR$(10),CHR$(10),CHR$(10),CHR$(10),CHR$(13),
3620 FOR I=1 TO 5
3630 PRINT %8E1,G1-G1/5*I,:IF I=5 THEN 3650
3640 PRINT CHR$(10),CHR$(10),CHR$(10),CHR$(10),CHR$(13),
3650 NEXT I
3660 PRINT CHR$(13)
3670 FOR I=1 TO 5
3680 I1=I*14+2
3690 PRINT TAB(I1),%7E1,F1/5*I,
3700 NEXT I
3710 PRINT CHR$(30)
3720 INPUT "ANOTHER PLOT FROM THIS FILE? (1=YES;0=NO) ",U2
3730 PRINT CHR$(11),CHR$(21),
3740 IF U2=1 THEN 3750 ELSE 3840
3750 Q7=43
3760 INPUT "CLEAR? (1=YES;0=NO)",U3
3770 IF U3=1 THEN 3780 ELSE 3820
3780 PRINT CHR$(16),CHR$(30),CHR$(21)
3790 FOR I=1 TO 21:PRINT CHR$(16),TAB(3),CHR$(16),
3800 PRINT
CHR$(12),CHR$(12),CHR$(12),CHR$(12),CHR$(12),CHR$(12),CHR$(21),
CHR$(12),CHR$(12)
3810 NEXT I:PRINT CHR$(16),:GOTO 3820
3820 PRINT CHR$(26),CHR$(30),:GOTO 3320
3830 GOTO 3320
3840 PRINT CHR$(11),CHR$(21),
3850 INPUT "DO YOU WANT HARD COPY (1=YES;0=NO)? ",U5
3860 IF U5=1 THEN 3870 ELSE 3890
3870 PRINT CHR$(30)," FILE ",N$, "
3880 X=CALL(256):GOTO 3710

```

```

3890 PRINT CHR$(16)
3900 PRINT CHR$(26)
3910 GOTO 80
3920 FILL 63487,8:PRINT CHR$(16),CHR$(26),:END
3930 DEF FNA(X(I,C))
3940 Y9=(X(I,C)+672.34)/7.7636E8
3950 RETURN Y9
3960 FNEND

```

Progress Curve Analysis. PROGCRV1, PROGCRV2 and MONODCRV are programs that fit data to the integrated forms of either the Michaelis-Menten equation (3) or the Monod equation (6). All three programs are similar in that they fit data to nonlinear models, and began as adaptations to the Progress Curve Analysis program listed in Michael R. Betlach's Ph.D. thesis (Michigan State University, 1979), which estimates  $K_m$  and  $V_{max}$  for substrate disappearance data that fit the integrated form of the Michaelis-Menten equation when the initial substrate concentration ( $S_0$ ) is known. In both Betlach's program and the three presented here, Gaussian linearization (1,4) is used to minimize the residual sum-of-squares. In addition to estimating the parameters for the above nonlinear models, these programs also estimate the standard errors of the parameters. The latter are calculated assuming no correlation among the measurement errors. A major difference between Betlach's program and the three that follow is it fits data to a 2-parameter model, whereas PROGCRV1, PROGCRV2 and MONODCRV fit data to 3-parameter models.

PROGCRV1 estimates  $K_m$ ,  $V_{max}$  and  $S_0$  for data that fit the integrated form of the Michaelis-Menten equation when  $S_0$  is unknown. It was essential that error in  $S_0$  be allowed for, since the initial  $H_2$  concentration in the progress curve experiments described in chapters I and III could not be directly measured. The substrate

concentration-time data pairs are read into PROGCRV1 in lines 80-220. An initial estimate of  $S_0$  is obtained by fitting the first 3-6  $H_2$  concentration-time data pairs to a straight line and extrapolating back to time  $t=0$  (lines 230-320). Initial estimates of  $K_m$  and  $V_{max}$  are obtained from linear regression analysis of the S-t data pairs, transformed according to equation [B.5] (lines 330-460). Once initial estimates of  $S_0$ ,  $K_m$  and  $V_{max}$  are obtained they are iteratively improved via nonlinear regression. This is accomplished using a 2-step procedure. Firstly, theoretical substrate concentrations are calculated given the current estimates of the three parameters (lines 1090-1170) using Newton's method for finding roots to implicit functions (2), which the integrated Michaelis-Menten equation is an example of. Changes to be made in the current parameter estimates are then calculated using the sensitivity equations for  $K_m$  [B.8],  $V_{max}$  [B.7] and  $S_0$  [B.10] (lines 1180-1700), and the iterations continue (lines 550-600) until changes in the parameters are less than some specified amount (e.g., 0.0001). Once this iterative process has converged the parameter estimates plus their respective standard errors are printed out to either the monitor or Decwriter (lines 610-670). Additionally, approximate estimates of (i) the covariance matrix, (ii) the determinant of the covariance matrix and (iii) the parameter correlation matrix for  $K_m$ ,  $V_{max}$  and  $S_0$  are outputted. After completion of the above nonlinear analysis, theoretical substrate and product concentrations plus the residuals (observed S-predicted S) and the sensitivity coefficients for  $K_m$ ,  $V_{max}$  and  $S_0$  may be calculated and stored on a minifloppy diskette (lines 880-1040), along with the original data file.



[illegible]

```

450 A9=Y1/N-B9*X1/N:K=A9/B9:V=1/B9
460 R=B9*(X9-X1*Y1/N)/(Y2-Y1*Y1/N)
470 PRINT#0:PRINT#0:PRINT#0
480 PRINT#0
*****
490 PRINT#0 "PROG CURV ANALYSIS Y=COLUMN NO. ",V3," X=COLUMN NO.
",V2
500 PRINT#0 "FILENAME--",N$:PRINT#0 "ID STRING-- ",IS
510 PRINT#0 "FIRST ESTIMATE FOR S0 IS",Z12E4,S0
520 PRINT#0 "FIRST ESTIMATE FOR K IS",Z12E4,K," FOR V IS",Z12E4,V
530 PRINT#0 "COEFFICIENT OF DETERMINATION IS ",Z12E6,R
540 E0=1E-8
550 E1=1E-4
560 GOSUB 1090
570 GOSUB 1180
580 IF ABS(V9)<E1 THEN 590 ELSE 560
590 IF ABS(K9)<E1 THEN 600 ELSE 560
600 IF ABS(S9)>=E1 THEN 560
610 PRINT#0 " ++++++"
620 PRINT#0 " + KM ESTIMATE IS",Z12E4,K,"
+/-",Z12E4,SQRT(C(1,1)*S2)," +" 630 PRINT#0 " + VMAX ESTIMATE
IS",Z12E4,V," +/-",Z12E4,SQRT(C(2,2)*S2)," +" 640 PRINT#0 " + S0
ESTIMATE IS",Z12E4,S0," +/-",Z12E4,SQRT(C(3,3)*S2)," +" 650 PRINT#0 "
+++++"
660 PRINT#0
-----
-----
670 PRINT#0
-----
-----
680 PRINT#0 "APPROXIMATE PARAMETER COVARIANCE MATRIX"
690 PRINT#0
-----
-----
700 FOR I=1 TO 3
710 FOR J=1 TO 3
715 C(I,J)=S2*C(I,J)
720 PRINT#0 Z12E4,C(I,J),:IF J=3 THEN PRINT#0
730 NEXT J
740 NEXT I
750 C9=C(1,1)*C(2,2)*C(3,3)+2*C(1,2)*C(1,3)*C(2,3)
760 C9=C9-(C(1,1)*C(2,3)*C(2,3)+C(2,2)*C(1,3)*C(1,3)+
C(3,3)*C(1,2)*C(1,2))
770 PRINT#0 "DETERMINANT OF APPROXIMATE COVARIANCE MATRIX",Z12E4,C9
780 PRINT#0
-----
-----
790 PRINT#0 "APPROXIMATE PARAMETER CORRELATION MATRIX"
800 PRINT#0
-----
-----
810 FOR I=1 TO 3

```

```

820 FOR J=1 TO 3
830 R(I,J)=C(I,J)/SQRT(C(I,I)*C(J,J))
840 PRINT#0 %12E4,R(I,J),:IF J=3 THEN PRINT#0
850 NEXT J
860 NEXT I
870 PRINT#0
*****
880 INPUT "DO YOU WANT TO GENERATE A THEORETICAL CURVE? ",Q1
890 IF Q1=0 THEN 1050:IF Q1<>0 AND Q1<>1 THEN 880
900 INPUT "ENTER NAME OF DATAFILE TO BE CREATED? ",N$
910 PRINT#0 "ENTER AN ID STRING FOR YOUR FILE"
920 INPUT I$
930 B=INT((49*N+144)/256)+1
940 CREATE N$,B,3
950 OPEN#0,N$
960 WRITE#0%0,I$,N+1,7,NOENDMARK
970 WRITE#0%95,0,S0,0,-99,0,0,S0,NOENDMARK:Z=0
980 FOR I=1 TO N
990 D=1+K/S(I):X1=K*LOG(S0/S(I))/D:X2=V*-T(I)/D:X3=S0*(1+K/S0)/D
1000 WRITE#0%(Z*49+144),T(I),S(I),S0-S(I),S0(I)-S(I),X1,X2,X3,NOENDMARK
1010 Z=Z+1
1020 PRINT#0 %10E2,T(I),%10E2,S(I),%10E2,S0-S(I),%10E2,S0(I)-S(I)
1030 NEXT I
1040 CLOSE#0
1050 INPUT "DO YOU WISH TO CHAIN BACK TO FILEMAN? ",Q3
1060 IF Q3=0 THEN 1080:IF Q3<>0 AND Q3<>1 THEN 1050
1070 CHAIN "FILEMAN,2"
1080 END
1090 S1=S0:P1=0
1100 FOR I=1 TO N
1110 P2=P1-(P1+K*LOG(S0/(S0-P1))-V*T(I))/(1+K/(S0-P1))
1120 IF ABS(P2-P1)<=E0 THEN 1140
1130 P1=P2:GOTO 1110
1140 P1=P2:S1=S0-P1:S(I)=S1
1150 NEXT I
1160 RETURN
1170 END
1180 DATA 0,0,0,0,0,0,0,0,0,0,0,0,0,0,0
1190 READ A1,A2,A3,B1,B2,B3,C1,C2,C3,D1,D2,D3,D4,D5
1200 RESTORE
1210 FOR I=1 TO N
1220 D=1+K/S(I)
1230 Y=S0(I)-S(I)
1240 X1=LOG(S0/S(I))/D
1250 X2=-T(I)/D
1260 X3=(1+K/S0)/D
1270 A1=A1+X1
1280 A2=A2+X2
1290 A3=A3+X3
1300 B1=B1+X1*X1
1310 B2=B2+X2*X2
1320 B3=B3+X3*X3

```

```

1330 C1=C1+X1*X2
1340 C2=C2+X2*X3
1350 C3=C3+X1*X3
1360 D1=D1+Y
1370 D2=D2+Y*Y
1380 D3=D3+X1*Y
1390 D4=D4+X2*Y
1400 D5=D5+X3*Y
1410 NEXT I
1420 X(1,1)=B1:X(1,2)=C1:X(1,3)=C3
1430 X(2,1)=X(1,2):X(2,2)=B2:X(2,3)=C2
1440 X(3,1)=X(1,3):X(3,2)=X(2,3):X(3,3)=B3
1450 D(1)=D3:D(2)=D4:D(3)=D5
1460 D9=X(1,1)*X(2,2)*X(3,3)+2*X(1,2)*X(1,3)*X(2,3)
1470 D9=D9-(X(1,1)*X(2,3)*X(2,3)+X(2,2)*X(1,3)*X(1,3)+
X(3,3)*X(1,2)*X(1,2))
1480 C(1,1)=X(2,2)*X(3,3)-X(2,3)*X(2,3)
1490 C(1,2)=X(1,3)*X(2,3)-X(1,2)*X(3,3):C(2,1)=C(1,2)
1500 C(1,3)=X(1,2)*X(2,3)-X(1,3)*X(2,2):C(3,1)=C(1,3)
1510 C(2,2)=X(1,1)*X(3,3)-X(1,3)*X(1,3)
1520 C(2,3)=X(1,2)*X(1,3)-X(1,1)*X(2,3):C(3,2)=C(2,3)
1530 C(3,3)=X(1,1)*X(2,2)-X(1,2)*X(1,2)
1540 C(1,1)=C(1,1)/D9:C(1,2)=C(1,2)/D9:C(1,3)=C(1,3)/D9
1550 C(2,1)=C(1,2):C(2,2)=C(2,2)/D9:C(2,3)=C(2,3)/D9
1560 C(3,1)=C(1,3):C(3,2)=C(2,3):C(3,3)=C(3,3)/D9
1570 FOR I=1 TO 3
1580 B(I)=0
1590 NEXT I
1600 FOR I=1 TO 3
1610 FOR J=1 TO 3
1620 B(I)=C(I,J)*D(J)+B(I)
1630 NEXT J
1640 NEXT I
1650 K9=B(1):V9=B(2):S9=B(3)
1660 K=K+K9:V=V+V9:S0=S0+S9
1670 S2=(D2-D1*D1/N-K9*(D3-A1*D1/N)-V9*(D4-A2*D1/N)-
S9*(D5-A3*D1/N))/(N-3)
1680 PRINT#0 "INTERMEDIATE VALUES, K",%12E4,K," V",%12E4,V,"
S0",%12E4,S0
1690 RETURN
1700 END

```

PROGCRV2 fits product concentration-time data pairs to the integrated form of the Michaelis-Menten equation when the origin of the progress curve is unknown. It estimates  $K_m$  and  $V_{max}$  plus  $P_0$ , which is defined as a positive displacement above the origin on the product concentration axis. A progress curve of unknown origin arises when

product is present at the start of a progress curve in which product appearance is monitored. The concentration of the product present as background must be lower (e.g., 5-fold) than that derivable from  $S_0$  if accurate estimates of  $K_m$  and  $V_{max}$  are to be obtained. Like PROGCRV1, PROGCRV2 calculates initial estimates of the above parameters which are then improved via nonlinear regression. Initial estimates of  $K_m$  and  $V_{max}$  are obtained from linear regression analysis of the P-t data pairs transformed according to equation [B.6] (lines 350-490). An initial estimate of  $P_0$  is calculated by fitting the first 3 data pairs to a straight line and extrapolating back to the product concentration axis (lines 250-340). Unlike PROGCRV1,  $S_0$  is not updated and assumed to be known. Analogous to PROGCRV1, PROGCRV2 approximates the standard errors of the estimated parameters along with the covariance and parameter correlation matrices. The sensitivity equations (lines 1240 and 1260-1280) are not included in Appendix B since they have appeared elsewhere (4,5).

Many of the lines in PROGCRV2 are identical to those occurring in PROGCRV1. In the listing below, a line number followed by an "=" indicates that this line of code is identical in both programs. When a line number occurs after an "=" this line of code in PROGCRV2 is identical with that line number of PROGCRV1 following the "=".

#### LISTING OF PROGCRV2

```

10 =
20 =
30 PRINT#0 TAB(3), "><>NOTE THIS VERSION OF PROGCRV IS FOR ANALYSIS
   OF PRODUCT DATA ONLY<><"
40 =

```

```

50 DIM P(160),T(160),P0(160),IS(80),X(3,3),C(3,3),B(3),D(3)
60 -
70 -
80 -
90 -
100 -
110 -
120 -
130 -
140 -
150 -
160 -
170 -
180 -
190 READ#0%(Z9*V8+V1),P(I)
200 P0(I)=P(I)
210 =200
220 =210
230 =220
240 INPUT "ENTER INITIAL SUBSTRATE CONCENTRATION ",SO
250 =230
260 FOR I=1 TO 3
270 Y1=Y1+P(I)
280 X1=X1+T(I)
290 Y2=Y2+P(I)*P(I)
300 X2=X2+T(I)*T(I)
310 X9=X9+P(I)*T(I)
320 NEXT I
330 B9=(X9-X1*Y1/3)/(X2-X1*X1/3)
340 P0=Y1/3-B9*X1/3
350 Y1=0:X1=0:Y2=0:X2=0:X9=0:N9=N
360 =340
370 IF SO>(P(I)+P0) THEN 390
380 N9=N9-1:EXIT 470
390 Y=T(I)/LOG(S0/(S0-P(I)-P0))
400 X=(P(I)-P0)/LOG(S0-P(I)-P0)
410 =380
420 =390
430 =400
440 =410
450 =420
460 =430
470 B9=(X9-X1*Y1/N9)/(X2-X1*X1/N9)
480 A9=Y1/N9-B9*X1/N9:K=A9/B9:V=1/B9
500 =470
510 =480
520 =490
530 =500
540 PRINT#0 "INITIAL SUBSTRATE CONC. IS",X12E4,SO
550 =520
560 =530
570 =540
580 =550

```

```

590 GOSUB 1110
600 GOSUB 1200
610 IF ABS(V9)<E1 THEN 620 ELSE 590
620 IF ABS(K9)<E1 THEN 630 ELSE 590
630 IF ABS(P9)<E1 THEN 640 ELSE 590
640 =610
650 =620
660 =630
670 PRINT#0 "    + P0 ESTIMATE IS",%12E4,P0," +/-",%12E4,SQRT(C(3,
3)*S2," +"
680 =650
690 =660
700 =670
710 =680
720 =690
730 =700
740 =710
745 =715
750 =720
760 =730
770 =740
780 =750
790 =760
800 =770
810 =780
820 =790
830 =800
840 =810
850 =820
860 =830
870 =840
880 =850
890 =860
900 =870
910 =880
920 =890
930 =900
940 =910
950 =920
960 =930
970 =940
980 =950
990 =960
1000 WRITE#0%95,0,S0,0,-99,0,0,0,NOENDMARK:Z=0
1010 =980
1020 D=1+K/(S0-P(I)):X1=K*-LOG(S0/(S0-P(I)):X2=V*T(I)/D:X3=P0
1025 WRITE#0 %10E2,T(I),%10E2,S0-P(I)-P0,%10E2,P(I)-P0,%10E2,
(P0(I)-P0)-(P(I)-P0),%10E2,X1,%10E2,X2,%10E2,X3,NOENDMARK
1030 =1010
1040 PRINT#0 %12E4,T(I),%12E4,S0-P(I)-P0,%12E4,P(I)-P0,%12E4,
(P0(I)-P0)-(P(I)-P0)
1050 =1030
1060 =1040

```

```
1070  =1050
1080  =1060
1090  =1070
1100  =1080
1110  P1=0
1120  =1100
1130  P2=P1-((P1-P0)-K*LOG(1-(P1-P0/S0)-V*T(I)))/(1+K/(S0-P1-P0))
1140  IF ABS(P2-P1)<=E0 THEN 1160
1150  P1=P2:GOTO 1130
1160  P1=P2:P(I)=P1
1170  =1150
1180  =1160
1190  =1170
1200  =1180
1210  =1190
1220  =1200
1230  =1210
1240  D=1+K/(S0-P(I)-P0)
1250  Y=P0(I)-P(I)
1260  X1=LOG(1-(P(I)-P0)/S0)/D
1270  X2=T(I)/D
1280  X3=1
1290  =1270
1300  =1280
1310  =1290
1320  =1300
1330  =1310
1340  =1320
1350  =1330
1360  =1340
1370  =1350
1380  =1360
1390  =1370
1400  =1380
1410  =1390
1420  =1400
1430  =1410
1440  =1420
1450  =1430
1460  =1440
1470  =1450
1480  =1460
1490  =1470
1500  =1480
1510  =1490
1520  =1500
1530  =1510
1540  =1520
1550  =1530
1560  =1540
1570  =1550
1580  =1560
1590  =1570
```



```

1600  =1580
1610  =1590
1620  =1600
1630  =1610
1640  =1620
1650  =1630
1660  =1640
1670  K9=B(1):V9=B(2):P9=B(3)
1680  K=K+K9:V=V+V9:P0=P0+P9
1690  S2=(D2-D1*D1/N-K9*(D3-A1*D1/N)-V9*(D4-A2*D1/N)-P9*(D5-A3*D1/N))/
(N-3)
1700  PRINT#O "INTERMEDIATE VALUES,  K",%12E4,K,"  V",%12E4,V,"  P0",
%12E4,S0
1710  =1690
1720  =1700

```

MONODCRV fits substrate disappearance data to the integrated form of the Monod equation [B.15], derived assuming constant yield. It estimates  $u_{\max}$ ,  $K_s$  and  $Y$  which respectively are the maximum growth rate, substrate concentration at which growth rate is half-maximal and the yield coefficient. The major difference between MONODCRV and the above 2 programs is it requires the user to input initial estimates of the 3 parameters; MONODCRV does not calculate initial estimates of  $u_{\max}$ ,  $K_s$  and  $Y$ . Initial estimates of the growth kinetic parameters are obtained using discretized approximations to the Monod equations [B.21], [B.22] describing the rates of change of substrate [B.12] and biomass [B.16] (details in Appendix B). These provisional estimates along with initial substrate ( $S_0$ ) and biomass ( $X_0$ ) concentrations are entered at lines 200-210. A second important difference between MONODCRV and the other 2 progress curve analysis programs is the former numerically integrates the derivative form of the Monod equation to calculate theoretical substrate and biomass concentrations (lines 830-960), whereas PROGCRV1 and PROGCRV2 numerically approximate solutions to integrated Michaelis-Menten equations. The parameter updating subroutine (lines

970-1500) is nearly identical with those of PROGCRV1 and PROGCRV2.

As was true for PROGCRV2, MONODCRV shares identical lines of code with PROGCRV1. These are indicated in the same way as was done for PROGCRV2.

#### MONODCRV LISTING

```

10 DIM S(160),X1(160),T(160),S0(160),IS(80),X(3,3),C(3,3),B(3),D(3)
20 DIM R(3,3): LINE 90
30 =70
40 =80
50 =90
60 =100
70 =110
80 =120
90 =130
100 =140
110 =150
120 =160
130 =170
140 =180
150 =190
160 =350
170 =200
180 =210
190 =220
200 =INPUT "ENTER INITIAL SUBSTRATE AND BIOMASS CONCENTRATIONS  ",
S0,X0
210 INPUT "ENTER INITIAL ESTIMATES OF KS,UMAX AND Y  ",K,V,Y
220 =470
230 =480
240 !#0 "MONODCRV ANALYSIS  Y=COLUMN NO.  ",V3,"  X=COLUMN NO.  ",V2
250 =500
260 =!#0 "S0= ",Z12E4,S0," X0= ",Z12E4,X0
270 =520
280 !#0 "FIRST ESTIMATE FOR Y IS",Z12E4,Y
290 =550
300 GOSUB 830
310 GOSUB 970
320 IF ABS(V9)<=E1 THEN 330 ELSE 300
330 IF ABS(K9)<=E1 THEN 340 ELSE 300
340 IF ABS(Y9)<=E1 THEN 350 ELSE 300
350 =610
360 PRINT#0 "  +  Ks ESTIMATE IS",Z12E4,K,"  +/-",Z12E4,SQRT(C(1,
1)*S2)," +"
370 PRINT#0 "  +  UMAX ESTIMATE IS",Z12E4,V,"  +/-",Z12E4,SQRT(C(2,

```

```

2)*S2)," +
380 PRINT#0 " + Y ESTIMATE IS",%12E4,Y," +/-",%12E4,SQRT(C(3,
3)*S2),"+"
390 =650
400 =660
410 =670
420 =680
430 =690
440 =700
450 =710
460 =715
470 =720
480 =730
490 =740
500 =750
510 =760
520 =770
530 =780
540 =790
550 =800
560 =810
570 =820
580 =830
590 =840
600 =850
610 =860
620 =870
630 =880
640 IF Q=1 THEN 790: IF Q1<>0 AND Q1<>1 THEN 630
650 =900
660 =910
670 =920
680 B=INT((28*N+123)/256)+1
690 =930
700 =940
710 WRITE#0%0,I$,N+1,4,NOENDMARK
720 WRITE#0%95,0,S0,0,-99,NOENDMARK:Z=0
730 =980
740 WRITE#0%(Z*28+123),T(I),S(I),S0-S(I),S0(I)-S(I),NOENDMARK
750 =1010
760 =1020
770 =1030
780 =1040
790 =1050
800 =1060
810 =1070
820 =1080
830 X1=X0:C2=2:C6=6:D0=.01
840 FOR I=1 TO T(N)
850 FOR J=1 TO 1/D0
860 K1=(V*(X0-X1+Y*S0)*X1)/(Y*K+X0-X1+Y*S0)*D0
870 K2=(V*(X0-(K1/C2+X1)+Y*S0)*(K1/C2+X1))/Y*K+X0-(K1/C2+X1)+Y*S0)*D0
880 K3=(V*(X0-(K2/C2+X1)+Y*S0)*(K2/C2+X1))/Y*K+X0-(K2/C2+X1)+Y*S0)*D0

```

```

890 K4=(V*(X0-(K3+X1)+Y*S0)*(K3+X1))/Y*K+X0-(K3+X1)+Y*S0)*D0
900 X1=X1+(K1+C2*K2+C2*K3+K4)/C6
910 NEXT J
920 X1(I)=X1:S(I)=(X0-X1)/Y+S0
930 !#0 Z6I,T(I),Z12E4,S(I),Z12E4,S0(I)-S(I),Z12E4,X1(I)
940 =1150
950 =1160
960 =1170
970 =1180
980 =1190
990 =1200
1000 P9=(K*Y+YS0+X0)/(Y*S0+X0):Q9=K*Y/(Y*S0+X0):R9=Y*S0+X0
1010 =1210
1020 D9=P9*Y/X1(I)+Q9/S(I)
1030 E=S0(I)-S(I)
1040 X1=Y/R9*(LOG(X1(I)/X0)-LOG(S(I)/S0))/D9
1050 X2=-T(I)/D9
1060 X3=(P9*(S0-S(I))/X1(I)+LOG(X1(I)/X0)/R9*(K+(1-P9)*S0)
-LOG(S(I)/S0)/R9*(K-Q9*S0))/D9
1070 =1270
1080 =1280
1090 =1290
1100 =1300
1110 =1310
1120 =1320
1130 =1330
1140 =1340
1150 =1350
1160 D1=D1+E
1170 D2=D2+E*E
1180 D3=D3+X1*E
1190 D4=D4+X2*E
1200 D5=D5+X3*E
1210 =1410
1220 =1420
1230 =1430
1240 =1440
1250 =1450
1260 =1460
1270 =1470
1280 =1480
1290 =1490
1300 =1500
1310 =1510
1320 =1520
1330 =1530
1340 =1540
1350 =1550
1360 =1560
1370 =1570
1380 =1580
1390 =1590
1400 =1600

```

```

1410  =1610
1420  =1620
1430  =1630
1440  =1640
1450  K9=B(1):V9=B(2):Y9=B(3)
1460  K=K+K9:V=V+V9:Y=Y+Y9
1470  S2=(D2-D1*D1/N-K9*(D3-A1*D1/N)-V9*(D4-A2*D1/N)-Y9*(D5-A3*D1/N))/
(N-3)
1480  PRINT#O "INTERMEDIATE VALUES,  K",%12E4,K,"  V",%12E4,V,"  Y",
%12E4,Y
1490  RETURN
1500  END

```

Numerical integration of PHASIM model equations. PHASIM

simultaneously numerically integrates the equations [A.1], [A.2] for gaseous substrate consumption by resting cells in a liquid phase described in Appendix A. A third equation for first-order increase in  $V_{\max}$  with time is numerically integrated concomitant with the above 2. The user has the option of storing the gaseous and aqueous phase concentrations of the gaseous substrate on a minifloppy diskette, in a data file that may be read by FILEMAN (lines 10-40, 370-390 and 420-430). The initial gaseous and aqueous phase concentrations of the gaseous substrate along with the  $K_{1a}$ ,  $V_{\max}$ ,  $K_m$ ,  $K$  (first-order coefficient for increase in  $V_{\max}$  with time) and  $R$  (linear rate of endogenous substrate production) are entered at lines 50-80. The user then enters the Bunsen absorption coefficient plus the time-step for integration ( $\Delta t$ ) and length of the simulation ( $T_{\max}$ ) at lines 90-100. The time-step for integration must be a number whose reciprocal is an integer. A fourth-order Runge-Kutta procedure (2) is used to estimate the solution curves (i.e.,  $G$  vs.  $t$  and  $A$  vs.  $t$ ) for the PHASIM system of ordinary differential equations (lines 170-350, 400 and 480-520). The time and concentrations of the substrate in the gaseous and aqueous phases is then outputted to the Decwriter (line 360).

Lastly, the user may decrease the delta t (lines 440-450) and re-run the simulation or a new set of parameter values may be entered (lines 460-470) and the solution curves estimated once more.

## PHASIM LISTING

```

10 DIM I$(80)
20 INPUT "IF YOU WISH TO SAVE DATA ON A FILE TYPE 'SAVE' ",S$
30 INPUT "ENTER THE NAME OF THE DATAFILE ",N$
40 INPUT "ENTER AN IDENTIFICATION STRING FOR YOUR FILE "I$
50 PRINT "ENTER INITIAL CONCENTRATIONS OF THE GAS IN THE GASEOUS
AND AQUEOUS PHASES"
60 INPUT G0,A0
70 PRINT "WHAT ARE THE VALUES OF KLA,VMAX,KM,K, AND R?"
80 INPUT K1,V,K3,K2,R
90 INPUT "ENTER THE BUNSEN ABSORPTION COEFFICIENT ",B9
100 INPUT "ENTER VALUES FOR TMAX AND DELTAT ",T9,D
110 D1=1/D:G1=G0:V1=V:A1=A0:Z=0
120 IF S$<>"SAVE" THEN 170
130 B=INT(7*T9*3+100)/256)+1
140 CREATE N$,B,3
150 OPEN,N$
160 WRITE #0%0,I$,T9,3,NOENDMARK
170 FOR I=1 TO T9
180 FOR J=1 TO D1
190 G2=-K1*(B9*G1-A1)*D
200 V2=K2*V1*D
210 A2=(K1*(B9*G1-A1)+R-V1*A1/(K3+A1))*D
220 G3=(-K1*(B9*(G2/2+G1)-(A2/2+A1)))*D
230 V3=K2*(V2/2+V1)*D
240 A3=(K1*(B9*(G2/2+G1)-(A2/2+A1))+R-(V2/2+V1)*(A2/2+A1)/(K3+
(A2/2+A1)))*D
250 G4=(-K1*(B9*(G3/2+G1)-(A3/2+A1)))*D
260 V4=K2*(V3/2+V1)*D
270 A4=(K1*(B9*(G3/2+G1)-(A3/2+A1))+R-(V3/2+V1)*(A3/2+A1)/(K3+
(A3/2+A1)))*D
280 G5=(-K1*(B9*(G4+G1)-(A4+A1)))*D
290 V5=K2*(V4+V1)*D
300 A5=(K1*(B9*(G4+G1)-(A4+A1))+R-(V4+V1)*(A4+A1)/(K3+(A4+A1)))*D
310 G6=FNA(G1,G2,G3,G4,G5)
320 V6=FNA(V1,V2,V3,V4,V5)
330 A6=FNA(A1,A2,A3,A4,A5)
340 G1=G6:V1=V6:A1=A6
350 NEXT J
360 PRINT#0 %4I,I,%12E4,G1,%12E4,A1
370 IF S$<>"SAVE" THEN 400
380 WRITE#0%(Z*21+95),I,G1,A1,NOENDMARK

```

```
390 Z=Z+1
400 NEXT I
410 PRINT#0:PRINT#0:PRINT#0
420 IF S$<>"SAVE" THEN 440
430 CLOSE #0
440 INPUT "HOW ABOUT ANOTHER DELTAT? (YES OR NO) ",A$
450 IF A$="YES" THEN 130
460 INPUT "HOW ABOUT ANOTHER SET OF PARAMTERS? (YES OR NO) ",F$
470 IF F$="YES" THEN 10 ELSE END
480 DEF FNA(Q1,Q2,Q3,Q4,Q5)
490 V=Q1+(Q2+2*Q3+2*Q4+Q5)/6
500 RETURN V
510 FNEND
```

#### LITERATURE CITED

1. Beck, J. V., and K. J. Arnold. 1977. Parameter estimation in engineering and science. John Wiley and Sons, New York.
2. Burden, R. L., J. D. Faires, and A. C. Reynolds. 1978. Numerical analysis. Prindle, Schmidt, and Weber, Boston.
3. Cornish-Bowden, A. 1976. Principles of enzyme kinetics. Butterworths, Boston.
4. Duggleby, R. G., and J. F. Morrison. 1977. The analysis of progress curve data for enzyme-catalyzed reactions by non-linear analysis. *Biochem. Biophys. Acta.* 481: 297-312.
5. Nimmo, I. A., and G. L. Atkins. 1974. A comparison of two methods for fitting the integrated Michaelis-Menten equation. *Biochem. J.* 141: 913-914.
6. Pirt, S. J. 1975. Principles of microbe and cell cultivation. John Wiley and Sons, New York.



MICHIGAN STATE UNIV. LIBRARIES



31293104760461